SYNTHESIS AND PROPERTIES OF SOME NOVEL CONDUCTING POLYMERS

By ADELINE PREVOST

A thesis submitted in partial fulfilment of the
requirements of Kingston University
for the degree of Doctor of Philosophy

October 2002

The following figures have been omitted on request of the University –

Fig. I-11	pg. 12
Fig. I-12	pg. 12
Fig. I-16	pg. 17
Fig. I-17	pg. 18
Fig. I-19	pg. 22
Fig. IV-1	pg. 162

AKNOWLEDGMENTS

From the beginning of this project I have discovered the most caring and helpful side of the people around me. Without their help, support, advice and sometimes criticism, this project would not have succeeded.

I would like to thank the technical staff of the Science Faculty, for having always found the time to help and advise me. I would also like to thank the lecturers and staff who have encouraged me to carry on.

A big thank you also goes to my friends and to my family, for caring, supporting, staying my friend throughout the rough patches, and for trying to understand.

The biggest thanks of all go to John and Peter, for their help and guidance, time and patience, and most of all for believing in me when even I did not believe in myself anymore.

ABSTRACT

Because of the nature of conduction in conjugated polymers, an improvement in the planarity of the backbone results in a smaller energy gap and increased electron mobility, and hence in a higher conductivity. From this consideration was born the idea of combining two types of material to create a new one: a side-chain liquid crystal conducting polymer possessing externally controllable backbone planarity.

Firstly, a small number of potentially conducting polymer backbones was chosen. For a polymer to be conducting a stable conjugated system is required, therefore an obvious choice was a type of backbone that includes aromatic or heteroaromatic rings. Three different backbone units were used in this project: aniline, pyrrole, and carbazole.

The aniline derivatives were chosen to be ortho-substituted so as to favour a regular 'head to tail' polymerisation in positions 1 (N) and 4. Both pyrrole and carbazole are symmetrical when substituted on the nitrogen, making the 'head' position equivalent to the 'tail' one. This property maximises the chances of a regular polymerisation pattern.

The next stage of the project was to produce suitable monomers. Previous work was considered to choose the liquid crystal moieties that would be attached.

This was achieved by optimising the synthetic route using model compounds before synthesising liquid crystal monomers. The model monomers, and some commercially available compounds, were employed in the following step of the project to optimise the polymerisation route for the various types of polymers. Both oxidative chemical polymerisation and electropolymerisation in different media were used.

The novel polymeric products were characterised and their electronic conductivities were measured. Films of the polymer that showed the greatest potential for alignment (liquid crystalline polypyrrole) were studied in more detail, and treated with a focussed laser beam to locally align the polymer backbone. This significantly increased the local conductivity. Most of the monomers and polymers were modelled using a software package (CAChe 3.2) to predict and compare some of their properties. The results of modelling the pyrrole derivative were combined with preliminary X-ray diffraction data for the aligned and unaligned polymer, allowing the proposal of a new explanation for the alignment phenomenon at a molecular level.

TABLE OF CONTENTS

I INTRODUCTION

Plastics have already replaced traditional materials such as wood, ceramic or glass in many applications. Their widespread use arises from the combination of their physical and mechanical properties together with ease of processability. Over the past 30 years these lightweight materials have triggered a renewed interest from industry, one reason for which was the discovery of the potential electronic uses of several classes of them. These applications have already found their way into our everyday life, in the form of anti-static films, batteries, sensors, and even light emitting devices such as video displays.

Although the polymers used are fairly efficient, much could still be done to optimise their properties. The main area of interest for this project is the manipulation of the conductivity of a specific class of polymers. The conductivity of polymers can be increased by the use of a doping agent, but it does not always suffice to produce a lasting processible conducting material. Amongst other factors, the conductivity in polymers is affected by the ease with which the electrons move along the backbone of the polymer. In an ideal world, the chains of polymer would therefore need to be neatly lined up. Unfortunately, when it comes to the reality of a film cast from solution, the resulting arrangement would be closer to a plate of spaghetti! The idea behind this project is to encourage the polymer chains to arrange themselves in a more orderly manner, thus increasing the potential conductivity, but without affecting the other properties. One way of achieving this would be to firstly organise the monomer molecules and then proceed with the polymerisation, and this general approach is under investigation by several research groups. We chose to alter the structure of the monomers so as to make possible the alignment of the backbone of the final polymer.

In order to achieve this result, it was logical to look at materials that have a natural tendency to order themselves. Liquid crystals have been studied for decades for precisely that reason. In appropriate conditions, the liquid crystal or mesogenic molecules have a preferred arrangement following one or more characteristic patterns. Even some polymers behave like this. Strangely enough the concept of combining polymers and liquid crystals did not wait for mankind to be invented. Spiders have been webbing polymer liquid crystal structures for hundreds, maybe even thousands of years. The enormous tensile strength of spider silk is the result of the liquid crystal molecules being part of the polymer backbone itself[1]. The polymer thus tends naturally to form strong fibres due to self-alignment. The same principle applies for the structure of man-made materials such as Kevlar, but unfortunately such molecules are, for structural reasons, bad candidates for conductivity.

For this reason, we decided to take the other option for the production of liquid crystal polymers. By attaching the liquid crystal moieties as side chains to a conducting polymer backbone, a more controllable material could be obtained that retains its conductive properties. By choosing liquid crystal phases that depend on temperature, we might be able to vary the planarity of the polymer backbone simply by heating it to the appropriate temperature[2]. By using a laser to do this, we may gain the advantage of precision drawing of conductive tracks. All of this will be discussed further below.

A lexicon can be found as Appendix V.1 to this thesis. A more detailed presentation of the above topics can be found in the introduction together with prior research work. The experimental section describes the techniques and experiments that were used in the project, together with some computer aided molecular modelling of the target molecules. Following the Results and Discussion part, a section suggests the future work that could be undertaken to follow up that project.

I.1 Liquid crystals

I.1.1 Historical background

In 1888 the Australian botanist Reinitzer[3] recorded for the first time the unusual chromic behaviour undergone by cholesteryl benzoate upon heating or cooling. The importance of the discovery was not really in that the colour of the compound changed to a deep blue colour upon apparent liquefaction, since that behaviour had already been reported thirty-eight years earlier[4] for different cholesteryl compounds, but in that the liquid phase became cloudy and colourless. As the temperature was increased further, the sample took the usual appearance of a fluid and clear melt. The most remarkable aspect of those observations came from the two apparent distinct melting points, when only one had ever been previously observed for purified solids, and also from the surprising accuracy with which the transition temperatures could be reproduced. Further experiments suggested to Reinitzer that he was witnessing the fluidity of a liquid combined with the anisotropic optical properties of a crystalline solid. His request to Lehman to study the strange observations using polarised light only confirmed the transitions[5], and the properties then observed led to the invention of the term 'liquid crystal' to describe these compounds that were neither true liquids nor true solids.

Since then, many names have been created to describe that intermediate state of matter, such as mesophase, crystalline liquid, mesomorphic phase, paracrystal and paracrystalline phase[6]. Still, the original name of Liquid Crystal remains the most widely used.

Strangely in his publication of 1922 accounting for the progress in the field of those compounds[7], Friedel was opposed to the name but nevertheless produced the first clarified systematisation and nomenclature, both of which were soon widely adopted.

A new class of compounds had emerged, and the interest they generated was to grow rapidly for the next seventy years, with numerous new properties being discovered, and even more new compounds exhibiting them being synthesised and studied. That is not to say that research on liquid crystals came to a sudden end in 1960. On the contrary that decade saw the major turn in the destiny of those peculiar chemicals. The electronic and display industry finally invented some applications. They are now part of a massive display industry, the products of which are found in our everyday life. Research is still very active on that front as the numerous properties of liquid crystals are still to be fully exploited.

So what gives a liquid crystal those specific properties that make it an intermediate phase (mesophase) between a crystalline solid and an isotropic liquid?

I.1.2 Structural Concepts

It is well understood that the higher the temperature, the more the molecules are moving and vibrating in a random way, hence the lower the order of the system. The structure of an ordered crystal is very simply described using three parameters per atom: positional order, bond orientational order, and molecular orientation. A solid phase possesses positional and orientational order that a liquid does not. When a solid 'melts' to a liquid crystal, the positional order may be lost although some of the orientational order may remain. As a result, the molecules in a liquid crystal phase are free to move in much the same way as they would in a liquid, but they tend to remain oriented in a certain direction, even though the orientational order is not as perfect as in a solid. A measure of the degree of orientational order or alignment is given by the order parameter[8,9]: $S = \frac{1}{2}\left(3 \cdot \cos^2\theta - 1\right)$ where θ is the angle between the long axis of a

representative molecule and some preferred direction which is denoted as the director (n), as illustrated in Figure I-1.

For a crystalline solid S=1, for an isotropic liquid S=0, and for a liquid crystal S ranges typically from 0.3 to 0.9[10].

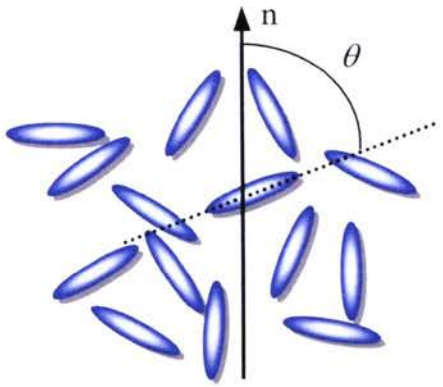

Figure I-1 Possibly restricted orientation of liquid crystal molecule with respect to the director.

To make the subject even more interesting to scientists, it was soon discovered that liquid crystals came in many different shapes and forms, so to speak, each new compound displaying its own range of properties and characteristics. The overall shape of the liquid crystal molecule is usually found to be disk-like (discotic) or rod-like (calamitic).

I.1.2.1 Discotic liquid crystals

Although discotic liquid crystals will not be discussed any further it seems relevant to briefly mention their general structure and properties. The mesomorphophic properties of those peculiar molecules were first reported in 1977 by Chandrasekhar for hexaalkanoylbenzenes[11]. Discotic liquid crystals usually consist of flat, polyaromatic molecules. An example of such a molecule can be found in Figure I-2.

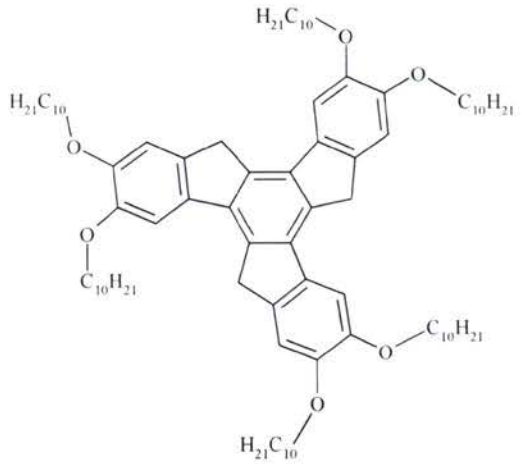

Figure I-2Discotic molecule of hexaalkoxytruxene

The discs are anisotropic and possess a short axis that tends to favour their lying parallel to each other.

Discotic liquid crystals usually exhibit one of two discotic mesophases: nematic or columnar. The nematic phase (characteristics of which will be detailed later in this chapter for calamitic materials) is the least ordered and the least viscous of the mesophases. A representation of the molecular arrangement can be found illustrated in Figure I-3.

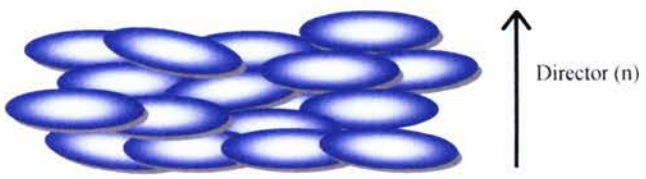

Figure I-3 Molecular arrangement within the discotic nematic phase

The columnar phases, specific to discotic materials, are characterised by two-dimensional lattices of columns with a variety of symmetry classes and various degrees of order of the molecular stacking within the columns. A representation of rectangular and hexagonal columnar phases can be found illustrated in Figure I-4.

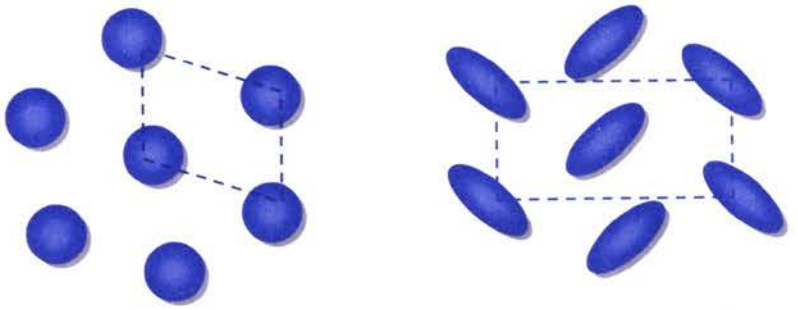

Figure I-4 Molecular positions within the hexagonal (left) and rectangular (right) columnar phase

I.1.2.2 Calamitic liquid crystals

The other shape of molecule that can exhibit a liquid crystal behaviour is elongated, often referred to as rod-like or lath-like, a good example of which is hexylcyanobiphenyl, illustrated in Figure I-5.

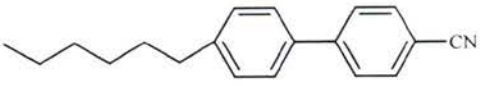

Figure I-5 Calamitic hexylcyanobiphenyl molecule

The rest of this chapter is dedicated to this class of material, starting with the two basic classifications of liquid crystals. The phase transition of a thermotropic liquid crystal depends on the temperature, while that of a lyotropic crystal depends on the concentration of that compound in a suitable solvent[12].

I.1.3 Lyotropic Liquid Crystals

Lyotropic liquid crystals were actually discovered long before the thermotropic liquid crystals. The observation of a texture was reported in 1850 for a mixture of myelin and water, but at the time little notice was taken of the phenomenon[13].

The molecules that form lyotropic liquid crystals are usually surface-active agents (surfactants). They consist of a polar, often ionic, 'head' and a distinct non-polar, often hydrocarbon, 'tail'.

A very simple yet typical example is sodium stearate (Figure I-6).

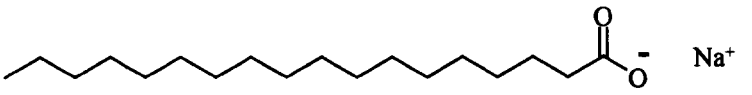

Figure I-6 Sodium stearate molecule

The head is attracted to water, so it is said to be hydrophilic. As the tail is repelled by water it is said to be hydrophobic. NB: in the case of a polar solvent different from water the head would be said to be lyophilic and the tail, lyophobic.

When the concentration of surfactant molecules become high enough, the molecules arrange themselves so that the polar heads are in contact with a polar solvent and/or the non-polar tails are in contact with a non-polar solvent. The 3-dimensional systems formed are called micelles. Micelles come in a variety of sizes, but the shape is usually spherical or rod-like.

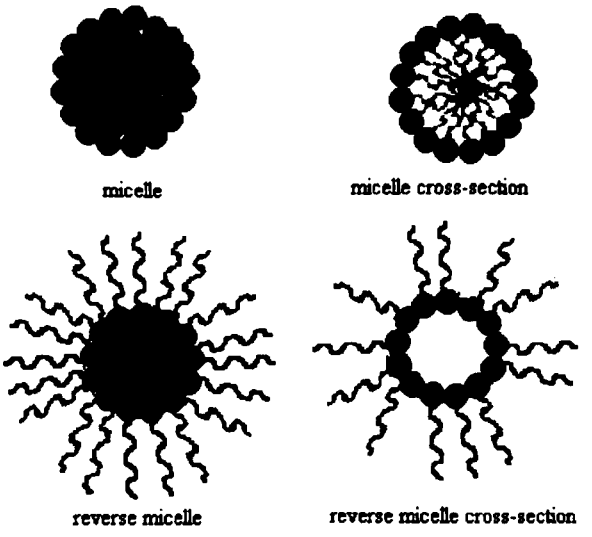

Figure I-7 Micelles formed by amphiphilic molecules

As the concentration increases, the micelles swell up and the micro-emulsion becomes a cloudy emulsion. As the concentration increases further, the micelles start arranging themselves in patterns. Those patterns give the system the ability to exhibit the characteristic, mainly optical, properties of a liquid crystal phase.

As the concentration is increased even more, a different liquid crystalline phase starts to form. Called a lyotropic liquid crystal bi-layer, it has a double layer of molecules arranged so that the heads of one layer face the heads of the next layer. The tails of that layer are arranged so as to face the tails of the previous layer.

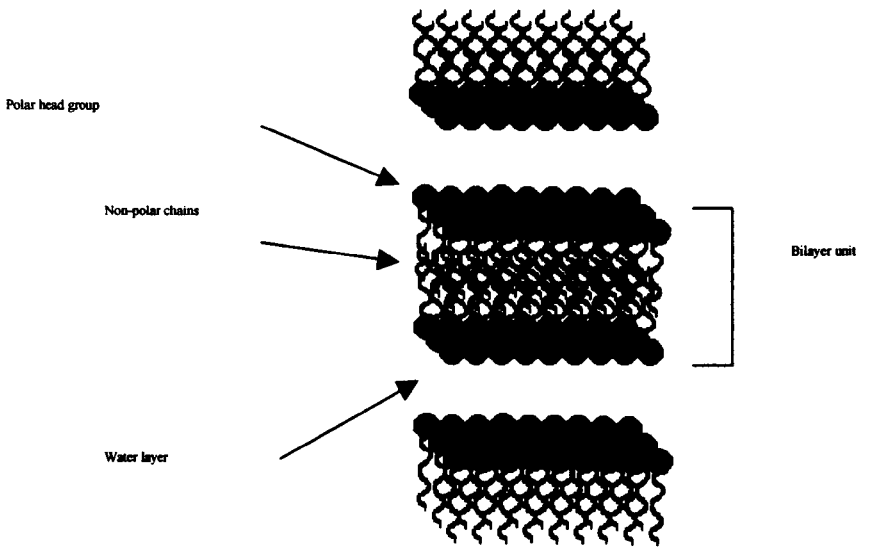

Figure I-8 Structure of the lamellar lyotropic liquid crystal phase

The system, also referred to as lamellar, is similar to a thermotropic smectic system (see section I.1.4.3 for more details on this type of structure). Figure I-9 summarises the changes in structure with concentration.

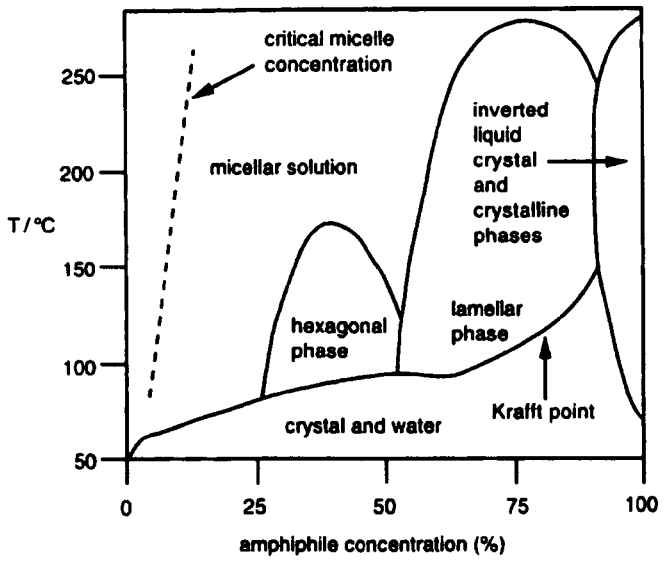

Figure I-9 Phase diagram for a typical soap (sodium stearate) in water

If the concentration becomes such that the amount of surfactant is greater (in weight) than the amount of solvent, the system reverses to an arrangement of droplets. However this time the lyophilic heads point towards the inside of the droplet in which the solvent is situated. The tails of the molecules separate the droplets from each other.

Lyotropic liquid crystals are found in countless everyday situations. The most obvious examples are soap and detergents when they are mixed with water, but biological membranes also display lyotropic liquid crystal behaviour.

I.1.4 Thermotropic Liquid Crystals

A thermotropic liquid crystal, also referred to as a non-amphiphilic mesophase, results from the melting of a mesogenic solid and is also called a thermally activated mesophase, formed from organic or organometallic molecules, mainly rod or disc shaped.

The liquid crystals involved in this project were exclusively thermotropic, so a much greater emphasis will be put on their study and investigation.

As mentioned previously, liquid crystals can be divided into many classes and a typical thermotropic liquid crystal will usually belong to one of three structural classes[14], best described through the mesophase they give rise to. These structures are:

- Nematic structure
- Smectic structure
- Cholesteric structure

All are related to the packing aspects and the dimensionality of the residual molecular order.

I.1.4.1 The Nematic Phase

It is the least ordered of the mesophase types as it has the most liquid-like properties. The long axes of molecules remain substantially parallel but the centres of gravity are more disorganised than for example in a smectic structure. The orientation of the molecules provides this phase with a low viscosity, as the flowing along this axis is easier than in the isotropic melt.

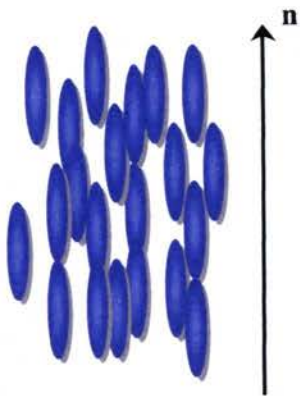

Figure I-10 Nematic mesophase for rod shaped liquid crystal molecules.

The textures most commonly observed in a nematic phase using polarised microscope are Schlieren (Figure I-11) and threaded textures. In addition less common textures can sometimes be observed, such as homogeneous and homeotropic.

I.1.4.2 The Cholesteric Mesophase

The cholesteric mesophase takes its name from the obvious reason that many compounds forming this mesophase derive from cholesterol[15]. Here a chiral centre is required, which makes the whole structure chiral. The cholesteric mesophase (Figure I-12) could be compared closely to the nematic one if the director were constant in space, but a helical distortion occurs, as if the structure were formed from layers of nematic liquid crystal.

The director of an individual layer is rotated through a small angle with respect to the director of the adjacent layers. After a regular succession of layers the director turns through 360° and this thickness represents the pitch length for the helix.

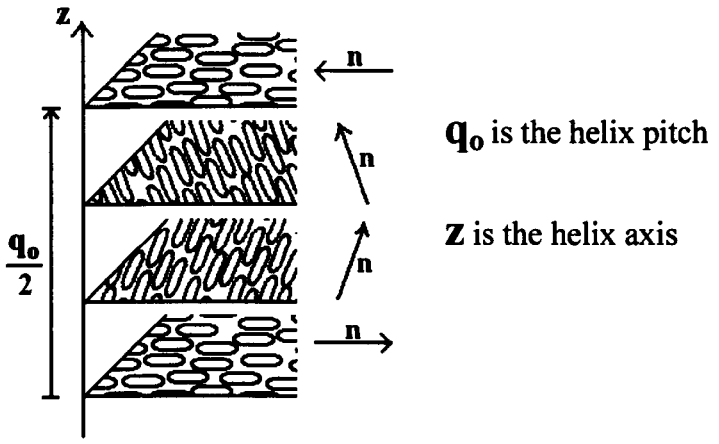

Figure I-13 A representation of the cholesteric mesophase.

I.1.4.3 The Smectic Mesophase

The smectic mesophase finds its characteristics in two features: the parallelism of molecular long axes, and the layering of molecular centres of gravity in two-dimensional planes or sheets.

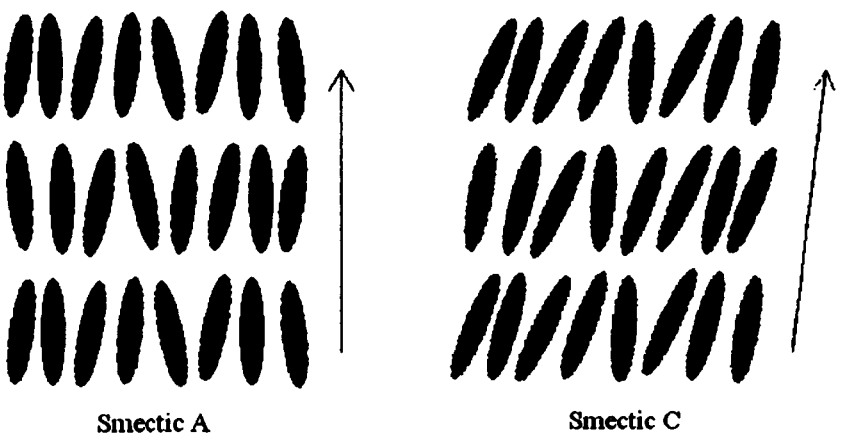

Figure I-14 Representation of smectic A and smectic C mesophase

As well as some orientational order, some positional order is kept, even though molecules remain free to move around quite randomly. Nevertheless, they tend to line themselves up with the director and are observed to arrange themselves in layers. It is the most solid-like of the liquid crystal mesophases. Its order parameter can be as high as 0.9, as some of the two-dimensional order is retained.

Because of the layering of the molecules, the angle adopted by the molecules with respect to the plane of the layers can vary greatly. Each different angle the molecules adopt, combined with the degree of order of the molecules within the layers, defines a different smectic phase. No less than 11 smectic phases have been reported in the literature, designated with letters ranging from A to K, and divided in two groups, depending on whether the director is perpendicular to the layer plane (1st group), or at a different angle (2nd group). Thanks to the progress of structural studies in the past fifteen years, the understanding of the smectic phases has increased greatly. This has led to some of the phases originally described as smectic phases to be re-classified as being crystal phases, since they possess some 3D order. The classification of smectic phases still remains difficult, with the D phase not completely defined, although it is believed to be cubic. A representation of the main smectic phases is illustrated in Figure I-15[16].

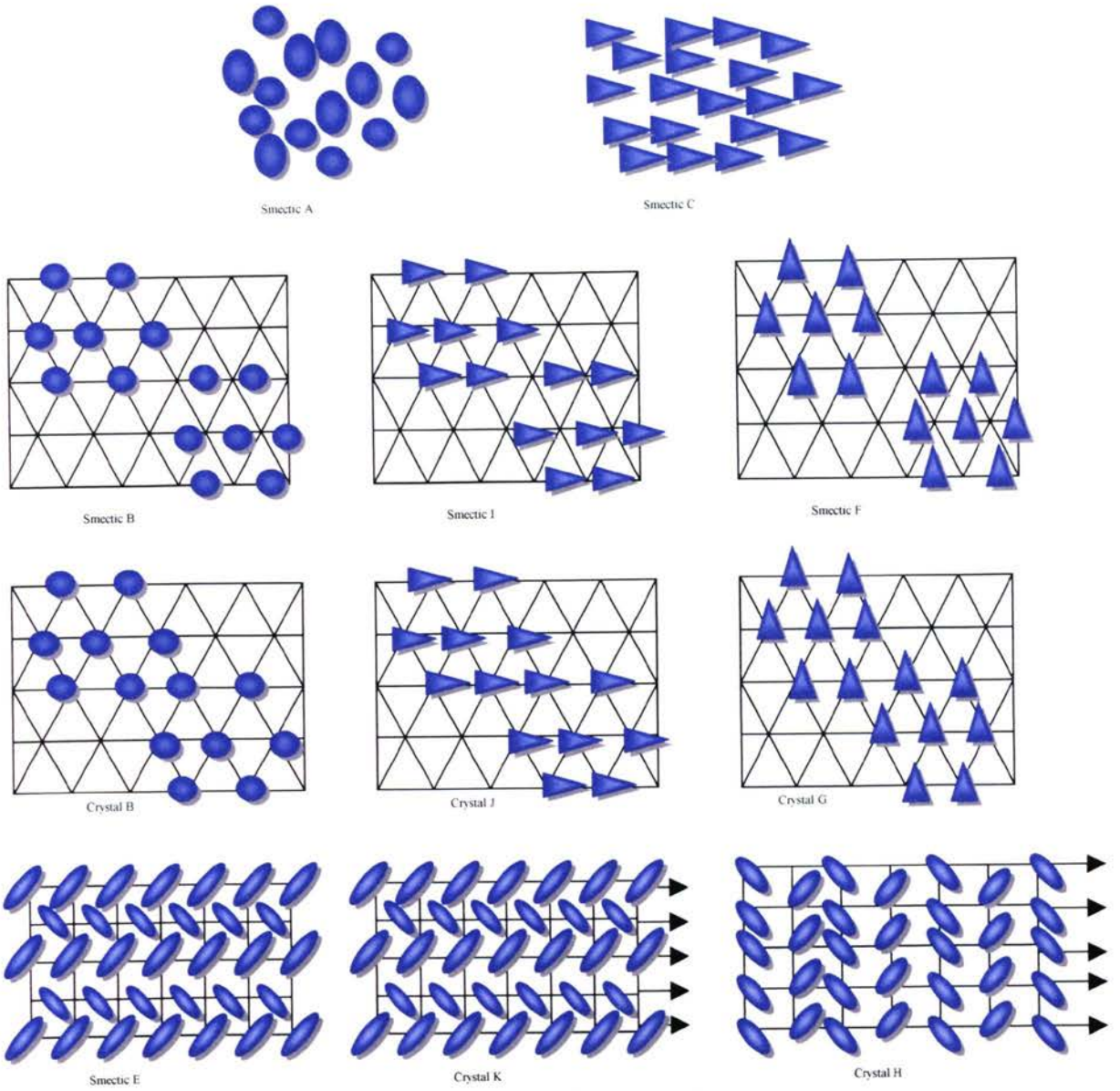

Figure I-15 Idealised plan view of smectic mesophase structures.

The constituent units of S_A are not tilted and they have no positional order within the layers. The smectic C (S_C) is the tilted analogue of the S_A phase. The smectic B phase is more ordered than the smectic A phase with the constituent molecules adopting a hexagonal ordering (bond orientational ordering) but the hexagonal lattices only have a repeat positional order over ~150-600Å. The hexagonal nature of the S_B phase generates two tilted analogues. They are called the smectic I (S_I) and the smectic F (S_F) phase, where the molecules are tilted such that the hexagonal lattice tilts toward the apex and the side respectively (the tilt direction is depicted by the direction of the

'triangular' molecules in Figure I-15). In the crystal B (B) phase the molecules are also hexagonally ordered but additionally the positions of the hexagonal lattice are predictable over a long range in 3-dimensions. The crystal E (E) phase develops from a contraction of the hexagonal lattice, which confers a herringbone-like structure with restricted rotation. The crystal J (J) and the crystal G (G) phases are tilted analogues of the B phase and the crystal K (K) and the crystal H (H) phases are the respective tilted analogues of the E phase; the tilt direction is shown by the arrows.

The other difficulty encountered comes from the fact that some phases form upon cooling another smectic phase. When a LC phase develops upon cooling an isotropic liquid or a nematic phase, it is said to be 'natural'. When the observed phase forms from the cooling of a higher temperature smectic phase, it is said to be paramorphotic.

I.1.4.3.1 1st group of smectic mesophases

The smectic phases found in this group are smectic A, smectic B, and crystal E. Smectic A and B are usually referred to as S_A and S_B. S_A possesses the least order and is the most common. It can typically be observed as two textures:

- The homeotropic texture, which appears isotropic and dark under crossed polarisers, due to the director being parallel to the light beam.
- The focal conic, recognisable by its fan-shaped needle regions that merge into a complete structure. This texture is illustrated in Figure I-16.

S_B and E differ by the greater order that exist within the layers. If S_A is present in a sequence of textures, it is always the first one to show itself upon cooling after isotropic and nematic.

I.1.4.3.2 2nd group of smectic mesophases

This group comprises all the smectic and crystal phases in which the director forms an angle with the layer plane that is different from 90°. Those phases are smectic C, the most common, smectic F, crystal G, crystal J, crystal H, crystal K. S_C can be compared to S_A, but the molecules within the layers exhibit a tilt with respect to the plane of the layer. As for S_A there is no specific order for the molecules within a layer. S_C can be formed paramorphotically from S_A, generally exhibiting a focal conic fan structure (illustrated as Figure I-17).

Since it is rarely observed, the D phase is not yet very well defined. The difficulty comes from the fact that D appears as a viscous isotropic phase easily mistaken for a liquid phase. The smectic C usually exhibits two natural textures: the focal conic (described previously), which is rarely seen, and the Schlieren. The Schlieren texture differs from the nematic texture by virtue of the fact that it is far less mobile and that it only consists of four brushes joined at a single point, giving it the appearance of a cross.

Although all the properties of a new liquid crystal compound cannot be completely predicted from first principles, certain rules can be used to predict the occurrence of liquid crystallinity [17].

I.1.5 Requirements for liquid crystallinity

As a general feature, calamitic (lath-like) liquid crystals show an elongated, narrow molecular framework [18], but other points also have to be considered. The strength and position of polar groups, the overall polarisability of the molecule and the presence of a

chiral centre [19] are amongst the factors that would affect the possible liquid crystalline behaviour of the molecule. To summarise, the molecule must contain a polar group and/or be highly polarisable. The terminal and lateral attractions between molecules maintain their parallel arrangement and determine the thermal stability of the nematic mesophase. In the case of a smectic mesophase, the attraction is only of the lateral type.

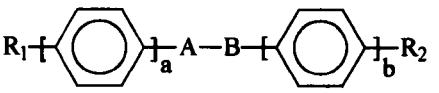

Figure I-18 Typical candidate molecule for liquid crystallinity

The figure above shows the most common type of molecule that would exhibit a nematic or smectic mesophase [20-21,22,23,24].

• a, b have small integral values.

• A-B is the linking unit in the core structure. It contains multiple bonds to maintain the rigidity and the linearity of the molecule. The most efficient one for a nematic liquid crystal is CH=CH (trans) followed by N=N-O, CH=N-O, C=C, N=N, CH=N, and COO.

• R1, R2 are terminal substituents such as alkyl, alkoxy or cyano groups. The efficiency of the different substituents has been quantified and found to be in the following sequence for the nematic mesophase[25]:

Ph > $NHCOCH_3$ > CN > OCH_3 > NO_2 > Cl > Br > $N(CH_3)_2$ > CH_3 > F > H

For the smectic mesophase, the order of efficiency is different[26]:

$NHCOCH_3$ > Ph > Br > Cl > F > $N(CH_3)_2$ > CH_3 > NO_2 > OCH_3 > CN

In both cases the highly polarisable groups Ph and $NHCOCH_3$ remain the most efficient.

After years of interest limited to the properties of single molecules for their liquid crystallinity, macromolecules are being studied. By following a similar route to that for simple molecules we can already predict the liquid crystal potential for some larger, more complex molecules, but there is still a lot of potential for improvement and new

discoveries. The compounds of main interest in this area are the ones comprising several repeat units: liquid crystal polymers.

I.2 Liquid Crystal Polymers

These polymers combine properties which are specific to polymers (such as strength and film-forming ability) with the anisotropic behaviour of liquid crystals, their optical and electrical properties have resulted in increasing theoretical and technological interest for the past couple of decades.

As the model for a liquid crystal is a semi-rigid, anisotropic molecule [27,28], the concept can be directly applied to polymers, considering that the monomer units of the polymer backbone contain the mesogenic group. Either thermotropic or lyotropic monomers could be used, and the monomer molecules could be attached in two different ways to form a macromolecule with mesogenic liquid crystal substituents :

- The mesogenic moieties are attached head to tail forming a liquid crystal main chain polymer.
- The mesogenic moieties are attached as side chains to the monomer units of the polymer backbone, to form a liquid crystal side chain polymer.

In both cases, a spacer chain (long or short) links the liquid crystal group to the polymer chain. The longer the spacer group, the more flexible, hence the more freedom of motion.

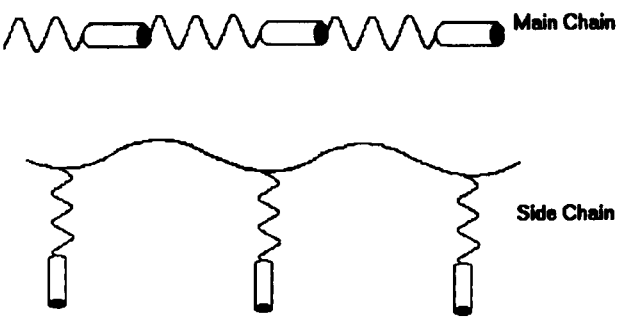

Figure 1.5.Main chain and side chain liquid crystal polymer

There are three main elements to be considered in a thermotropic liquid crystal side-chain polymer[29]:

- Polymer backbone (wide range of possible different chemical and physical properties).
- Mesogenic side chain (with lots of potential different constituents).
- Flexible spacer group.

A major question to take into consideration is whether the properties specific to the polymer are affected by the anisotropic state of the mesogenic side chain and vice versa. A polymer in its solid phase can be crystalline or amorphous, which means the molecules are arranged either in a regular or a random way, but have virtually no freedom of movement. The amorphous phase of the polymer is also said to be the 'glassy' phase and can co-exist with the crystalline phase over a quite large range of temperatures. A solid polymer, no matter if crystalline or glassy, will melt when heated, and if it melts to a liquid crystalline phase, it will be said to be a polymer liquid crystal. In principle, it appears easy to prepare liquid crystal side chain polymers. The main difficulty comes from the mesogenic group, since its self-arranging properties are opposed by the rigidity of the polymer backbone. In order to minimise this, several points have to be considered, amongst which is the nature of the spacer group. This has to be flexible, since for rigid ones, only an isotropic polymer melt is observed. Direct linkage of the mesogenic group to the main chain of the polymer thus results in a loss of liquid crystal properties as its motion is reduced. Large mesogenic groups are prevented from achieving parallel alignment because of strong steric hindrance, and often result in an increase in the glass transition temperature, indicating a stiffening of the polymer. The use of a flexible spacer group such as an alkyl or an alkoxy chain can help overcome these problems by allowing to a certain extent the decoupling of the motion

of the mesogenic group from the motion of the backbone. Although the polymer main chains tend to adopt a statistical distribution of chain conformations above Tg, the flexible spacer allows the anisotropic ordering of the mesogenic group to proceed.

The length of the spacer also influences the type of liquid crystal order of the side chain. The use of a long spacer gives the mesogenic groups enough freedom to adopt a more ordered structure, so that smectic phases only are obtained. If too short, the spacer does not allow motion and no anisotropic alignment is observed. The effect of this freedom of movement is the reason why liquid crystal polymers can be produced which exhibit nematic, smectic, or cholesteric mesophases, depending on their molecular structure. If we compare a mesogenic monomer with the corresponding polymer, two major changes would be noticed:

- increased tendency toward formation of smectic phase.
- increased liquid crystal phase transition temperature with increase in the degree of polymerisation.

The tendency to form smectic mesophases (illustrated in Figure I-19[c]) can be explained by the restrictions in both rotational and translational motion because of the connection to the polymer backbone[30].

Higher mobility is required to form a nematic mesophase as well as a flexible spacer, so that sufficient flexibility of the chain segments will be needed. The reduction of the free volume during the polymerisation process accounts for the observed increase in the liquid crystal transition temperatures.

I.3 Conducting polymers

Due to the fact that polymers (generally known as 'plastics') are supposed to be electrically insulating, it is difficult at first to imagine that some of them could conduct electricity with nearly the same efficiency as metals or semi-conductors. This may be the reason why scientists only came to this idea in the 60's. In 1960, when Kallman and Pope [31] first reported the possibility of an organic electrode after observing charge injection and conductance in anthracene, they were probably not aware of the increasing interest this discovery would start for materials with the important electronic and optical properties of semi-conductors together with the attractive mechanical properties and processing advantages of polymers[32].

Study of any polymer with a conjugated π-electron backbone would show that unusual electronic properties are displayed, such as low energy optical transition, low ionisation potential, and high electron affinities[33].

So in fact a whole class of polymers has to be considered which can be reduced or oxidised more easily and more reversibly than conventional polymers. Charge transfer agents (dopants) effect this oxidation or reduction, and in doing so convert an insulating polymer to a conducting material with near metallic conductivity in many cases. Two key developments can be pointed out in the early stages of conducting polymer research: First, the discovery of a synthetic route to free-standing high quality films of

polyacetylene (PA) in 1974[34]. Secondly, the discovery in 1977[35] that these films could be doped by electron donors or acceptors to conductivity levels (about 100 Scm^{-1}) approaching those of some metals.

A significant breakthrough was achieved in 1982[36] when it was discovered that poly(p-phenylene) could also be doped to high conductivity: polyacetylene was not unique any more, and shortly afterwards a number of new poly-aromatic conducting systems (including poly(p-phenylene sulphide), polypyrrole, polythiophene, and polyaniline) were added to the increasing list.

From the very beginning, the ultimate goal of research on conducting polymers has been to optimise the combination of electronic properties with processability, but there is no singular method for synthesising polymers that can be transformed into conductors. In designing polymer syntheses, extended π-electron conjugation must be incorporated. The monomeric starting materials therefore typically have an aromatic constitution that is preserved in the final backbone. Conjugation can also be achieved in a subsequent step that transforms the initial polymeric product into a conjugated polymer. Consistently polymerisation of acetylene yields the prototype of conjugated polymer (conjugated ethylene units), and polymerisation of benzene produces a chain of covalently linked aromatic units: poly(p-phenylene).

As represented in Figure I-20, a large class of conducting polymer candidates is constituted by polymers in which phenyl rings are incorporated in the backbone as repeat units of aniline (in polyaniline), phenol (poly(p-phenylene oxide)), thiophenol (poly(p-phenylene sulphide)) or simply phenylene (poly(p-phenylene)).

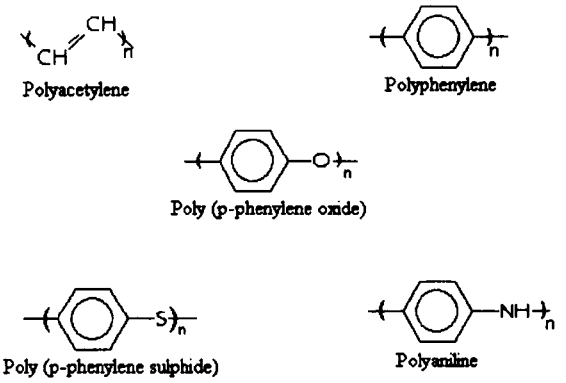

Figure I-20 Examples of electrically conductive polymers

The good environmental stability of polyaniline makes it of great interest as an electroactive (potentially conductive) polymer. The acid doped polymer is the precipitated product from an aqueous solution containing typically ammonium persulfate, hydrochloric acid and aniline. Amongst other variables the pH of the solution will affect the structure of the polymer backbone. A scheme of structures and corresponding names has been devised to describe these protonated, unprotonated, oxidised, and reduced forms. They are illustrated in Figure I-21. As can be seen in the centre of the figure, the normal representation of the polyaniline repeat unit takes into consideration the reduced and the oxidised forms.

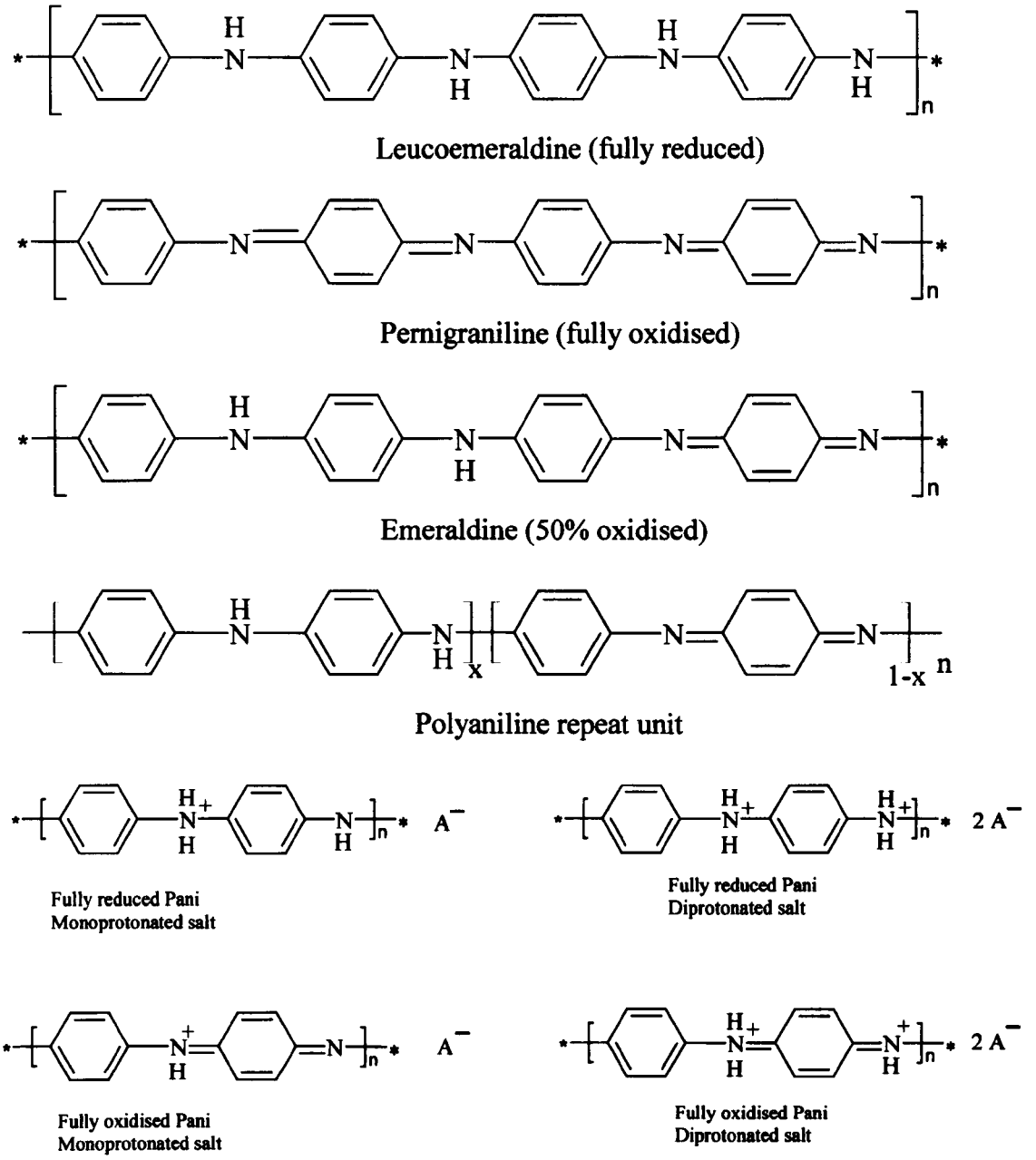

Figure I-21 The various forms of polyaniline (Pani)

Conjugated polymers, which can be made metallic by oxidation or reduction, are intrinsically semi-conductors; the occupied and the unoccupied molecular orbitals can, through intrachain covalent interactions, give rise to valence and conduction bands respectively, as illustrated in Figure I-22.

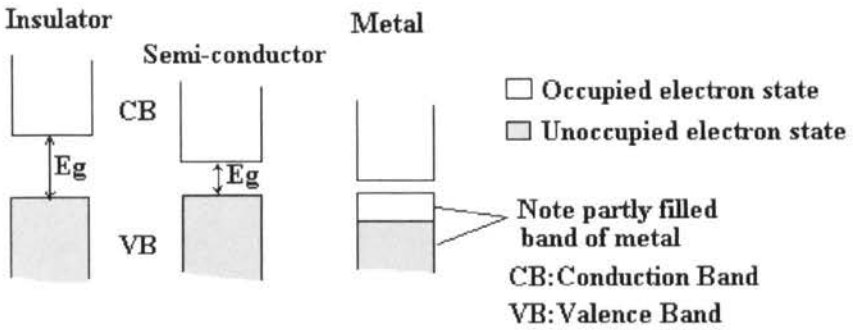

Figure I-22 Electron occupation of bands in different types of materials

These energy bands are the result of the bonding of thousands of atoms in the polymeric chains. The valence band involves pi-bonding orbitals, and the conduction band, pi-antibonding orbitals. The bands are separated by an energy gap, Eg, measured in electronVolts (eV). According to conventional band theory, as the value of Eg increases, the conductivity of the material decreases [30]. For a material to conduct electricity, the electrons must be able to 'jump' from the valence band to the conduction band. In insulators, the value of Eg is far too great for the electrons to cross, but a decrease in Eg to below 3eV yields semi-conducting material, where thermal excitation results in a few valence electrons passing to the conduction band. When Eg is small enough to become negligible, we have a metallic material, which is conducting without influence of the temperature. As shown above, in a metal the valence band is only partly filled: the highest occupied state within the valence band is called the Fermi Level, and electrons in or very near this level are the ones associated with conduction. For semiconductors a decrease in temperature implies there is less thermal energy available to promote electrons in the valence band across the energy gap to the conduction band, hence conductivity decreases.

However the physics of conducting polymers is very different from that of inorganic elemental and compound semiconductors such as Si or GaAs. In carbon backbone polymers, an added charge produces relatively large local changes in bond lengths, and

distinctive new energy states appear in the gap between the conduction and valence bands. In polyacetylene, a bond alternation reversal zone effectively forms an extended radical (known as a soliton in physics), which produces a mid gap energy state.

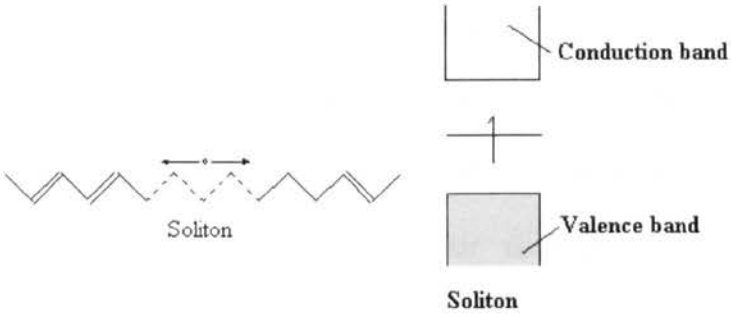

Figure I-23 Soliton in polyacetylene

This defect is mobile along a perfect chain ('delocalised') but may become pinned down by chemical defects in real chains.

In other polymers, added charges give rise to localised changes in bond alternation in the form of radical cations or dications (polarons and bipolarons respectively)[37].

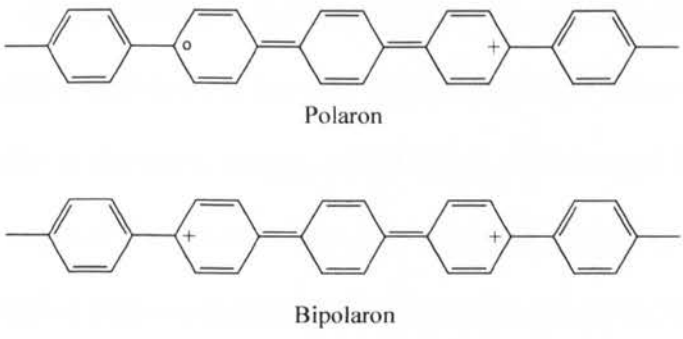

Figure I-24 Polaron and bi-polaron in polyphenylene

The best description of conjugated organic polymers in their pure (undoped) state is electrical insulators. The conductivities of polyacetylene (ranging from 10^{-9} Scm^{-1} for the cis isomer to 10^{-5} Scm^{-1} for the trans one) are detectable but are probably not intrinsic to the polymer, and so are best attributed to defects and impurities.

The conductivity, σ, is proportional to the product of the free-carrier concentration (n) and the carrier mobility (μ). $\sigma = e\ n\ \mu$, where e is the unit electronic charge (1.6×10^{-19} C).

For intrinsic conductivity, the carrier concentration decreases exponentially with increasing band gap. Conjugated polymers often have relatively large band gaps, which makes the concentration of free-carriers low at normal temperature, and hence, even though the backbone structure is suitable for conduction, there is negligible conductivity.

By doping the conjugated polymers, it is possible to generate high conductivities by increasing the carrier concentration[33]. Doping is achieved by oxidation or reduction with electron acceptors or donors. For example, if a polymer is oxidised by an acceptor's removal of an electron, it produces a radical cation (which can also be seen as a hole) in the chain. If the hole can overcome the coulombic binding energy to the acceptor anion with thermal energy or, at high dopant concentration via screening of the coulombic charge of the anion, it moves through the polymer and contributes to conductivity. Dopant concentrations are very high compared to those in inorganic semi-conductors (typically in the ppm range), and it is not unknown to find the dopant to represent 50% or more of the final weight of conducting polymer, making it more a charge transfer complex than a doped polymer. However, the term 'dopant' is accepted for common use.

By attaching a mesogenic side chain to the conducting polymer backbone, an improvement of the planarity of the backbone may result from the tendency of the liquid crystalline moieties to order themselves. If the planarity is increased, the charge carriers have more ease of motion and the overall result should be an increase in the conductivity. The problems of the choice of the polymer, of the side chain, and of attaching the side chain, to ensure that the resulting polymer will still be conducting are

all relevant to both previously described areas of investigation. In the past it has been often reported that the substitution of a conducting polymeric backbone often decreased or suppressed the original conductivity, and more importantly affected its glass transition temperature. In the meantime the liquid crystalline characteristics of a moiety can suffer from its being attached to a rigid polymer backbone which restrains its movement. Because the liquid crystal phase transition temperature needs to be higher than the glass transition of the polymer for it to exhibit itself, much thought has to be put into combining the right elements to create a 'working' combination. The right backbone will allow the glass transition to remain low enough while still remaining electrically conducting, a carefully chosen liquid crystal moiety will exhibit a liquid phase when attached to the backbone by a spacer of the right length so that the ordering effect may force some alignment of the polymer backbone.

I.4 Self-organisation of conducting polymers

As discussed earlier in this chapter, although conducting polymers can display high conductivity, it is still true that polymers in their natural state are generally reluctant conductors. Since the day of the discovery of the wide range of their potential applications, the quest for a better polymer has been pursued. As well as the structural requirements, there are many factors that influence the conductivity of a polymer. They include the concentration of charge carriers, the mobility of the electrons, and the width of the band gap. The task was thus set for researchers to minimise those factors that limit the conductivity. The following lists only a few of the means that were developed over the years.

Doping: Whether it is included within the polymerisation process or inflicted afterwards on the polymeric material, doping works by increasing the concentration of charge carriers.

Alignment: When it comes to long-range mobility, one of the main problems encountered is the fact that the polymer chains tend not to be organised, especially when cast from solution. However if we can force the backbone to be more planar, the mobility of the electrons along the chain will be improved. This problem can be addressed in two ways: externally or internally. In the case of an external intervention, the structure of the polymer remains untouched, but an outside action forces the chains to be more aligned. If the alignment factor is internal, the polymer structure will be modified to incorporate some new, useful properties. The external means of aligning polymer chains have been the most widely investigated, mainly because they apply not only to conducting polymers, and can be produced easily in industrial processing. Extrusion for example, which forces the polymeric material through a small orifice to form fibres, can lead to the organisation of polymer chains in many cases[1]. The fibres produced by this process show good strength, and in the case of liquid crystal polymers such as Kevlar the process is enough to promote the aligning properties of the liquid crystal moieties. This results in polymer fibres with a built-in ordering of the polymer molecules, and a material with increased strength. However, the scale on which extrusion is performed and the need for the polymer to form fibres does not make it an obvious candidate for expensive LCCPs.

Another route for research focuses on orienting the monomers before polymerisation. One way this can be achieved is by placing the monomers in a liquid crystalline matrix in which the polymerisation will be performed after the system has been oriented, using a magnetic or electric field, and then 'frozen' in place[38, 39, 40]. Another possibility would be to attach the monomer units to a fixed substrate, forcing the organisation before the polymerisation is carried out.

The alternative method, with an internal factor to induce organisation, requires the structure of the polymer to be modified. An organisation-inducing molecule, namely a

liquid crystal moiety is affixed to or incorporated inside the polymer backbone, transmitting its properties to the polymer. By doing so we can potentially produce an externally switchable system. However the original conductive ability of the polymer must not be lost from the addition, and consequently a side-chain substitution is a lot less invasive than a main-chain addition.

Side-chain substitution is the method we have been investigating in this project, and although the idea is still quite novel, it has already generated international interest.

I.5 Side Chain Liquid crystal conducting polymers.

As discussed in the previous section, the improvement of conductivity in organic materials relies heavily on increasing the planarity of the polymer backbone. Another aspect that needs to be addressed is the processability of such materials. Both of those properties have been improved successfully by attaching side groups to the conjugated backbone. Soluble 3-substituted polythiophenes for example have been synthesised[41]. But the route that appears most promising is the introduction of mesogens as those pendant groups to the benefit of their self-organising properties, and several research teams in the early 1990's started to develop this idea.

The first breakthrough came in 1988, when Tsibouklis *et al*[42] reported the polymerisation of diacetylenes exhibiting liquid crystalline behaviour. This communication was followed a year later by the work of another research team[43] on the preparation of liquid crystalline acetylene and diacetylene. No value of conductivity was published for any of those potentially conducting materials, but as they were only dimers of acetylene, it would probably have been almost as low as for simple acetylene molecules. Nevertheless they had shown that the synthesis could be done and in 1991 Bryce succeeded in electro-polymerising a thiophene bearing a side-chain mesogen[44]. This time, the polymer was reported to be conducting (15 mS cm^{-1} for a film), but the

only clue to a possible liquid crystalline behaviour was a reversible DSC peak at 58°C. The molar mass was not discussed in the publication. The same year another research team[45] published their results on the preparation of polyheptadiynes bearing liquid crystalline side chains using transition-metal catalysts for the cyclopolymerisation. For the first time there was a full account of observed liquid crystalline behaviour (smectic phase at 92°C, isotropic melt at 105°C), as well as the undoped and I_2-doped conductivity (6.3×10^{-11} S cm^{-1} and 10^{-2} S cm^{-1} respectively). The molar mass of the polymer was reported to be 10.5×10^4 $g.mol^{-1}$. The same research group carried on their investigation on this type of polymer and in 1993 published their results[46] on a polyheptadiyne bearing not just one but two identical mesogens on the same site. This new polymer exhibited a smectic phase over the temperature range 90-110°C. Its conductivity appeared to increase with temperature, from 10^{-16} S cm^{-1} at 50°C to around 5×10^{-10} S cm^{-1} at 150°C. Two inflection points were observed at the temperatures corresponding to the liquid crystalline transitions. Although no thermochromic behaviour was observed for the undoped material, indicating the thermal stability of the molecule conformation, electrochemical doping of the polymer led to the observation of different colour, from dark red (0V) to colourless (1V), and more intriguingly, to light blue (1.4V), which seemed to indicate not one but two doping states. The higher doping state was attributed to the biphenyl rings of the mesogenic moiety.

A communication[47] of the same year indicated that a polythiophene with mesogenic pendant groups was prepared using a Stille coupling reaction, yielding a thermally stable polymeric material that exhibited a nematic mesophase close to room temperature, with variations depending on the side-chain length, while the isotropic melt occurred about 200°C. 1993 also marked the first report by Langley *et al*[48] of a successful preparation of liquid crystal substituted polypyrrole, but the polymer did not exhibit any liquid crystal behaviour. The same year Awaji *et al* claimed in 3

patents[49,50,51] to have synthesised a variety of conducting oligomers and polymers derived from polythiophene and polypyrrole. Both types of monomer were polymerised and doped using $FeCl_3$, and exhibited a liquid crystalline mesophase (smectic for the polymers substituted with one pendant group per monomer unit, nematic for the polythiophene di-substituted on the same position) with all transitions reported to occur between 90°C and 100°C. A subsequent patent in 1994 by Koide reported the polymerisation of 3-substituted polythiophene and the resulting liquid crystalline and thermochromic material. Although both polymers would have made ideal candidates for conductivity, no investigation seems to have been made in that direction at the time, and there have been no subsequent publications of Awaji's or Koide's patented work.

While the main focus for the Japanese teams was on hetero-aromatic backbones, the research team of F. Vicentini was continuing work on acetylenic and di-acetylenic ones[52] as well as on pyrrole[53] based liquid crystalline polymers. For the first time there was a mention made of the resulting electrical anisotropy of the material when the oriented liquid crystalline monomer molecules were bulk-polymerised under the influence of a magnetic field. This was made possible by the fact the nematic mesophase of the monomers was thermally stable over a wide range of temperatures. The resulting polymers exhibited a smectic mesophase stable over a wide range of temperatures, and after doping with iodine a nematic phase also appeared. A conductimetric study of LC-substituted polyacetylene showed the conductivity of the amorphous undoped polymer increased from 10^{-11} S cm^{-1} to 5×10^{-8} S cm^{-1} after iodine doping. However when the polymer was oriented by heating it to isotropic melt and slowly cooling it in the mesophase while subjecting it to a magnetic field, the homeotropic orientation was 'frozen' when a temperature below glass transition was reached. The conductivity of the undoped polymer was increased to 10^{-9} S cm^{-1}, but no value was mentioned for doped material at the time. Their study of derivatives of

polypyrroles proved more successful in terms of conductivity, as the values obtained were in the 10^{-3}-10^{-2} S cm^{-1} range. When the oriented polymer was studied, the conductivity was measured both parallel and perpendicular to the direction of the mesogens. The value obtained for the perpendicular measurement was 10 times greater than that parallel to the direction of the liquid crystal moieties. This was in agreement with the expectation of unidirectional conductivity in the direction of the polymer chain (hence perpendicular to the pendant group).

Other research teams published papers on derivatives of polypyrrole and polythiophene at a similar time. While the paper by Thobie-Gautier[54] *et al* still addressed the substitution in the 3-position of thiophene, Ibison[2] *et al* as well as Melamed[55] *et al* chose to investigate the N-substitution of pyrrole with a mesogen. While the latter group failed to successfully produce a polymer from the mesogenic pyrrole monomer by electropolymerisation, Ibison *et al* at Kingston University prepared polymers electrochemically and chemically, and the product from the latter method exhibited a monotropic liquid crystal phase as well as being soluble in chloroform.

By 1995 the increased interest from Japanese teams had reverted to the derivatives of polyacetylene. Yoshino *et al* set out to investigate the optical and electrical properties of a substituted polyacetylene that exhibited the fan-shaped texture characteristic of a homogeneously aligned smectic A phase[56]. Measurement of the transmission of laser light as a function of temperature showed a drastic change at the transition temperatures, which corresponded to a change in the scattering properties of the sample. Values were obtained for the dielectric constant, but there was no mention of conductivity. However, when the polymer was mixed with a ferro-electric liquid crystal, a two-fold increase in the dielectric constant was observed at the transition temperature. An absorption spectrum was also recorded for polarised light with its electric component perpendicular and parallel to the director of the liquid crystals, and the perpendicular

absorption (parallel to polymer backbone) was much greater than that parallel. This indicated the absorption originated from the backbone, and although the observed band-gap was larger than that of polyacetylene despite the increased alignment, there may have been a twisting effect from the steric hindrance of the large liquid crystal substituents. In the meantime, Akagi *et al* were focussing on investigating the possibility of I_2-doping a liquid crystal substituted polyacetylene, as well as studying the stabilisation effect of using longer alkyl chains on the smectic A phase[57]. Their results suggested that the electron mobility in substituted polyacetylene might be lower than in non-substituted, accounting for the lower conductivity. The same group also investigated the possibility of inducing a greater alignment in similar polymers using shear stress and magnetic fields[58]. The shear stress resulted in the observation of a bâtonet texture of smectic phase aligned along the direction of the shear. The effect of the magnetic field was investigated using polymer melted on a substrate bearing a four-probe gold connection. The system was heated to the isotropic melt temperature then slowly cooled while being subjected to a 0.7T magnetic field until room temperature was reached. The alignment induced was found to remain frozen in at room temperature, and although the conductivity remained small, it showed a two-fold increase when measured parallel to the polymer backbone compared to that obtained parallel to the liquid crystal moieties. A further increase was observed after doping with iodine vapour, but the impact of the doping was found to depend on what catalyst had been used to induce the polymerisation, with Mo-based metathesis catalyst giving the largest increase (x70) upon doping. The UV-visible spectra of doped polymer revealed two new absorption bands at 420nm and 700nm which were associated with the creation of two new electronic transitions on positively charged segments of polyene. The resulting electrical anisotropies measured ranged from $2\text{-}10^5$, which seemed to indicate an increase in the coplanarity as well as a parallel alignment of the polymer chains.

Akagi *et al* also investigated the formation of mono-domains in LC substituted polyacetylenes[59]. The ^{13}CNMR study of monomers and polymers on the respective cooling cycles from the isotropic melt to the liquid crystal phase revealed that whereas the monomer exhibited a nematic liquid crystal phase, the polymer mesophase was of the more highly ordered smectic type. The observed difference in chemical shift was due to the liquid crystal side-chain and the monomer positioning themselves parallel to the magnetic field of the NMR apparatus. This resulted in the liquid crystal moieties being macroscopically aligned and forcing the polymer to adopt a structure where all the molecules in one domain are oriented along a unique director (referred to as a 'mono-domain').

Polyheptadiyne substituted with two identical moieties continued to generate interest, and Yoshino[60] investigated the effect of mixing the resulting polymer with a ferro-electric liquid crystal, but no ferro-electric behaviour was recorded. His attempt to electro-polymerise the monomer resulted however in the observation of a temperature dependency that only allowed the liquid crystalline monomer solution to undergo an oxidation-reduction cycle above 50°C. The diffusion of the BF_4^- dopant ions was found to be maximal between 80°C and 120°C which was almost identical to the limits of the liquid crystal phase, and this seemed to indicate the diffusion coefficient to be greater in the liquid crystal phase.

A Japanese patent[61] the same year reported the preparation of liquid crystal side-chain polythiophenes with molar mass ranging from 1,000 to 20,000 $g.mol^{-1}$ and exhibiting electrochromic properties, with the oligomers yielding a smectic mesophase.

Another research group prolific in the same area at the same time was Vicentini *et al*, with three papers in 1995[62,63,64] on derivatives of polyacetylene and polypyrrole. The main emphasis was made on the utilisation of the liquid crystal properties of the monomer units whilst polymerising them, and the effect of the end component of the

mesogenic moiety on these properties. Polyacetylene derivatives were polymerised using a catalytic bulk reaction with the monomer aligned by a magnetic field. The aligned samples showed an increase in the clearing temperature indicating, as expected, a greater organisation of the polymer. However most of the research was in fact focussed on β-substituted pyrrole derivatives, as they were stable to oxidation and - unlike acetylene based polymers- allowed for the preservation of the electronic transport after substitution. The use of a methylene link between the pyrrole ring and the carbonyl group in the mesogen prevented the decrease in conductivity that might occur through conjugation of electrons from the polymer backbone with the functional group. The polymerisation was carried out both in bulk using iodine and in solution with ferric chloride. Both methods gave soluble and fusible polymers of respectable molar mass. The effect of orientating the mesogen was investigated as part of the polymerisation process as well on the readily produced amorphous polymer via the application of a magnetic field to the cooling melt. Increase in the spacer length yielded an increase in the enantiotropic behaviour[62], where the phase stability (upper limit at which the liquid crystal phase exists) is higher than the melting point. The X-ray diffraction pattern (Figure I-25) also showed the characteristic condensation in two spots of an anisotropic material.

Figure I-25 X-ray diffraction of aligned PCBT

This indicated that the main-chain was in fact confined between two smectic layers, producing high order in the polymer. It also gave an indication of the spacing of the

layers, confirming the assumption that a monolayer is the length of the moiety in its most extended conformation. It emerged that the values obtained for both lengths of spacer did correspond to monolayers. These concepts will be further discussed in the 'Results and Discussion' section.

Further study[63] showed that for the polymer prepared in solution the ratio of ferric chloride to monomer had to be optimised to obtain processible liquid crystalline material of high enough molar mass, but with a doping level high enough for the conductivity to be satisfactory (note: no ratio was found to satisfy all conditions). Similarly for bulk polymerisation the molar mass was influenced by the temperature of the reaction. GPC analysis indicated the complete conversion of the monomer regardless of temperature, but when the polymerisation was carried out in the liquid crystal phase, the polydispersity of the molar mass was found to be very low, with the range of molar mass remaining the same throughout the LC range, and the polymers being completely fusible. Although the polymerisation happened more quickly at higher temperature with a much higher but more broadly distributed molar mass, the material produced was only partially fusible. This experiment indicated that the kinetics of polymerisation are influenced by the mesogenic order. The use of I_2 as a polymerisation medium yielded a polymer that did not require any purification other than removal of excess iodine using dynamic vacuum. Under UV-visible investigation, the final product was found to contain 1 I_3^- (absorption at 350nm) per 3 units of monomer, which corresponds to total doping. As a result, the conductivity of these samples was found to be higher than those produced from solution. However, whereas the polymerisation medium influenced the conductivity and the ability to form a liquid crystal phase of the polymer, the nature of the phase produced was derived from the molecule itself, with the spacer playing an important role in the transmission of the mesogenic properties to the polymer backbone. The conformation of the polymer chain

was studied in order to verify the efficiency of the coupling between the main chain and the mesogen, by small-angle neutron scattering on a 50% deuterated-spacer polymer mixture. The result was that in the case of the polymer prepared from solution, the smectic monomer yielded a polymer exhibiting not one but two smectic phases, with the lower temperature one appearing to be partially bi-layered, and the higher temperature one being completely monolayered. The main chain exhibited a preferred direction (hence an anisotropic behaviour of the material), and the results also showed that the polymer and the moiety had arranged themselves in distinct layers, with the polymer being completely excluded from the layers of moiety and vice-versa. This arrangement is illustrated in Figure I-26.

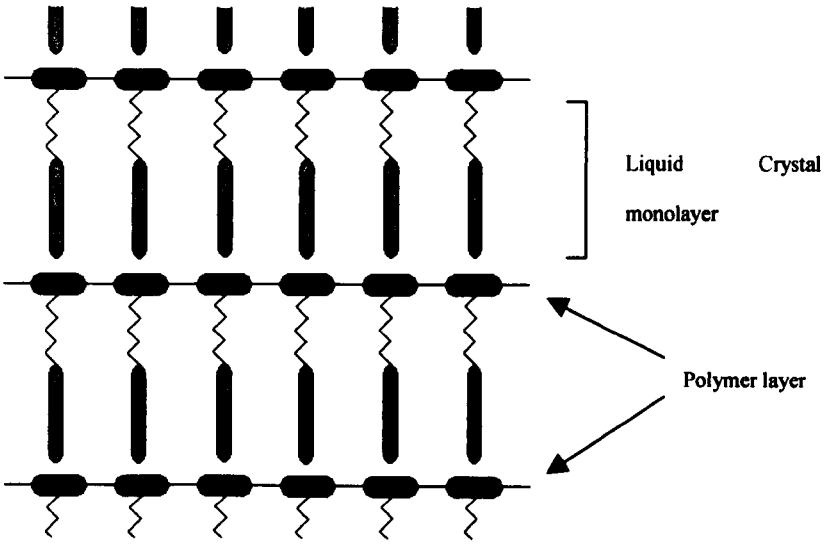

Figure I-26 Suggested layer arrangement in aligned side-chain liquid crystal polymer

At low frequency, high ⊥ / // anisotropy (values as high as 6 were reported) was observed, and the conductivity perpendicular to the axis of the mesogens in smectic planes was much greater than that in the parallel direction.

In 1996 Akagi *et al* were refining even more their studies of polyacetylenes[65]. By using miscibility tests to assess the true nature of the liquid crystal phase of the monomer and the polymer and confirming the results with DSC and polarising optical microscopy,

they found that although all the acetylene based monomers gave nematic phases, the resulting polymers were all smectic A. The investigation of polymers prepared using different catalysts revealed an influence of the catalytic agent on the size and the thermal stability of the domains, Mo-based catalysts giving more satisfactory results than Fe-based catalysts. However UV-visible study of the same polymers showed that the conjugation length in the polyene was shorter in the Mo prepared polymer, the absorption band being at shorter wavelength. Moreover, in the liquid crystal domain of the Fe prepared polymer, the absorption wavelength was 70nm greater than the wavelength observed for the initial solution, indicating that there was a spontaneous orientation of the liquid crystal side chain leading to alignment of the polymer backbone. This resulted in longer conjugation lengths in the domains due to coplanarity. An ESR investigation confirmed the findings of their 1995 paper that the mobility of electrons was lower for substituted polyacetylene than for un-substituted, but also that the concentration of carriers was lower, both accounting for the decrease in conductivity.

1996 also saw the first successful preparation of a conducting liquid crystal side-chain polyaniline (monomer of which is illustrated in Figure I-27), by Gabaston *et al* at Kingston University[66]. The ortho-substituted monomers were prepared through the hydrogenation of more stable nitrobenzenes. A variety of alkyl spacer lengths was produced, and revealed strong odd-even effects on the transition temperatures of the nitrobenzene molecules when investigated using DSC and hot-stage polarising optical microscopy. Whereas the molecules possessing an even number of methylene groups in the spacer exhibited a homeotropic Schlieren liquid crystal texture above room temperature, the ones with an odd number did not! The monomers with even spacers were hydrogenated and the resulting monomers were also found to have liquid crystal properties. The use of a Brönsted acid medium ensured that the polymer would be

regio-specific head-to-tail and partially protonated, with the assistance of a surfactant (DBSA) to allow the dispersion of the chloroform based monomer solution in acid. Although many mesogenic side groups were investigated to obtain liquid crystal behaviour above Tg, only two of the polymers did in fact exhibit a Schlieren texture under mechanical stress as well as an increase of the conductivity with temperature (despite a thermal limitation due to loss of protonation at 130°C).

Figure I-27 Liquid crystalline 1- [(aniline-2-yl) oxy]-6-[(4'-biphenylcarboxylic acid-4-yl)oxy] hexane

The conductivity values found ranged from 10^{-5}-10^{-3} Scm^{-1}, but the band gap remained

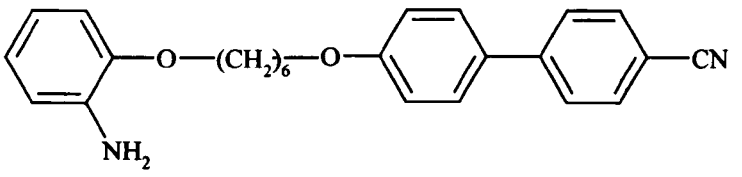

large at 3.3eV, which was attributed to the fact that the bulky mesogens forced a twist in the backbone because of steric hindrance.

The research team led by Akagi decided to try and improve the properties of derivatives of polyacetylene by introducing for the first time a ferro-electric liquid crystal as the side-chain[67]. Because of the ability of such molecules to produce spontaneous polarisation, the resulting material was expected to display a much greater susceptibility to an electric field than a normal liquid crystal would, as well as a very fast response time. Ferro-electric properties however require a non-zero dipole perpendicular to the molecular long axis, best represented by a smectic C phase. Because of the use of carbonyl containing moieties, the choice of catalyst also had to be carefully considered. Consequently, only the polymer (S)-(-)-PBP9*003A prepared using the molybdenum based catalyst (illustrated in Figure I-28) exhibited a smectic C phase as well as a smectic A, with a high molar mass (45,000 $g.mol^{-1}$).

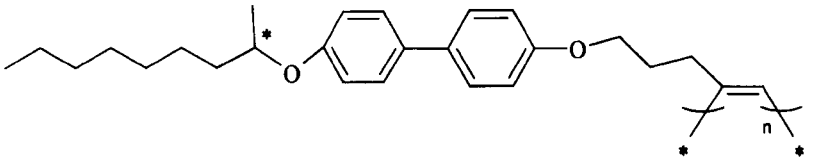

Figure I-28 (S)-(-)-PBP9*003A (Mo)

The circular dichroism spectrum indicated that the laevorotatory configuration was retained in the polymer. The S_C^* phase range was found to be very narrow (95-100°C). The observed texture at 96°C was striated fan-shaped, which enabled one to estimate the helical pitch of the ferroelectric liquid crystal phase, itself correlated to the helical pitch of the polymer. This was found to be about 10μm, which is three to five times larger than that of the typical ferroelectric liquid crystal.

A new route to LC conducting polymers was also opened in 1997 when Goto *et al* reported the preparation of methine bridged polymers (Figure I-29) with alternate aromatic and quinoid units to produce small band-gap LC conducting polymers[68].

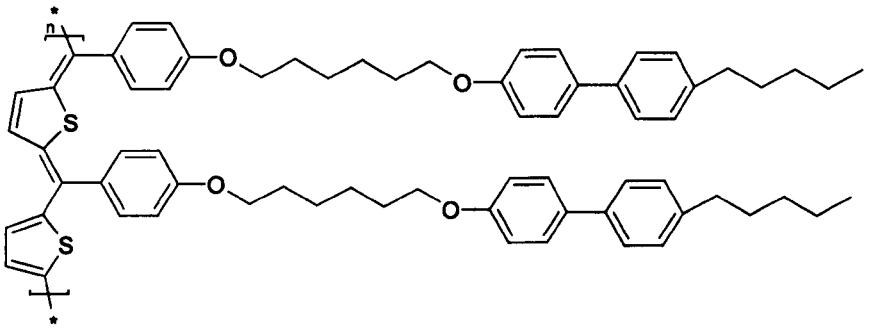

Figure I-29 Example of methyne bridged side-chain liquid crystal polymer

The pendant LC group was placed on the methine unit, and the polymerisation derived from the coupling reaction between an arylene (either a pyrrole or a thiophene) and a liquid crystal aldehyde. The protonation during polymerisation was complete yielding a conjugated methine bridged sequence. All but one polymer was fusible and soluble as well as exhibiting a S_E or S_A smectic mesophase. The band-gap for the polymer was

found to be as low as 1.45eV, and the best combination (illustrated in Figure I-29) was found to incorporate a longer liquid crystal side chain and the use of a benzene ring instead of the usual alkyl chain to link the mesogen to the main chain. This seemed to instigate an intra-molecular electron resonance interaction between the main chain and the phenyl moiety in the liquid crystal group. This phenomenon was probably responsible for a shorter effective conjugation length yielding the modest conductivity observed (10^{-6} Scm^{-1} undoped, 10^{-4} Scm^{-1} I_2 doped).

In 1998, Kijima *et al* decided to focus on the use of an N-substituted pyrrole to avoid the irregular linkage of the polymer[69]. The monomers were prepared not from pyrrole but from 6-(1-pyrrolyl)hexanol. The liquid crystal moieties were prepared separately and studied as model compounds. All the monomers and model compounds were observed to be liquid crystalline, and were all found to exhibit either a nematic or smectic mesophase, with the transition temperature depending on the mesogenic core: ketobiphenyl>cyanobiphenyl>cyclohexylbenzene. The polymers were prepared chemically and electrochemically, and had a good processability and average molar mass (2,600-10,300 $g.mol^{-1}$). Unfortunately the CV suggested the possible occurrence of coupling between the pyrrole moiety and the mesogen leading to irregularity in the polymer structure. The ring bending observed in the monomer by infrared spectroscopy was found to disappear after polymerisation. The conclusion of those observations was that a high degree of order in the monomer does not automatically yield a liquid crystal polymer, and the mesogenic core is in fact what determines the stability of the mesophase. For a conducting polymer to be produced there has to be a rigid backbone and a flexible spacer, to produce a weak Van der Waals interaction. In the case of a smectic mesophase, the polymer chains are orientated parallel to one another, making it an ideal candidate for electrical anisotropy. However the poor fluidity of the resulting system makes it unsuitable for magnetic field alignment to a monodomain.

The potential and technique for alignment of liquid crystal N-substituted polypyrrole, and of polythiophenes and polyanilines, was to be drastically changed by Foot *et al*, when they published a patent describing a totally novel way to locally align films of liquid crystal polymers[70]. The use of a focussed laser beam to locally melt films of carefully selected polymers led to anisotropy and great improvement in the conductivity (over 60,000 times) without the external influence of a magnetic or electric field. Furthermore, the resulting patterns could be easily wiped out and re-written repeatedly without any major loss in the polymer properties. The same research group joined forces with the University of Surrey to help validate the first report of a theoretical study of liquid crystal polypyrrole by molecular modelling of substituted pyrrole monomers and polymers using Cerius® and comparing the predicted results with the corresponding experimental data[71]. Although no indication was obtained for the prediction of liquid crystallinity, the models showed that the Tg of the polymers could be simulated with success by modelling the influence of the temperature on the density of the unit cell. An optimal conformation could be predicted, as well as physical properties.

It was not until 1999 that the production of a nematic phase for the polymers was investigated. Percec *et al* set out to study the mechanism of formation of liquid crystal phases[72]. Their paper described a novel approach to the problem since they suggested that it is the backbone that dictates the ability to yield a nematic mesophase, and not the mesogenic group. By using a rigid rod-like backbone such as poly-p-phenylene, with a side chain based on cyanobiphenyloxy and an alkyl spacer of various lengths, it was found that all the generated polymers produced an enantiotropic nematic phase over a wide range of temperatures. This was attributed to the fact the backbone was not distorted by the addition of the mesogen.

As research progressed, more and more backbones were considered as possible skeletons for liquid crystal conducting polymers, in the quest for the perfect combination of properties. One of the latest backbones to be considered was poly(isothianaphthene methines) with liquid crystal substituents. Kiebooms *et al* first reported work on those in 2001[73]. The use of this greatly conjugated backbone arose from the desire to lower the band-gap and to stabilise the system through the phenyl moiety in the mesogen. A polycondensation reaction produced polymers of the type pictured in Figure I-30 with a low band-gap around 1.2-1.3eV.

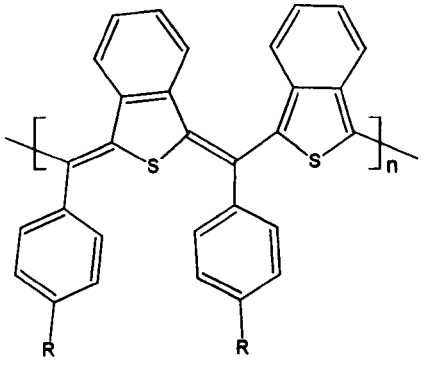

Figure I-30 Example of poly(isothianaphthene methines) with liquid crystal substituents

The conductivity increased from 10^{-8} to 10^{-4} Scm^{-1} after doping, however, no LC texture was observed under optical microscope, despite an obvious transition being observable by DSC.

Dai *et al* set out to improve even more on the concept of chiral liquid crystal side chains by using a fluorine containing one[74]. They expected that the 3-substitution of a polythiophene would allow the control of the properties via the orientation of the liquid crystal, with the ferroelectric LC producing a faster response. The result was the production of high molar mass (13,000-55,000 $g.mol^{-1}$) soluble polymers displaying liquid crystallinity. Only one of the three polymers produced exhibited a S_C^* mesophase, and its ferroelectric behaviour was confirmed by investigating the temperature dependence of the dielectric constant. Meanwhile Abe *et al* were

establishing a correlation between the polarity of the side-chain, hence the dipole moment, and the domain size for N-substituted polypyrroles[75]. A series of polymers was produced, all exhibiting a smectic mesophase. In order to lower the transition temperature, side-chains with intrinsic nematic properties were introduced, and a longer spacer group was used to increase the mobility of the side-chain. The result was the formation of larger domains, and/or the formation and stabilisation of a highly ordered smectic phase.

A further step was taken in the study of liquid crystal conducting polymers with the report from Osaka *et al* on 3-substituted polythiophenes and polythienylenevinylenes bearing liquid crystal side-chains[76]. Not only did the resulting polymers exhibit a smectic A (S_A) mesophase, they were also found to be fluorescent, and susceptible to alignment using a magnetic field. The fluorescence was found to be polarised, with a dichroic ratio after magnetic field alignment of 3.8. The fluorescence was greater parallel to the chain (perpendicular to liquid crystal side chain and direction of field). The electrical anisotropy was found to be as high as 8 despite the conductivity only being $10^{-6}/10^{-5}$ Scm^{-1}. A new type of material with linearly polarised fluorescence and electrical conductivity had been produced, opening a whole new range of possible applications.

I.6 The Project

Among the polymers with potential conductivity, the ones involving the presence of hetero-atoms in their backbone now have an established place. The nitrogen based aromatics, such as anilines and pyrroles[2, 77, 78, 79,80] as well as carbazoles, with their good stability and conductivity, combined with a high processability, represent a major field of interest.

Even though polypyrrole had been prepared in 1916[81], it was only in 1979 that its electrical properties were discovered, and it became of great interest for electrochemists. Polymers formed from substituted pyrroles have been widely studied, but almost all of the molecules considered had the substituent in the 3 position, leading to non-symmetrical monomers. These are therefore said to have a head (H) and a tail (T). When the polymerisation occurs under normal conditions, and considering the polymerisation to occur only between positions 2 and 5 (Figure I-31–b), the connections between the molecules seem to happen somewhat randomly, as a mixture of HH, HT, TH, and TT is formed[82,83]. As any linkage other than HT decreases the planarity of the molecule by creating twists or kinks in the backbone, it decreases the conductivity of the polymer. The bulkier the substituent, the less π-orbital overlap there is, and hence the greater the loss in conductivity. Some studies have shown that backbones consisting of nearly exclusive HT linkages can be produced from 3-substituted thiophenes brominated in positions 2 and 5, but only hydrocarbon side chains can be used, reducing their potential applications[84]. N-substituted pyrroles and their polymers may prove to be far more versatile, as the equivalence of their head and tail positions makes the monomers symmetrical. Polymerisation of these leads to nearly strict HT connections (provided that only 2-5 linkage occurs), and hence to a more planar backbone, as the side chains are unlikely to overlap.

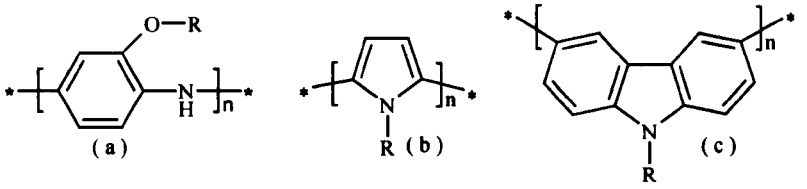

Figure I-31 Preferred polymerisation sites for the polymer backbones used in the project.

Aniline on the other hand offers different properties because of its six-membered ring structure. Polymerisation will usually occur between positions 1 (N) and 4 (Figure I-31-a), and to favour these connections the molecule is substituted in its ortho-position [29], yielding a fairly linear backbone.

Carbazole shows properties quite similar to those of pyrrole but as a fused ring system its application as a conducting polymer has only been investigated recently[85, 86, 87]. When N-substituted, the carbazole monomer tends to favour polymerisation on the meta-site of the benzene rings (Figure I-31-c). As a stable conjugated system with a regular polymerisation pattern it makes an excellent candidate to be a conducting polymer.

The main concern with conductive polymers consists of making the most of their properties, and the optimum planarity for their backbone is thus necessary to promote the conductivity. Even though the (idealised) backbones of all three types of polymer show a reasonably good planarity, any improvement in this property (and the conjugation length) would increase the electron mobility, and thus improve the conductivity. Several methods have been considered so far, but introducing within the monomer structure an element that would increase the planarity of the polymer seems the most promising, as the alignment could then occur at the same time as the polymerisation with no need for extra equipment or manipulation.

Liquid crystals have a great tendency for organisation and the idea was to use this property to promote self-alignment of the molecules within the polymer backbone.

Liquid crystalline units were thus used as substituents in this project, in the hope that by ordering themselves in a planar pattern they would induce a more linear backbone. The conductivity of the produced polymer might then be improved by the use of laser alignment or by the application of electric or magnetic fields at the appropriate transition temperature.

As mentioned in the earlier parts of this chapter, research on liquid crystal conducting polymers has only grown in the past few years. Therefore at the start of this project the idea was novel and not very well understood. The project set out to study possible ways to improve (or control) the conductivity of conducting polymers through an improvement of the planarity of the backbone. The backbones of aniline and pyrrole were originally chosen, as some previous work had shown them to be good candidates with the properties we were trying to develop [2, 66, 70]. The carbazole backbone was added to the list, as it appeared to have a similar potential for conductivity with the advantage of stabilisation of the charge through delocalisation on the aromatic rings, while still being based around a nitrogen heterocycle. Similarly, liquid crystal moieties were chosen that had successfully led to polymer alignment in previous work[2, 66, 70].

The first step was to be the synthesis of monomers that could be polymerised. Model molecules were first to be used to optimise the synthetic route before working with liquid crystal substituted molecules. These would be based on *o*-substituted anilines, N-substituted pyrroles and N-substituted carbazoles. Once the monomers had been prepared and characterised, the model monomers were to be used to optimise the polymerisation route, by trying a variety of both oxidative chemical polymerisation routes and electropolymerisation. The resulting polymers were to be characterised and their electronic properties were studied in various conditions. The novel method of 'laser alignment'[70] would finally be used on the sample that was to be found most suitable and the resulting change in the properties studied by polarised optical

microscopy, electrical measurements and X-ray diffraction. More details on this method and the results can be found in section III.8. To help predict and better understand the various properties of the monomers and polymers it was planned to use molecular modelling. The details and results of the modelling work can be found in section II.5 and from section III.2 onwards.

Summary of the aims of the project:

- Selection of suitable backbones and liquid crystal moieties.
- Preparation and characterisation of novel liquid crystalline monomers suitable as candidates to yield conducting polymers
- Preparation and characterisation of polymers using chemical and electrochemical methods
- Optical microscopic study of the liquid crystal phases for monomers and polymer under cross-polarised light.
- Study of the effects of laser alignment on the microscopic conductivity of a film of liquid crystal conducting polymer.
- Investigation of the conducting properties of the aligned and un-aligned polymeric materials under various conditions
- Investigation of the anisotropy of the aligned material using optical microscopy (cross-polarised light) and X-ray diffraction.
- Computer assisted modelling of various properties to investigate the mechanisms of alignment and the effects of structural changes on the properties of the molecules.

II EXPERIMENTAL

II.1 General procedures and instrumentation

II.1.1 Solvents and Chemicals

The chemicals that were used for the completion of this project were obtained from Aldrich, Avocado or Merck, unless stated differently. The solvents required for reactions as well as purifications were generally used as supplied.

II.1.2 Analysis Techniques

II.1.2.1 Chromatography:

Thin layer chromatography was carried out using silica gel (mesh 60) on a PET plastic substrate. After eluting with the appropriate mixture of solvents, the plates were looked at under UV light, both long (365nm) and short wave (254nm).

Flash column chromatography was performed using silica gel of grade 60-80 mesh.

II.1.2.2 Spectroscopy

Infrared spectra were obtained using a Perkin Elmer Paragon 1000 Fourier Transform Infrared Spectrophotometer. Samples were analysed as pressed pellets (where the sample was mixed with KBr), or on NaCl windows as thin films cast from solution, or as nujol mull.

Proton nuclear magnetic resonance (^{1}H NMR) spectra were recorded on a Bruker AC-300F Fourier transform magnetic resonance spectrometer. The frequency used was 300 MHz. The machine was also used at variable temperature (variable temperature unit Bruker VT1000) to allow for the observation of polymerisation in situ. The tubes used for variable temperature work were thick wall tubes (5mm, Fluorochem).

Mass spectra were obtained using a VG Trio 2 Quadrupole mass spectrometer. The mass range available was m/e40-2000 and the source temperature was set at 150°C.

Ultra-violet/visible spectra were recorded using a Kontron Uvikon 940 UV/VIS. spectrophotometer. The solvent used for most samples was chloroform, which gave a cut-off wavelength of 250nm. The spectra were typically run between 200nm and 900nm.

II.1.3 Determination of Transition Temperatures

II.1.3.1 Differential Scanning Calorimetry

Glass transition temperatures and liquid crystal transitions were recorded by differential scanning calorimetry (DSC) using a Mettler DSC 25 together with the software STARe for analysis. The reference was an empty aluminium pan of the same type as the one holding the sample (40μl).

In this technique the sample and an inert reference are heated separately. The power supply to the sample heater is variable so that the temperature difference can be maintained at zero even when exothermic or endothermic changes occur. The difference in power supplied to the two heaters is monitored as the analytical signal ΔE. On the graph any exothermic change shows as an upward peak, and any endothermic

change shows as a downward peak. The sample needs to be homogeneous (usually finely powdered) to ensure an even distribution of the heat. The experiments were carried out in air or under nitrogen flow. In the latter case, all oxidation peaks are removed, and only the thermal transitions of the material are seen. This technique provides information about the transition temperatures characteristic to the sample, such as melting, vaporising or liquid crystalline transition, or degradation, as well as any other phenomena requiring or expending energy.

II.1.3.2 Hot Stage Microscopy

Liquid crystal transition temperatures and textures were observed using a heating stage (Linkam THMS-600) fitted onto a polarising microscope (Nikon Optiphot-2). The set-up also included a colour video camera (JVC TK-1085E) and a colour video monitor (TM-1500PS), as well as a control unit (Linkam) comprising a cooling system (CS 196), a display and keyboard (TMS 91) and a video-text overlay (VTO 232).

II.1.3.3 Microscopy using cross-polarised light

The facilities used for the observation of the laser aligned samples prepared at Kingston University (see further) were those of School of Earth Science and Geography. The equipment used included a Leitz microscope with a LinkSystem image acquisition and analysis system.

II.1.4 Elemental analysis

Some of the samples produced were sent away for elemental analysis*. The technique allows one to quantify the amounts of various elements present in a sample from the

* MEDAC Ltd, Brunel Science Center

gaseous products of its thermal degradation. The samples were sent for bromine analysis when appropriate as well as for the usual C, H, N, O analysis. Results are discussed in the Results and Discussion section.

II.1.5 Other techniques

II.1.5.1 Cyclic voltammetry

The cyclic voltammetry experiments were carried out using an electrochemical workstation (BioAnalytical systems 100B/W). The conditions for each experiment are described in chapter II.3.4.

II.1.5.2 Conductivity measurements

II.1.5.2.1 General features

The samples were used in different forms: as film cast from solvent on microscope glass cover slip; as free standing film fixed on glass substrate with double-sided tape; and as film cast from solvent on commercial four probe conductivity cells (AU MB4000 and PT MB4000 both supplied by Windsor Scientific Ltd). The substrates consist of an oxidised Si substrate, with 4-in-line gold or platinum electrodes deposited photolithographically so that the gap between the electrodes is 10μm. A diagram of the conductivity cell is illustrated in Figure II-1.

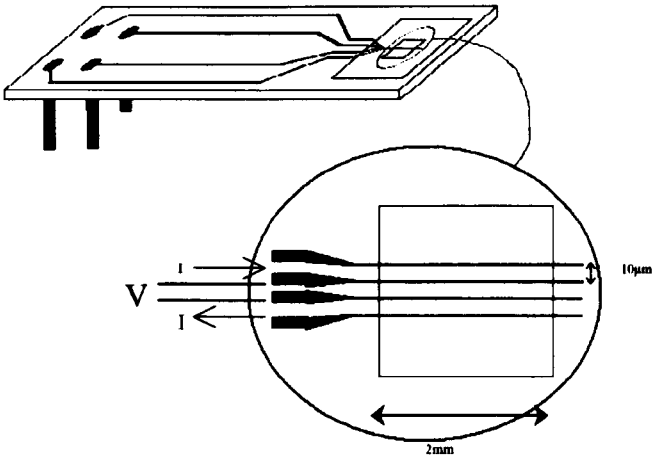

Figure II-1 Representation of a commercial substrate for conductivity measurements

The polymer film was cast over the platinum lines, which are 10μm apart. The current was applied between the two external lines, and the voltage measured between the two inner lines. The conductivity was obtained from the measured current (I) and voltage (V) using the following equation: σ=current density (Am^{-2})/electric field (Vm^{-1}) or $\sigma = \frac{I/A}{V/\ell}$ where A is the cross sectional area of the film (in this case, thickness (d, typically about $10x10^{-6}$m) x $2x10^{-3}$ m^2), and ℓ the distance between two electrodes ($10x10^{-6}$m). Since V/I is in fact the apparent resistance (Ω) that can be obtained as the slope from the plot of I vs V, the conductivity was obtained as $\sigma = \frac{A}{slope.\ell}$ in Sm^{-1}.

Conductivity measurements for undoped and doped samples were obtained using a programmable electrometer (Keithley 617) and a programmable current source (Keithley 224). A computer allowed for control of the set-up through a custom-designed software (Keith4, written in Turbo-Pascal language by Dr. Pete Spearman).

II.1.5.2.2 Measurement of conductivity as a function of temperature.

The thin film of deprotonated poly-2-methoxyaniline was produced by rotary evaporation of the chloroform solution. The 1 cm^2 square piece was stuck to a glass slide to allow the contacts to be put into place using silver dag. The device was placed on an electronically controlled Linkam hot stage and the temperature was increased stepwise, allowing for 5 minutes stabilisation of the temperature reading before a conductivity measurement was recorded using the same set of Keithley equipment as mentioned before.

Although different techniques were used, the principle remained the same: a known current was applied to the sample and the resulting voltage measured. The value of the resistance R (Ω) was obtained from the formula V=R I.

Van der Pauw's method using a four probe system yields a value of the resistivity of the polymer, which takes into account the thickness of the sample, but is independent of the distance between the contacts. In this method, the sample bears four contacts consisting of fine copper wires fixed to the sample using silver paint. The current is passed through an adjacent pair of contacts while the voltage is measured between the other two contacts.

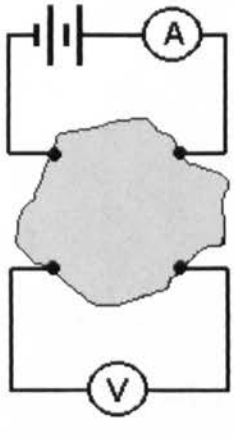

Figure II-2 Illustration of the typical set-up for four-probe measurement

Measurements were taken for different values of the current so that the slope of the plot of voltage versus current was obtained. The resistance value obtained using this method was then used in the following formula to calculate the resistivity of the sample.

In the formula $\rho = \frac{tR\pi}{\ln 2}$ ρ is the resistivity (Ωcm), t is the thickness of the sample (cm) and R is the resistance (Ω). The conductivities (Scm^{-1}) were easily obtained, being the inverse of the resistivity σ(Ωcm), with $\sigma = \frac{1}{\rho}$.

In the case of the two-probe measurements, in which the current and the voltage were going through the same contact points the shape of the sample had to be taken in consideration. The resistivity was obtained from the equation $\rho = \frac{RA}{\ell}$ where A (cm^2) is the area of the cross section of the sample and ℓ (cm) the distance between the contacts.

II.1.5.3 Laser alignment

The original laser experiments were performed using the purpose-designed facilities kindly provided by Greenwich University.

The experiments were later successfully repeated at Kingston University using a He-Ne laser (20mW), dampened with a 60% filter. The beam was focussed using a microscope lens of focal length 0.4 mm, and the scanning was achieved by moving the sample in the beam using an X-Y translation stage.

II.1.5.4 Molecular modelling

Molecular modelling work was carried out at Kingston University using Quantum CAChe 3.2. Further details of the procedure will be provided in the following chapter.

II.1.5.5 Hydrogenator

A hydrogenator, also referred to as a rocking autoclave (Chas. W. Cook & Sons Ltd) was used to perform the hydrogenation for compounds under pressure. The apparatus allowed for pressures up to 500 psi (pound per square inch; 14 psi =1bar) and temperatures up to 300°C. The reaction vessel was made of glass and the metal casing of the temperature probe was glass-coated to prevent the contamination of the metal by mixed catalysts.

II.2 Synthesis and characterisation of monomers

II.2.1 N-propyl carbazole [88, 89]

Into a round bottom flask was added in order: carbazole (2.00 g, 11.96×10^{-3}mol), acetone (20ml), 66% potassium hydroxide aqueous solution (2ml), and 1-n-bromopropane (3.03 g, 2.47×10^{-3}mol). The reaction mixture was refluxed for 12 hours, and then poured into water (50ml). A light brown paste was obtained, which solidified upon cooling with ice. After filtration, the crude product was recrystallised (0.78 g, 3.73×10^{-3}mol) from methylated spirit. Since the solubility of both starting material and product are very similar, the product mixture was purified using flash chromatography, eluting with ethyl acetate and petroleum spirit (1:4). (0.395g, 1.89×10^{-3}mol, 77%)

NMR δ_H (acetone-d_6): 8.00 (2H, d, aromatic <u>H</u>-C-N-), 7.60-7.00 (6H, m, aromatic H), 4.30 (2H, t, N-<u>CH_2</u>-CH_2-CH_3), 1.90 (2H, m, -CH_2-<u>CH_2</u>-CH_3), 0.95 (3H, t, -CH_2-<u>CH_3</u>).

m/z = 209(M^+).

ν_{max} (film cast from chloroform solution): 3421(<u>C-N</u>-CH_2), 2957(CH_3 stretch), 2849(CH_2 stretch), 1598(aromatic C-H), 1448(CH_2 deformation), 1376(CH_3 deformation) cm^{-1}.

II.2.2 N-butyl carbazole

The method used for preparation and purification was the same as for N-propyl carbazole, but 1-iodobutane (2.68 g, 14.56×10^{-3}mol) was used instead of bromopropane, to react with the carbazole (3.00 g, 17.94×10^{-3}mol). A mixture of waxy solid and yellow oil was obtained, that still contained unreacted carbazole. Flash chromatography purification (same conditions) was necessary. (2.695g, 12.08×10^{-3}mol, 83%)

ν_{max} (film cast from chloroform solution): 3419(C-N-CH_2), 3050(aromatic C-H), 2952(CH_3 stretch), 2868(CH_2 stretch), 1600(aromatic C-H), 1451(CH_2 deformation), 1378(CH_3 deformation) cm^{-1}.

II.2.3 N-propyl carbazole using the cyclohexanone method [29]

The following reagents were placed in a round bottom flask: carbazole (3.97 g, 23.8 $\times 10^{-3}$mol), potassium carbonate (15.84 g, 11.5 $\times 10^{-3}$mol), 1-bromopropane (5.0 ml, 55×10^{-3}mol), and cyclohexanone (35 ml). The mixture was refluxed for 48 hours, after which a brownish solid was filtered off. The cyclohexanone was difficult to remove completely, because of its high boiling point. (4.038g, 19.32×10^{-3}mol, 81%)

ν_{max} (film cast from chloroform solution): 3417(C-N-CH_2), 2922(CH_3 stretch), 2853(CH_2 stretch), 1600(aromatic C-H), 1450(CH_2 deformation), 1378(CH_3 deformation) cm^{-1}.

NMR δ_H (acetone-d_6): 8.00 (2H, d, aromatic H-C-N-), 7.70-6.90 (6H, m, aromatic H), 4.25 (2H, t, N-CH_2-CH_2-CH_3), 1.80 (2H, m, -CH_2-CH_2-CH_3), 0.85 (3H, t, -CH_2-CH_3).

II.2.4 N-butyl carbazole using the crown ether method [2,90,91]

To a solution of 18-crown-6 (0.52 g, 2.0 x10^{-3}mol) in dry diethyl ether, potassium *tert*-butoxide was added (2.24 g, 2.0 x10^{-3}mol). The flask was fitted with an anhydrous magnesium sulphate guard tube, and was stirred for a few minutes. Carbazole was then added at once (3.32 g, 20 x10^{-3}mol), and the resulting mixture was left to stir for 15 minutes. A solution of bromobutane (0.43 ml, 4.0 x10^{-3}mol) in dry diethyl ether was prepared. The solution was added dropwise to the reaction mixture over 10 minutes, and the mixture left to stir at room temperature for 48 hours. The reaction was then quenched with water (20 ml). The aqueous phase was extracted with two portions of diethyl ether (2x20 ml). The combined organic fractions were washed firstly with a saturated sodium chloride solution (50 ml), and then with water, dried over anhydrous magnesium sulphate and evaporated. The product was purified using flash chromatography, eluting with a 1:4 mixture of ethyl acetate and petroleum spirit 40-60. (0.268g, 1.20 x10^{-3}mol, 30%)

NMR δ_H ($CDCl_3$): 7.95 (2H, dd, aromatic H closer to N), 7.50-6.85 (6H, m, aromatic H), 3.75 (2H, t, N-$\underline{CH_2}$-CH_2-), 2.00-0.60 (7H, m, alkyl chain CH_2-CH_2-CH_3).

ν_{max} (KBr): 3446(C-N-CH_2), 3043(aromatic C-H), 2952(CH_3), 2868(CH_2), 1625(aromatic C-H), 1452(CH_2), 1384(CH_3) cm^{-1}. M/z = 223(M^+)

II.2.5 Model monomer for the N-substitution of carbazole: 1-(N-carbazole)-6-[(4'-bromobiphenyl-4-yl)oxy]hexane

The synthetic route chosen was the 18-crown-6 one, as described in section II.2.4, since the product proved to be much easier to recover for a similar yield. A ratio of 3.5:1 of carbazole to the bromo-substituent was taken to ensure an optimum yield with respect to the substituent.

To the solution of 18-crown-6 (0.81 g,3.0 x10^{-3}mol) in diethyl ether (80ml), potassium *tert*-butoxide was added(3.91 g, 3.5 x10^{-3}mol). Under the same experimental conditions, carbazole was added (5.02 g, 30 x10^{-3}mol). While this was left to stir, a solution of 1-bromo-6-[(4'-bromobiphenyl-4-yl)oxy]hexane (4.12 g, 10 x10^{-3}mol) in dry diethyl ether (50ml) was prepared. The rest of the experiment was carried out as in section II.2.4.

The bromo compound did not dissolve easily in ether but the experiment was nevertheless carried on for 18 hours. After quenching the reaction with water (20ml) a waxy solid was obtained and washed with diethyl ether. It was dissolved (partially) in dichloromethane and after purification by flash chromatography (ethyl acetate/petroleum spirit 1:15) a white solid was obtained (1.30g, 2.61 x10^{-3}mol, 26%).

NMR δ_H ($CDCl_3$): 8.0 (2H, d, aromatic H closer to N), 7.55-6.55 (14H, m, aromatic H), 4.4-3.6 (4H, m, CH_2-N + CH_2-O) + 2.1-0.85 (8H, m, 4xCH_2), m/z (FAB) = 499 (M+1)

ν_{max} (KBr): 3446(C-N-C), 2927(CH_3), 1608(aromatic C-H), 1491(CH_2), 1473(CH_3), 1251(C-O-C) cm^{-1}.

II.2.6 Carbazole monomers bearing a liquid crystal N-substituent

The synthetic route for 1-(N-carbazole)-6-[(4-cyanobiphenyl-4'-yl)oxy]hexane is shown in Figure II-3.

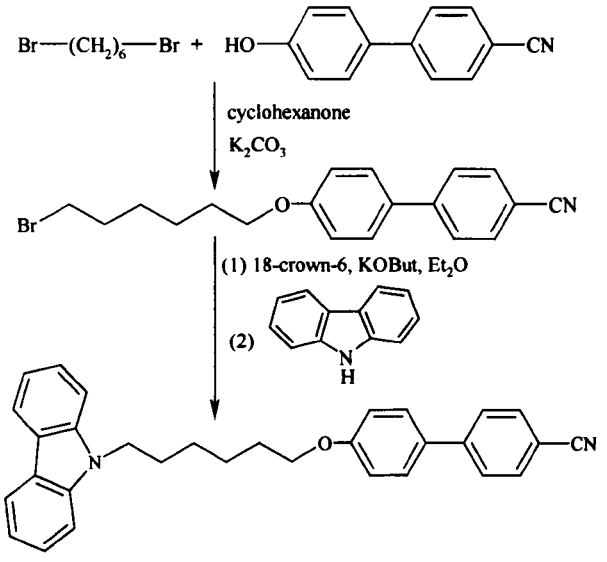

Figure II-3 Synthetic route for 1-(N-carbazole)-6-[(4-cyanobiphenyl-4'-yl)oxy]hexane

II.2.6.1 Synthesis of a liquid crystal moiety: 1-bromo-6-[(4-cyanobiphenyl-4'-yl)oxy]hexane[2]

4-cyano-4'-hydroxybiphenyl (0.979g, 5 x10^{-3}mol) was added to a mixture of 1,6-dibromohexane (5.49g, 23 x10^{-3}mol), and potassium carbonate (3.174g, 0.023 mol) in cyclohexanone (70cm^3). The mixture was refluxed for 6 hours, and filtered under reduced pressure. The obtained solid was purified using vacuum distillation and column ($CHCl_3$). (1.360g, 3.80 x10^{-3}mol, 76%)

NMR δ_H ($CDCl_3$): 7.66(4H, q), 7.53(2H, d), 6.99(2H, d), 4.02 (2H, t), 3.44 (2H, t), 1.87 (4H, m) + 1.53 (4H, m)

ν_{max} (KBr): 3446(C-N-C), 2937(CH_3), 2862(CH_3), 2222(C≡N), 1602(aromatic C-H), 1495(CH_2), 1474(CH_3), 1251(C-O-C) cm^{-1}.

II.2.6.2 Preparation of the liquid crystal substituted carbazole monomer 1-(N-carbazole)-6-[(4-cyanobiphenyl-4'-yl)oxy]hexane

The method described in section II.2.4 was used to prepare the carbazole monomer, but using an excess of carbazole. To the mixture of 18-crown-6 ether (0.045g, 1.5×10^{-3}mol), diethyl ether (10ml), potassium *tert*-butoxide (0.201g, 18×10^{-3}mol) and carbazole (0.500g, 3.0×10^{-3}mol), the solution of 1-bromo,6-[(4-cyanobiphenyl-4'-yl)oxy]hexane (0.65g, 1.82×10^{-3}mol) in diethyl ether (10ml) was added dropwise. The reaction was stirred for 20h before being quenched with water (10ml). The reaction mixture was extracted with diethyl ether (2x5ml). The organic fractions were combined and washed with a saturated solution of sodium chloride (2.5ml). The organic phase was dried over anhydrous magnesium sulphate. The filtered solution was evaporated and recrystallised (0.218g, 4.91×10^{-4}mol, 27%) from diethyl ether.

NMR δ_H ($CDCl_3$): 8.2-6.85 (16H, m, aromatic H), 4.34(2H, t, CH_2-O), 3.95 (2H, t, CH_2-N), 1.94 (2H, quint., alkane CH_2), 1.78 (2H, quint., alkane CH_2), 1.5 (4H, m., alkane CH_2)

ν_{max} (KBr): 3448(C-N-C), 3052(arom), 2930(CH_3), 2850(CH_2), 2220(C≡N), 1599(conjugated C=N), 1492(CH_2), 1465(CH_3), 1251(C-O-C) cm^{-1}.

II.2.7 Characterisation of readily available monomers

Some of the commercial compounds were analysed in order to identify the products of reactions in which they were used.

II.2.7.1 Carbazole:

ν_{max} (nujol mull): 3418(C-N-CH_2), 2924(aromatic C-H) cm^{-1}.

ν_{max} (KBr):3419(C-N-CH_2), 3050(aromatic C-H) cm^{-1}.

II.2.7.2 N-methyl carbazole

ν_{max} (nujol mull): 3425(C-N-C), 3049(aromatic C-H), 1597(conjug. C=N), 1466(-CH_3) cm^{-1}.

II.2.8 Hydrogenation of nitro compounds[29]

The use of high-pressure catalytic hydrogenation allows for a fast, clean and efficient conversion of readily available nitro compounds to anilines. Figure II-4 shows as an example the reaction path for the hydrogenation of 1- [(2-nitrophenyl-1-yl) oxy]-6-[(4-biphenylcarboxylic acid-4'-yl)oxy] hexane.

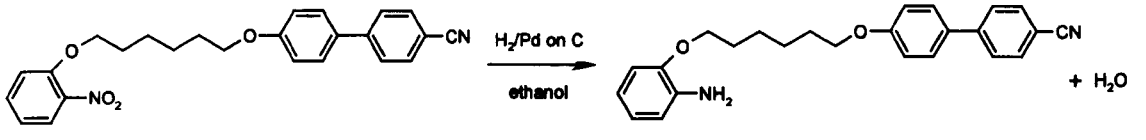

Figure II-4 Hydrogenation of 1- [(2-nitrophenyl-1-yl) oxy]-6-[(4-biphenylcarboxylic acid-4'-yl)oxy] hexane

II.2.8.1 Hydrogenation of 1-[(2-nitrophenyl-1-yl)oxy] -6-[(4-biphenylcarboxylic acid-4'-yl)oxy] hexane.

1- [(2-nitrophenyl-1-yl) oxy]-6-[(4-biphenylcarboxylic acid-4'-yl)oxy] hexane (0.40g, 9.60 x10^{-4}mol) was dissolved in ethanol (70ml) at 50°C. A catalytic amount of palladium on carbon (10%) was added to the solution in the glass vessel of the hydrogenator. After sealing the device, the pressure was set (30psi, ~2.3bar), and the temperature was increased to 70°C. The pressure gradually increased to 70psi. After 90min of gentle rocking, the mixture was allowed to cool down to room temperature.

The product having precipitated out of the solution, the mixture was warmed up (50°C), so as to allow hot filtration of the catalyst. For safety reasons the catalyst was de-activated by soaking it in water. The product (a creamy white solid) was filtered from the cooled solution and recrystallised from methylated spirit. (0.2988g, 7.73 x10^{-4}mol, 80%)

ν_{max} (KBr): 3463(NH_2), 2939(CH_2), 2867(CH_2),), 2549(COOH), 1679(C=NH_2), 1526(CH_2), 1506(CH_3), 1290(-OH), 1249(C-O-C) cm^{-1}.

II.2.8.2 Hydrogenation of 1-[(2-nitrophenyl-1-yl)oxy] -6-[(1-phenylcarboxylic acid-4-yl)oxy] hexane.

Using the method described in II.2.8.1, 1- [(2-nitrophenyl-1-yl) oxy]-6-[(1-phenylcarboxylic acid-4-yl)oxy] hexane (1.00g, 2.79 x10^{-3}mol) in ethanol (140ml) was reacted for 3.5 hours at 40psi, 75°C with palladium on carbon (catalytic amount). The resulting mixture was treated as described in II.2.8.1. The product, a pale brown solid yielded a pale creamy solid (0.911g, 2.77 x10^{-3}mol, 99%) upon treatment with activated charcoal.

ν_{max} (KBr): 3474(NH_2), 3380(NH), 2942(CH_2), 2855(CH_2), 2670(COOH), 2558(COOH), 1675(C=NH_2), 1505(CH_2), 1470(CH_3), 1306(-OH), 1259(C-O-C) cm^{-1}.

II.2.8.3 Hydrogenation of 1-[(2-nitrophenyl-1-yl)oxy] -6-[(4-cyanobiphenyl-4'-yl)oxy] hexane.

The experiment was carried out in similar conditions as described in II.2.8.1, 1-[(2-nitrophenyl-1-yl) oxy]-6-[(4-cyanobiphenyl-4'-yl)oxy] hexane (0.52g, 1.25 x10^{-3}mol) in ethanol (60ml) and palladium on carbon as catalyst. The autoclave was sealed and the pressure was set (45psi, ~3.1bar), and the temperature increased to 70°C. The pressure

exceeded the set limit again, to reach 80psi. After 75 minutes the system was allowed to cool down. The product was recovered as for II.2.8.1, and the resulting grey waxy solid was recrystallised from methylated spirit. (0.369g, 0.94 x10^{-3}mol, 75%)

ν_{max} (KBr): 3458(NH_2), 3368(NH), 2937(CH_2), 2862(CH_2), 2224(C≡N), 1500(CH_2), 1475(CH_3), 1252(C-O-C) cm^{-1}.

II.3 Preparation of polymers

Several techniques were studied for the polymerisation of the different monomers. The reason for this was as much the quality and quantity of the polymer produced as its properties or the information expected from the various experiments.

II.3.1 Emulsion polymerisation

The use of an emulsion medium for the polymerisation enables us in theory to have some control over the size of the particles of polymer produced. The production of aniline based polymers using an emulsion has been widely reported, but the use of a micro-emulsion, in which the micelles are much smaller, should enable the production of particles that reflect better the molecular size. The surfactants used for this type of experiment were usually of the ionic type, which meant they could produce very stable emulsions. However, the retrieval of the polymer could prove difficult because of the difficulty of breaking down the emulsion once the reaction was complete. The use of a non-ionic surfactant, by not allowing ionic bonding, yields an emulsion that was also very stable throughout the experiment, but should also be easily dispersed to retrieve the polymer.

II.3.1.1 Synthesis of poly(2-methoxyaniline) using an ionic surfactant[29]

A solution of 2-methoxyaniline (0.22 g, 1.8 x10^{-3}mol) in chloroform (20 ml) was cooled in ice to 5°C. This temperature was maintained as a mixture of dodecylbenzenesulphonic acid (DBSA) (2 ml) in 1M hydrochloric acid (18 ml) was added, with vigorous stirring. Once a stable emulsion had been obtained, a few milligrams of iron (II) chloride were added as a catalyst and a solution of ammonium persulphate (0.37 g, 1.6 x10^{-3}mol) in 1M hydrochloric acid (20 ml) was slowly added along a glass rod. The mixture was stirred overnight at 0-5°C. The green reaction mixture was then diluted with 1M hydrochloric acid and filtered to give a dark green solid and a green liquid. The solid residue was dissolved in chloroform (100 ml) and the solution obtained was then extracted with 1M hydrochloric acid (2x70 ml). The organic phase was then evaporated to yield a dark green solid. The liquid remaining from the reaction was centrifuged and the solid obtained treated as described previously. (0.10g, 8.25 x10^{-4}mol, 52%)

ν_{max} (KBr): 3389(NH), 2928(CH_3), 2348(NH^+), 1507(C-N-C), 1457(CH_3), 1253(C-O-C) cm^{-1}.

II.3.1.2 Synthesis of poly(2-methoxyaniline) using a non-ionic surfactant[92,78]

The surfactant Brij 35 (0.4g) was dissolved in a solution of 2-methoxyaniline (0.20 g, 1.7 x10^{-3}mol) in 3M hydrochloric acid (5 ml). Petroleum ether 60-80°C (15 ml) was then added with stirring at room temperature, to form a stable inverse microemulsion. Meanwhile a similar emulsion was prepared using sodium persulphate (0.38 g, 1.6 x10^{-3}mol) instead of 2-methoxyaniline and water instead of hydrochloric acid. After one hour's stirring, the two translucent emulsions were mixed and the

resulting mixture was stirred for 3 days at room temperature, during which the mixture turned successively from colourless to burgundy and finally dark green. Excess methanol was then added to 'break' the emulsion and the black solid particles formed were isolated using centrifugation. The solid phase was centrifuged several times with fresh portions of 3M hydrochloric acid (3 x 50ml) and then with water (2 x 50 ml). An aqueous solution of ammonia (2 %, 10 ml) was added to the resulting solid, which then turned purple, and this solution was extracted with chloroform. The organic phase, once evaporated, yielded a metallic-like blue film on the walls of the round bottom flask. Upon treatment with hydrochloric acid, the solid turned into a green powder partially soluble in chloroform (0.03 g, 2.53 x10^{-4}mol, 15%).

ν_{max} (KBr): 3395(NH), 2933(CH_3), 2353(NH^+), 1512(C-N-C), 1462(CH_3), 1258(C-O-C) cm^{-1}.

II.3.1.3 Synthesis of poly(2-propoxyaniline) using a non-ionic surfactant.

The synthesis was carried out following the procedure described for the preparation of poly(2-methoxyaniline) in section II.3.1.1. The monomer used was 2-propoxyaniline (0.20 g, 1.3 x10^{-3}mol). The other quantities used were the same as described previously and the experiment was carried out up to the centrifugation with acid and water. The wet product was left to dry on a watchglass in a desiccator, and yielded a black powder soluble in chloroform (0.0385 g, 2.47 x10^{-4}mol, 19%).

ν_{max} (film cast from chloroform solution): 3150/3050 (Ar. ring), 3000/2950 (CH_2, CH_3), 1582 (C-N), 1494 (C=C), 1351 (CH_2), 1291 (CH_3), 1202 (C-O-C), 1130 (C-O), 1010 (C-C), 837 (C-H) cm^{-1}.

II.3.1.4 Preparation of poly(2-butoxyaniline) using a non-ionic surfactant.

The procedure followed was the same as for 2-propoxyaniline but the monomer used was 2-butoxyaniline (0.21 g, 1.3 x10^{-3}mol). As for the poly(2-propoxyaniline), the obtained product was soluble in chloroform before treatment with ammonia and was left to dry on a watchglass to yield a green powder soluble in chloroform (0.072g, 4.47x10^{-4} mol, 34%).

ν_{max} (film cast from chloroform solution): 3150/3050 (Ar. ring), 2962/2868 (CH_2, CH_3), 1581 (C-N), 1496 (C=C), 1351 (CH_2), 1300 (CH_3), 1205 (C-O-C), 1124 (C-O), 1002 (C-C), 837 (C-H) cm^{-1}.

II.3.1.5 Polymerisation of 1-[(aniline-2-yl)oxy]-6-[(4-biphenylcarboxylic acid-4'-yl)oxy] hexane using a non-ionic surfactant

The two emulsions were prepared separately as described in II.3.1.2. Emulsion A consisted of 1-[(aniline-2-yl)oxy]-6-[(4-biphenylcarboxylic acid-4'-yl)oxy] (0.1g, 0.25x10^{-3} mol), petroleum spirit 40-60 (7ml), 3M hydrochloric acid (2ml) and Brij 35 (0.1g). Emulsion B consisted of $Na_2S_2O_8$ (0.24g, 1.00x10^{-3}mol), petroleum spirit 40-60 (7ml), 3M hydrochloric acid (2ml) and Brij 35 (0.1g). Both emulsions were mixed together to give a pinkish emulsion that gradually darkened to brown. The reaction was left to stir for 24 hours, after which it was treated as described in II.3.1.2. The product (0.037g, 0.09 x10^{-3}mol, 36%) was a dark brown solid.

ν_{max} (KBr): 2940/2868 (CH_2), 1603 (C-N), 1506 (C=C arom), 1430(CH_2), 1194(C-O-C), 1125 (C-O) cm^{-1}.

II.3.1.6 Emulsion polymerisation of 1-[(aniline-2-yl)oxy] -6-[(1-phenylcarboxylic acid-4-yl)oxy] hexane.

1-[(aniline-2-yl)oxy]-6-[(1-phenylcarboxylic acid-4-yl)oxy]hexane (0.1g, 0.30×10^{-3}mol) was dissolved in a mixture of acetone (15ml) and chloroform (5ml). To a solution of Brij35 (0.8g) in hydrochloric acid (10ml) was added ferric chloride (0.5g). Both solutions were cooled to 5°C before mixing. The reaction mixture was kept stirring while a solution of sodium persulphate (0.70g, 2.94×10^{-3}mol) in hydrochloric acid (10ml) was added along a glass rod. The mixture was reacted for 7 days before quenching with methanol and water. The product was an oily paste, but after a few days, it dried to a dull burgundy solid. (0.052g, 0.16×10^{-3}mol, 53%)

ν_{max} (KBr): 3025 (Ar. ring), 2942/2854 (CH_2), 2669/2557(COOH), 1675(C=C arom.), 1577 (C-NH), 1219 (C-O-C) cm^{-1}.

II.3.2 Polymerisation of N-methyl carbazole

Because of the structural similarities between carbazole, aniline and pyrrole, similar techniques were used to polymerise the carbazole monomers. NB: the usual methods reported for the polymerisation of carbazole and carbazole derivatives were electropolymerisation[93, 94, 95], and direct chemical polymerisation[96]

II.3.2.1 Using the straight emulsion method

Solutions of N-methyl carbazole (0.02g, 0.11×10^{-3}mol) in chloroform (2ml) and of Brij35 (0.2g) and ferric chloride (0.05g) in 3M hydrochloric acid (4ml) were mixed at 5°C before the solution of sodium persulfate (0.01g, 4.2×10^{-5}mol) in hydrochloric acid (2ml) was added along a glass rod. After 7 days stirring at room temperature the solution went from yellow to green with visible particles of blue material. The reaction

was quenched with methanol, yielding a dark sticky material (0.009g, 0.05 x10^{-3}mol, 45%) that was retrieved using centrifugation.

ν_{max} (KBr): 3423(C-N-C), 3047(aromatic C-H), 1595(conjug. C=N), 1464(-CH_3) cm^{-1}.

II.3.2.2 Using the inverse microemulsion method

The emulsions were prepared using the method described in section II.3.1.6. Emulsion A consisted of N-methyl carbazole (0.02g, 0.11 x10^{-3}mol) in 2M hydrochloric acid (2ml) and chloroform (4ml) with Brij35 (0.03g). Emulsion B consisted of sodium persulfate (0.01g, 4.2x10^{-5}mol) in water (4ml) with Brij35 (0.03g) in chloroform (5ml). The reaction was left running for 8 days before it turned khaki green. The product was washed as described for the polymerisation of the aniline derivative in section II.3.1.2. (0.010g, 0.54x10^{-4} mol, 49%)

Spectral data was found to be almost identical to that in II.3.2.1.

II.3.3 Chemical polymerisation of a liquid crystalline pyrrole derivative: polymerisation of 1-(N-pyrrole)-6-[(4-cyanobiphenyl-4'-yl)oxy]hexane

1-(N-pyrrole)-6-[(4-cyanobiphenyl-4'-yl)oxy]hexane (0.02g, 6.24×10^{-5}mol), supplied by Dr P. Ibison, was dissolved in a solution of ferric chloride (0.05g, 2.90×10^{-4}mol) in chloroform (10 ml). The mixture was heated to 40°C (no reflux) and stirred for two days, after which it was extracted with two fresh portions of an aqueous solution of sodium EDTA (0.1 mol.L^{-1}). The organic phase was then washed twice with water and dried with magnesium sulphate. After evaporation of the chloroform, the oily material was refluxed with methylated spirit to dissolve the oligomeric part. The solution was

decanted off and the residual solid polymer (<0.01 g) was redissolved in chloroform in order to cast a film for microscopic study. No liquid crystalline texture was observed but the compound melted (isotropic phase observed under the microscope) at about 65°C, and kept its initial appearance after cooling, which suggests that the obtained polymer was not too sensitive to oxidation. The non-observation of the texture was attributed to the excessively short period of microscopic study, as it may often take a few hours to develop in a liquid crystalline polymer, and the transition temperatures were only maintained for a few tens of minutes. The samples were observed both upon heating and cooling, but the rate of change in temperature, although quite low (1°C/min) may still have been too fast to allow the textures to develop.

ν_{max} (KBr): 2934/2858(CH_2), 2225(C≡N), 1494(CH_2), 1251(C-O-C) cm^{-1}.

II.3.4 Electrochemical polymerisation experiments[2, 97]

Although the yield of polymer obtained from electrochemical polymerisation (also referred to as electro-polymerisation) is not always very good, it gives useful information about the pattern of formation, and the properties of the polymer

In order to get a minimum volume of electrolyte for the monomers to be dissolved in, a three-compartment electrochemical cell was designed and tested, but the resistance proved to be too high for cyclic electrodeposition to take place. This was apparently due to the thickness of the sinters joining the compartments. The cell was thus replaced with a simple small glass container.

The platinum working electrode had to be replaced by ITO glass ones, as non conductive deposits seemed to form on the platinum after the first use, which inhibited the flow of the current when the experiment was repeated. This problem was easily overcome by using a new ITO electrode each time. As no major difference was

observed (in the chosen range of potentials) between degassed and non-degassed solutions most of the experiments were run on non-degassed solutions. For the experiments performed on pyrrole derivatives, tetramethylammonium tetrafluoroborate was tried at first as well as the use of acetonitrile as electrolyte solvent. The solubility of the former was not high enough and the latter did not confer any benefit, either in the spectra or in the films formed.

II.3.4.1 Pyrrole derivatives

All the experiments were carried out using a solution of tetraethylammonium tetrafluoroborate in propylene carbonate (0.2 $mol.L^{-1}$) as the electrolyte solution for cyclic voltammetry. The concentration used for the monomers was 0.01 $mol.L^{-1}$.

Both the working and the counter electrode were initially platinum, but in order to provide a larger contact surface as well as for greater ease of retrieval of the produced films, they were replaced by ITO glass working electrodes and a stainless steel counter electrode. The reference electrode used was a calomel electrode (MF 9244 RE 5 reference electrode).

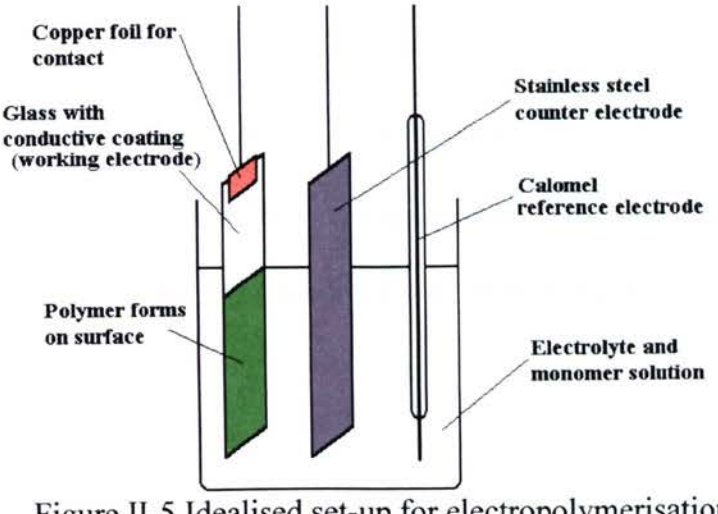

Figure II-5 Idealised set-up for electropolymerisation

A cyclic voltammogram was first run for the blank electrolyte solution to show that it was stable in the range of potentials to be studied (from -400 mV to 2000 mV).

A solution of ferrocene in the electrolyte was then prepared as calibrant by dissolving a few grains of ferrocene in the electrolyte solution. The voltammogram observed showed the expected sharp peak (around 40 mV), so the experiments were carried on.

The monomers studied were N-methyl pyrrole, 1-(2-cyanoethyl)pyrrole (both commercially available) and the liquid crystalline monomer: 1-(N-pyrrole)-6- [(4-cyanobiphenyl-4'-yl)oxy]hexane.

The infrared spectrum of the polymer from 1-(N-pyrrole)-6- [(4-cyanobiphenyl-4'-yl)oxy]hexane was run for the film obtained on ITO glass.

ν_{max}: 2936 (CH_2), 2224 (R-C≡N), 1602 (C-N), 1580 (C=C), 1494 (C-O), 1467 (CH_2), 1250 (C-O), 1180 (C-O-C) cm^{-1}.

II.3.4.2 Carbazole derivatives

II.3.4.2.1 Electropolymerisation of N-methylcarbazole

Sets of cyclic voltammetry experiments were performed under different conditions:

II.3.4.2.1.1 Using ITO glass as a working electrode

Since ITO glass electrodes can be produced cheaply, a series of experiments was devised using a different electrolyte medium and a new electrode every time.

II.3.4.2.1.2 Using tetraethylammonium tetrafluoroborate in propylene carbonate as electrolyte.

The electrolyte was made up to 0.2M and a solution of N-methyl carbazole (1.028g, 5.68×10^{-3} mol) was prepared in 19ml electrolyte solution. Some attempts had been made to use a lower concentration, but only with that kind of concentration was a film of polymer obtained. When the range of cycling potential was wide (-0.2/1.2V), no film formation was observed, only an electrochromic cloud (green/yellow) surrounding the working electrode that seemed to be attached, but would disperse if the electrode was moved. When the potential range was changed to a more static value (1.0/1.1V), a film growth was observed starting as dispersed spots on the ITO electrode. The spots would then increase in number so that after about 20,000 cycles at an almost stationary potential a film of satisfying thickness was obtained. The film was not peelable but could be removed as small turnings in order to get an infrared spectrum of the polymeric product (The use of reflectance mode infrared spectroscopy was considered, but the patchy nature of the obtained films did not permit one to get a satisfactory spectrum).

Poly N-methyl carbazole ν_{max} (KBr): 3442(C-N-CH_3), 3051(CH aromatic), 2929(CH_3), 1619(CH aromatic meta substitution), 1594(CH aromatic para substitution) cm^{-1}.

II.3.4.2.1.3 Using tetraethylammonium tetrafluoroborate in acetonitrile as electrolyte.

The concentrations used were consistent with the ones described in section II.3.4.2.1.2. for the propylene carbonate based method.

Although the green colour could be observed, no film formation occurred, even after the system had been left at 'growing potential' (1.0-1.1 V) for a long period of time (30,000 cycles). Further tests done on the films obtained from the propylene carbonate solution

suggested that the polymer was soluble in acetonitrile, therefore precluding the growth of the film on the electrode.

Infrared data was almost identical to that obtained for II.3.4.2.1.2.

II.3.4.2.2 Using platinum foil as a working electrode

An identical of concentration of electrolyte salt in propylene carbonate was used to that described in section II.3.4.2.1.2, together with a similar concentration of monomer. Film formation occurred more or less in the same way, but although the appearance of the film was a lot smoother the initial film growth was still in the form of dots.

Infrared data was almost identical to that obtained for II.3.4.2.1.2.

II.3.4.3 Electropolymerisation of N-methyl carbazole using an acid medium[98, 99, 100, 101].

The electrolyte solution was prepared by mixing 5M hydrochloric acid (20ml) with methanol (60ml). N-methyl carbazole (0.344g, 1.90×10^{-3} mol) was then dispersed using an ultrasonic bath for 5min. The cyclic voltammetry experiment was set up using the equipment described in section II.3.4.1 for the electropolymerisation of pyrrole derivatives. A series of 1000 cycles was run in the range 850-950mV. A patchy dark green film was obtained on the working electrode, and green particles were observed at the bottom of the vessel. The same solution was employed, but using a magnetic stirrer to keep the particles of monomer in suspension. 1000 cycles were run in the range 800-900mV. Although less patchy, the film obtained was not free-standing, because of its thinness.

Infrared data was almost identical to that obtained for II.3.4.2.1.2.

II.3.4.4 Electropolymerisation of N-butylcarbazole

When a 0.1M solution of N-butylcarbazole in Et_4NBF_4/propylene carbonate solution was used, no film formation was observed, but a green cloud could be seen at the working ITO electrode. The cyclic voltammogram obtained was encouraging as it clearly showed the characteristic stages of polymerisation and dedoping on the cycles. The shape of the cyclic voltammogram obtained was altogether very similar to the ones recorded in consistent conditions for pyrrole derivatives, which confirms the similarity of both types of polymers.

ν_{max} (thin film): 3420(C-N-CH_2), 3049(aromatic C-H), 2953(CH_3), 2867(CH_2), 1601(aromatic C-H), 1452(CH_2), 1377(CH_3) cm^{-1}.

II.3.4.5 Electropolymerisation of 1-(N-carbazole)-6-[(4'-bromobiphenyl-4-yl)oxy]hexane in acid medium.

The electrolyte solution was prepared using 2.5M sulphuric acid (10ml) and methanol (30ml). 1-(N-carbazole)-6-[(4'-bromobiphenyl-4-yl)oxy]hexane was added (0.1g, 2.0×10^{-4} mol), and the vessel was placed in an ultrasonic bath for 10 minutes. The experiment was carried out as described section II.3.4.3, with the mixture stirred throughout the experiment. Although no film could be observed even at growth potential (~1.05V), a voltammogram was obtained.

II.3.4.6 Electropolymerisation of 1-(N-carbazole)-6-[(4'-bromobiphenyl-4-yl)oxy]hexane in propylene carbonate based electrolyte.

A solution of Et_4NBF_4 (4.34g, 0.02mol) in propylene carbonate (100ml) was prepared. 1-(N-carbazole)-6-[(4'-bromobiphenyl-4-yl)oxy]hexane was dissolved in warm electrolyte solution (30ml). The cyclic voltammetry experiment was carried out as described in section II.3.4.2.1.2. Although no film was obtained, the shape of the voltammogram definitely shows the typical features of formation (~1.10V), doping (~0.85V) and dedoping (~0.62V) of a conducting material.

II.3.5 Polymerisation of N-methyl carbazole and 1-(N-carbazole)-6-[(4'-bromobiphenyl-4-yl)oxy]hexane using liquid iodine as a solvent and oxidising agent

The use of liquid iodine as a medium for polymerisation[102, 103] theoretically fulfils two requirements. Firstly it provides a fluid medium in which the monomer can dissolve, and secondly the oxidising property of iodine enables the polymerisation to take place without requiring the addition of any further chemical. The remaining iodine after polymerisation also acts as a doping agent for the obtained polymeric material.

The following polymerisations were attempted first as bench based experiments, using a heated oil bath to increase the temperature. In order to get a better idea of the progress of the reaction, the same experiments were scaled down and performed *in situ* in the NMR machine. Details of both experiments follow.

II.3.5.1 Bench top experiment

In separate test tubes were placed N-methyl carbazole (0.022g, $1.2x10^{-4}$ mol) and 1-(N-carbazole)-6-[(4'-bromobiphenyl-4-yl)oxy]hexane (0.020g, $4.0x10^{-5}$ mol) ground together with solid iodine (2.00g, $7.87x10^{-3}$ mol). The tubes were fitted with stoppers and placed in an oil bath. The temperature of the bath was increased to 130°C and the tubes were left heating overnight. The resulting products were insoluble very dark solids that were cleaned of iodine by first washing and centrifuging repeatedly the crushed samples with acetone, then evacuating them using a vacuum line (house vacuum, samples heated slightly with hot air). Because of the high apparent yield obtained (respectively 0.13g and 0.09g) it is likely that some iodine remained in the samples.

No infrared data were recorded as the samples were very contaminated with iodine.

II.3.5.2 NMR tube experiment

Note: Even though the literature mentioned the use of NMR to follow the evolution of the reaction, no mention was made of the method used and no example of the aspect of the spectra was available, so the method had to be devised from scratch.

Figure II-6 illustrates the set-up that was designed.

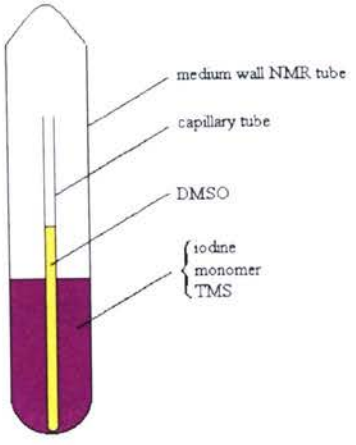

Figure II-6 Set up for the iodine polymerisation in NMR tube

Before the experiments were carried out, care had to be taken that the NMR tubes would withstand the pressure of the vapour inside as they were to be sealed off. After deciding the tubes to be used would be 175mmx4mm, the vapour pressure created by the reaction could be calculated. The amount of iodine (MW 181) used was decided not to be in excess of 1.00g, and the maximum temperature to be 400K. The relationship between pressure, volume and number of moles is generally known to be PV=nRT, therefore we can determine the value of P as being $P = \frac{nRT}{V}$, with the volume $V=h\pi r^2=2.2\times10^{-6}m^3$, with h and r being respectively the length and the radius of the tube. The maximum value for P was found to be 8.36×10^5 Pa, a value which although quite high was low enough for the tube to stand it. The following system was set up: the monomer (0.01g, 5.5×10^{-5} mol for the N-methyl carbazole, 0.013g, 2.60×10^{-5} mol for 1-(N-carbazole)-6-[(4'-bromobiphenyl-4-yl)oxy]hexane) was crushed with iodine (respectively 1.00g and 0.80g).

After inserting the sample in the NMR tube, 6 drops of TMS were added to the iodine mixture. A capillary tube filled with enough DMSO for its level to be higher than that of the iodine was then inserted in the middle of the NMR tube. Note: the DMSO was

needed for the NMR spectrometer to find a solvent 'lock' but did not interfere with the reaction. The NMR tube was then cooled and sealed off. The NMR spectra were recorded at intervals, with the machine set on temperature increase up to 440K.

No infrared data were recorded as the samples were very contaminated with iodine.

II.4 Conductivity measurements

The conductivity of the polymer samples was measured using a 4-point system. The equipment involved was that described in section II.1.5.2.1.

Depending on the quantities available and the solubility, the polymer samples were treated in one of the following ways:

- Casting of a film on a non-conductive glass surface from solution, and copper wires attached to the sample in a square pattern using silver dag. A representation of this set-up can be found in Figure II-2.

Alternatively, a free-standing film can be secured onto a non-conductive glass surface using double-sided sticky tape, with the copper contacts affixed as before.

- Casting of a film from solution onto a commercial substrate (as described in section II.1.5.2) of very small dimensions allowing conductivity measurements for small quantities of polymer.

In the case of conductivity measurements taken for samples doped with ferric chloride while on commercial substrates, a problem arose: it was observed that although the tracks were not effected (they were gold-coated), the contacts with the 'legs' of the substrate as well as those themselves corroded quite quickly when exposed to the dopant, even when great care was taken not to get any solution onto those parts. This same problem prevented the success of some attempts to monitor the doping in situ using iodine vapour in a pressurised cell. Even by coating all the contacts with a Teflon solution, the oxidising potential of the iodine damaged the metallic contacts in the cell.

It may be possible to remedy this problem by encasing as much as possible of the exposed metal in glass.

II.5 Molecular modelling

II.5.1 Background

The software package used during the project was Quantum CAChe (Version 3.2, CAChe Software/Fujitsu). The principle was standard for that type of software: using different sets of specific equations, it enabled the calculation of a number of solid-state materials properties. The optimisation of each model followed a similar process, as described below.

II.5.2 Creation of the molecule within the package:

Prior to any calculation, the chosen molecule had to be created within the package, using the 3-dimensional drawing facilities provided. As it was drawn manually, the bond lengths and the relative angles were not accurate. The software offered a 'beautification' facility. It repositioned the atoms so as to ensure that the bond lengths and angles were accurate, and adjusted the number of hydrogen atoms. This ensured that the valence, the hybridisation, the geometry, and the ring structure were correct at the time of drawing.

It was useful in some cases to obtain data on the un-optimised molecule. It was obtained using Molecular Mechanics. This term refers to the theoretical methods that were used to determine the molecular geometry, and to describe the forces acting on the atoms in the molecule. They use empirically derived equations from classical Newtonian physics[104]. Molecular mechanics force fields (also referred to as force fields

methods or Westheimer methods) calculated the potential energy* of the molecule. It typically included terms such as bond stretching, angle bending, torsional and non-bonding interactions such as Van der Waals and hydrogen bond interactions[f]. The sum of those terms represents the steric energy of the molecule.

II.5.3 Minimisation of the energy of the structure.

The nuclear positions of the atoms influence the potential energy of the molecule. The latter can be seen as a multidimensional potential energy surface. The surface shows hills corresponding to strained high-energy conformations, and valleys that correspond to stable low energy conformations.

After the molecule had been drawn and 'beautified', the next step was to assess whether the chosen conformation was the most stable one, i.e. the one of lowest energy. Molecular mechanics Optimisation adjusted the positions of the atoms in order to find an optimum molecular geometry. This corresponds to an energy minimum or valley on the potential energy surface. In order to achieve this goal, the software systematically moved the atoms until the net force acting on each atom came near zero, i.e. there is no more decrease in the resulting calculated potential energy. The method used in CAChe was to apply Allinger's standard MM2 and MM3 force fields, as well as implemented rules to estimate parameters in cases not addressed by standard force fields. As a result the force fields were considerably increased, which allowed minimisation calculations for square planar, trigonal pyramidal and octahedral coordinations of atoms throughout the periodic table. The direction and the distance moved by atoms depend on the slope of the potential energy surface. However, the energy minimisation process is iterative,

---

* Term used in the user manual, which might be inaccurate in a particular chemical/physical context.

[f] N.B: This list is non-exhaustive.

which means that unless there is only one minimum in the potential energy surface, the final structure will depend on the starting geometry. Figure II-7 illustrates how a structure minimisation started from two different points on the energy plot will yield two different (local) low-energy conformations.

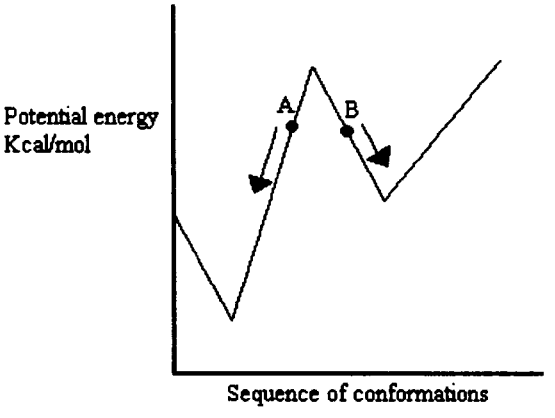

Figure II-7 Starting point dependence of minimised energy

It is also important to realise at this point that the way the 'double' bonds of the aromatic rings were allocated when drawing the molecule may affect the outcome of the minimisation process. The software-favoured structures where double bonds were drawn in a trans conformation rather than in a cis conformation.

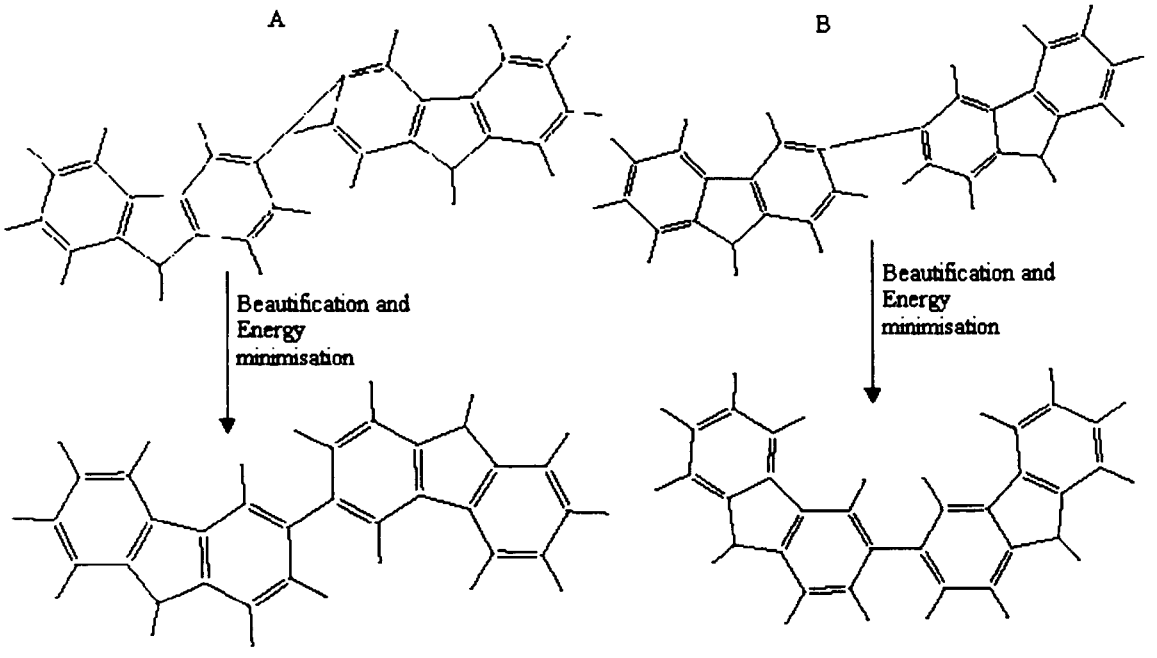

Figure II-8 Effect of position of double bond on minimised structure.

Although it makes little different to extended parts of molecules containing double bonds, it can completely change the outcome of a minimisation for aromatic ring-based molecules. Figure II-8 illustrates the minimisation of two representations of di-carbazole. In A, the 'double' bonds are identically drawn, and in B they are drawn inverted. In both cases the minimised structure shows that the double bonds on either side of the inter-monomer bond have adopted a trans configuration.

The information that was obtained will be detailed in Chapter III: Results and Discussion.

III RESULTS AND DISCUSSION

III.1 Introduction

The previous chapters of this thesis have been concerned with introducing the topic of self-organising conducting polymers, describing the design, synthesis and polymerisation of materials with such abilities, such as aniline and carbazole derivatives bearing mesogenic pendant groups. This chapter will describe the characterisation of the monomers and the polymers, as well as the optical and electrical properties of the latter. Techniques aimed at improving on those properties will also be discussed. Throughout the chapter the topic of molecular modelling will also be addressed as a means to predict some of the investigated properties, and also as a tool to better understand the configurations adopted by the different molecules.

III.2 General features of molecular modelling: Bond rotation and energy map

After considering the limitations mentioned in the Experimental part, models of the monomers and polymer molecules were created in the software, and various properties were calculated for each of them.

In order to address the problem of possible multiple energy minima, an energy map was plotted for each of the molecules. One or more 'search labels' were defined in the molecule and the optimised map experiment was run. The labels were implemented in steps to the specified final value and for each step the conformation was optimised. The rest of the structure was left as it was upon starting the experiment.

The bond(s) selected as 'search labels' were usually the connecting bond between monomer units because they could be freely rotated. The potential energy was then calculated and the bond(s) was then rotated by a set angle. The process was repeated until the final angle (usually 360°) was reached. A 2-dimensional (2D) diagram (3D in the case of 2 bonds) was then obtained of the potential energy as a function of the angle of the bond. The number 'n' of steps taken to reach that angle for one search label gave 'n+1' conformations. In the case of two search labels of 'n' steps each, '$(n+1)^2$' conformations are generated, which depending on the value of 'n' can mean a vast amount of data. Up to 8 labels could be studied at the same time, but because of computing possibilities and time required only experiments with one or two labels were carried on. The lowest energies corresponded to the most stable (most favoured) conformation and the highest energies, to the least stable (and least likely) conformation.

Figure III-1 shows the energy map for the rotation of di-carbazole and the structure that yields the lowest energy. Unlike the minimised structure for which all the atoms were taken into account this dimer has a twisted structure which is probably linked to the hydrogen atoms on the aromatic rings. The steric effect is lessened by the twisting of the molecule.

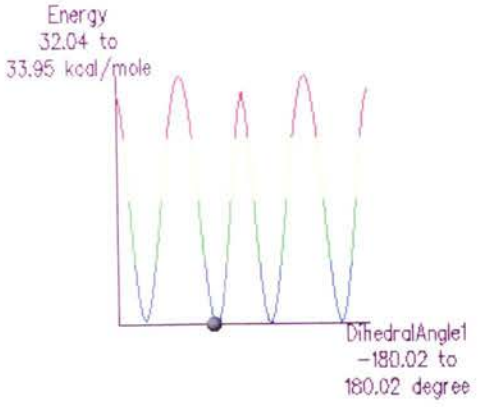

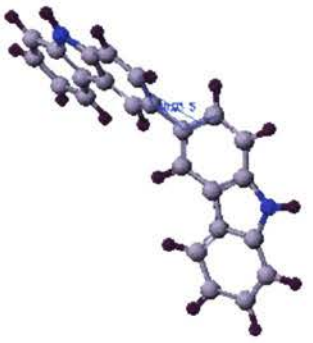

Minimum energy: 134.14 kJ/mole

DIHEDRAL ANGLE: -40.00 DEGREE

Figure III-1 Energy map for di-carbazole (the four different colours show the relative stability of the structure: blue = very stable, red = less stable, hence less favoured structure)

III.3 Synthesis and analysis of monomers.

The monomers synthesised were as follows: N-propyl carbazole, N-butyl carbazole (three methods), 1-(N-carbazole)-6-[(4'-bromobiphenyl-4-yl)oxy]hexane and 1-(N-carbazole)-6-[(4-cyanobiphenyl-4'-yl)oxy]hexane.

They were analysed using techniques described in the experimental section.

Infrared Spectroscopy (IR) was used to monitor the bond changes from starting material to final product. The substitution of carbazole with the liquid crystal moiety: 1-bromo-6-[(4-cyanobiphenyl-4'-yl)oxy]hexane (illustrated in Figure III-2) for example can be followed.

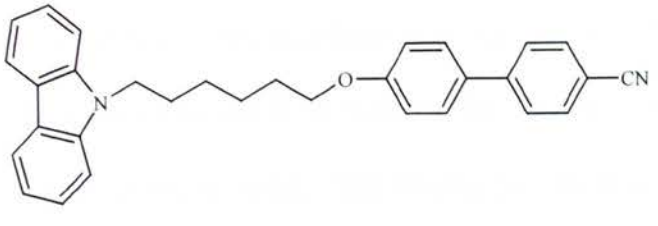

Figure III-2 1-(N-carbazole)-6-[(4-cyanobiphenyl-4'-yl)oxy]hexane

Comparison of the spectra from both starting materials (carbazole and 1-bromo-6-[(4-cyanobiphenyl-4'-yl)oxy]hexane) with that of the reaction product clearly shows the obvious combination of both molecules to form the latter. The spectra of both starting materials were very dissimilar but the spectrum obtained from the product combined almost all the features from both original spectra, as expected since only the linking groups from each 'half' of the molecule had been removed. The C≡N bond remained clearly visible at 2200cm^{-1}, indicating that the end group on the liquid crystal moiety was left unreacted. The various types of aromatic rings present in the product were distinguished by comparing the value of their peak to that in the spectra of the starting materials. The aromatic stretch peaks for the carbazole molecule were found to be at 722cm^{-1} and 756cm^{-1}, whereas that for benzene ring in the mesogenic moiety was found at 820cm^{-1}. All three distinct peaks were found in the substituted monomer at similar wavelengths. The other peaks were assigned using tables available on the Internet[105]. The values can be found in the Experimental section after the description of the synthesis.

Although the IR spectroscopy provided copious amounts of useful information about the molecules, a cross-reference with other techniques was required to confirm their identity. Proton NMR spectroscopy (^{1}H NMR) showed three distinct absorption areas for the product. (details in section II.2.6.2) As for the IR, the detailed values –when available- can be found in the Experimental section after the description of the synthesis. The data confirmed the results obtained from the IR spectra, but also allowed for the differentiation between the possible substitution sites on the aromatic rings. Confirmation of the occurrence of the substitution on the N- site of the carbazole was easily provided by the absence of an N-H peak in the spectrum (9-10ppm), together with no creation of a new hydrogen bond. The linking N-CH_2 bond can also be found as a triplet at 3.95ppm.

III.3.1 Mass Spectrometry (MS)

This method of analysis bases itself on the ionisation and fragmentation of the sample. This can be achieved by different means, such as bombardment with a high-energy electron beam (EI), chemical ionisation, field ionisation or fast atom bombardment (FAB). A mass analysis is then performed on the fragments obtained.

Although the standard (EI) technique of ionisation gave results for the simple molecules studied, the more complex molecules had to be studied using FAB, as their volatility was lower. The obtained results were fairly similar, but because the FAB technique resulted in the production of $(M+H)^+$ and $(M-H)^+$, the peaks were observed at (M+1) and/or (M-1), but not at M^+.

The illustrative example (Figure III-3) chosen here is 1-(N-carbazole)-6-[(4'-bromobiphenyl-4-yl)oxy]hexane (MW 498).

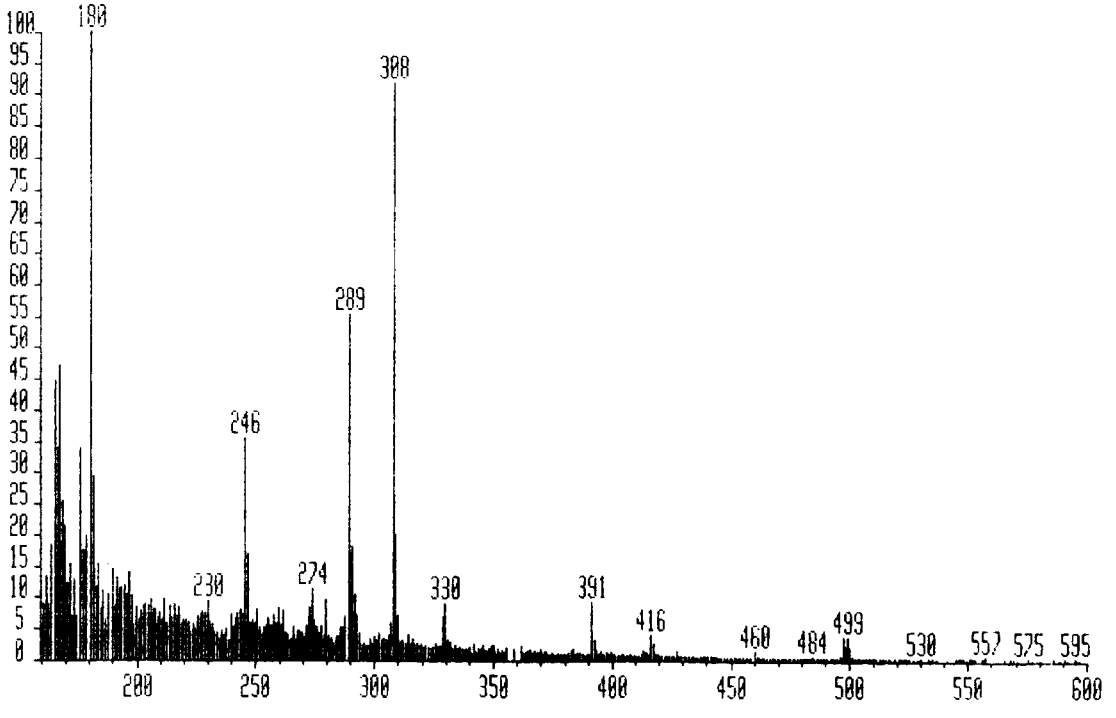

Figure III-3 FAB Mass spectroscopy data for 1-(N-carbazole)-6-[(4'-bromobiphenyl-4-yl)oxy]hexane

The FAB spectrum showed a double peak at m/e=499, which agreed with the expected M+1 value. More importantly, the two isotopic peaks were very close together and of similar intensity, confirming the presence of bromine in the molecule (isotopic

abundance Br^{79}=50%, Br^{81}=50%). Two other major peaks were observed at 289, which corresponds to $(carbazole+H)^+$, and at 308, corresponding to N-ethyl carbazole.

The data obtained from mass spectrometry are only of real significance in conjunction with the other techniques, but they give good information about the likelihood for the molecule to fragment at specific bonds, and about the stability of the fragments formed.

III.3.2 Visible and Ultraviolet (UV/Vis) Spectrometry

The absorption of electromagnetic radiation in both the visible and ultraviolet regions of the spectrum results in electronic transitions between molecular orbitals. The absorbance is measured versus the wavelength. Although of limited interest for the identification of molecular species, UV/Vis spectrometry provides information on the energy levels in the molecule. Its main purpose in the present work was to provide the value of Eg, the energy gap, of the polymeric products. The relation between the extrapolated wavelength of absorption onset (λ_0) and Eg is $1/\lambda_0$ = Eg/hc, with c the speed of light (299792458 ms^{-1}) and h is the Planck constant ($6.6260755 \times 10^{-34} Js^{-1}$). In the case of doped polymers, the position of the intermediate energy states were obtained from the absorption maximum of further peaks at longer wavelengths, using the same formula. The different energy levels are illustrated in Figure III-4.

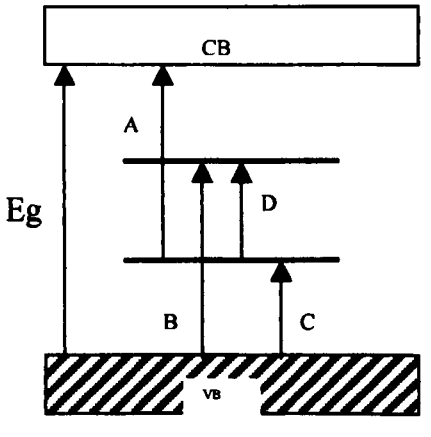

Figure III-4 Representation of the different energy levels between valence and conduction bands

If we consider the two polaron levels between the valence and the conduction band, then gaps A and B would be of approximately the same value, C would be small, and D would be even smaller (not detectable in the UV/Visible region).

Poly(N-methylcarbazole) (pNMC), prepared using emulsion polymerisation was studied undoped as well as doped and provides a good illustrative example (Table III-1).

Sample	Colour	Peaks /nm	Shoulder /nm	λ (nm), Eg (eV)	λ (nm), Polaron (eV)
pNMC	Pinkish	241 (S), 266 (M/S), 295(M)	≅ 330(w)	415, 2.99	890, 1.39
pNMC + ammonia	Pinkish	241 (S), 266 (M/S), 295(M)	≅ 330(w)	375, 3.30	N/A
pNMC + H_2SO_4	Pinky-brown	241 (S), 266 (M/S), 295(M)	≅ 330(w)	550, 2.25	850, 1.46
pNMC + H_2SO_4 +$Na_2S_2O_4$	Green	287 (v.S)	N/A	365, 3.39	N/A
pNMC + $Na_2S_2O_4$	Green	260 (w), 285 (v.S), 330(v.w)	N/A	320, 3.87	N/A

Table III-1 UV/visible data for poly-N-methyl carbazole (pNMC) under different conditions

As expected, it was observed that doping with sulphuric acid resulted in a narrowing of the band gap and a decrease in the polaron energy, whereas deprotonation using ammonia yielded a larger band gap than that of the starting material, and moreover the polaron could not be detected any more. The value observed for the Eg of the original sample was slightly lower than expected, probably due to some residual ferric chloride from the polymerisation medium. This value increased when the sample was treated with sodium dithionite, as its strong reducing properties removed the last traces of dopant (ferric chloride). The decrease in Eg and polaron energy in the sample treated with sulphuric acid was linked to the fact the doping was of a different type from the residual dopant initially observed (combined with the residual dopant effect). For the initial sample, the value of the polaron transition energy (about half that of Eg) seemed to indicate a single polaron level between the valence band and the conduction band. In the case of the protonated sample, the value obtained for the polaron was closer to two

third of Eg, consistent with two polaron levels (distances shown as A and B in Figure III-4). In the case of treatment with both sodium dithionite and sulphuric acid, the protonation effect only was observed, as the reduction process counteracted the residual dopant. The ammonia treated sample was fully deprotonated, but still showed the oxidising effect of the residual ferric chloride.

III.3.3 Elemental Analysis

The results for Elemental Analysis can be found in Appendix V.2. Although the required amount of compound was very small (2-5 mg/analysis) some samples (e.g. the liquid crystal carbazole derivative) were still too small for significant data to be obtained. In the case of the polymeric materials, two problems arose: the molecules were difficult to pyrolise, which also made mass spectrometry difficult, and two of the samples still contained residual iodine from the polymerisation. This is likely to be the reason for the absence of evidence for bromine in the polymer of the model carbazole, and for the lack of exploitable data from poly(N-methyl carbazole).

Although three of the samples provided data of exploitable quality, two of them had non-negligible amounts of contaminant, possibly from degradation of the sample, or in the case of carbazole, from the difficulty of separation after synthesis.

III.3.4 Molecular modelling and the monomers

The molecular modelling software was used to predict properties as well as assist the interpretation of the spectroscopic data for monomers.

III.3.4.1 Simulation of properties of monomer molecules

After molecules had been created in the molecular modelling package, it became possible to obtain information quickly that, although possible to calculate manually, would otherwise take some time to process. Such information includes molecular formula, molecular mass, and the expected values for elemental analysis. More advanced calculations allowed values for properties such as polarisability to be obtained.

Chemical Sample	Molar mass $g.mol^{-1}$	Polarizability	Dipole Moment (debye)	Lambda Max UV-Visible (nm)	Total Energy (Hartree)	Heat of Formation (kcal/mole)
1-[(aniline-2-yl)oxy]-6-[(4-cyanobiphenyl-4'-yl)oxy] hexane	386.493	36.807	5.568	197.493	-199.531	18.314
1-(N-carbazole)-6-[(4-cyanobiphenyl-4'-yl)oxy]hexane	444.575	43.628	3.535	232.917	-222.12	85.414
1-(N-pyrrole)-6- [(4-cyanobiphenyl-4'-yl)oxy]hexane	344.455	32.687	2.942	288.719	-174.765	57.006
1-[(aniline-2-yl)oxy]-6-[(4-biphenylcarboxylic acid-4'-yl)oxy] hexane	405.493	35.781	3.829	197.75	-216.479	-105.881
1-(N-carbazole)-6-[(4-biphenylcarboxylic acid -4'-yl)oxy]hexane	463.575	43.31	2.51	239.375	-239.054	-39.323
1-(N-pyrrole)-6- [(4-biphenylcarboxylic acid -4'-yl)oxy]hexane	363.455	32.472	2.352	191.876	-191.682	-67.44
1-(N-carbazole)-6-[(4'-bromobiphenyl-4-yl)oxy]hexane	498.461	42.646	1.285	236.916	-219.215	58.103
Carbazole	167.21	16.705	1.03	231.768	-81.83	53.921
1-bromo-6-[(4-cyanobiphenyl-4'-yl)oxy]hexane	358.277	29.022	3.156	289.091	-151.605	26.186
N-butylcarbazole	223.317	21.361	1.737	235.485	-110.423	36.195
N-methylcarbazole	181.237	18.196	1.605	238.572	-88.961	53.406
N-propylcarbazole	209.29	20.329	1.365	238.247	-103.274	41.465

Table III-2 Modelled properties of various monomers

The package also provided the possibility to obtain reasonably accurate predictions for spectroscopic data.

III.3.4.2 Simulation of Infrared and UltraViolet/Visible spectra.

After the molecule had been optimised, one of the features that could be related to experimental results very easily was the prediction of the spectrometric data.

III.3.4.2.1 Infrared

Cache enabled the user to view an infrared spectrum of transitions for a molecule. To simulate the co-ordinated motion of the atoms as electromagnetic radiation in the infrared region is absorbed by the molecule, quantum mechanics was used to compute the necessary force to distort the molecule from its equilibrium geometry. By doing so the frequency of vibrational transitions could be predicted. Absorptions are associated with bending as well as stretching of particular bonds, and by selecting a point on the vibrational spectrum, motion vectors appear in the workspace, indicating what type of transition yielded that specific peak, as featured in Figure III-5.

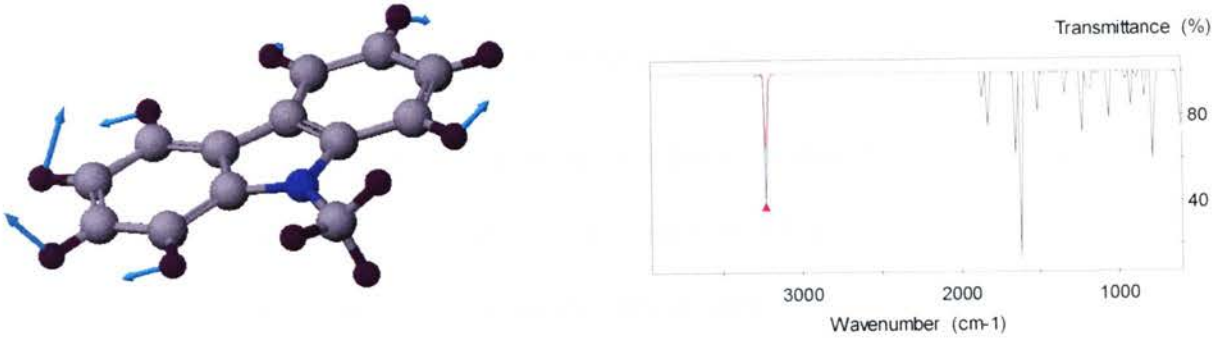

Figure III-5 Infrared spectrum of N-methyl carbazole showing the molecular vibration

III.3.4.2.2 UV/visible

Cache was also used to view UV/visible spectra as created by electron transitions between molecular orbitals in the molecules. Quantum mechanics was used to compute

the energies of excited electronic states. As for infrared spectra, when a particular transition point was selected on the spectrum, the molecule was displayed in the workspace with the molecular orbitals superimposed on it, as shown in Figure III-6.

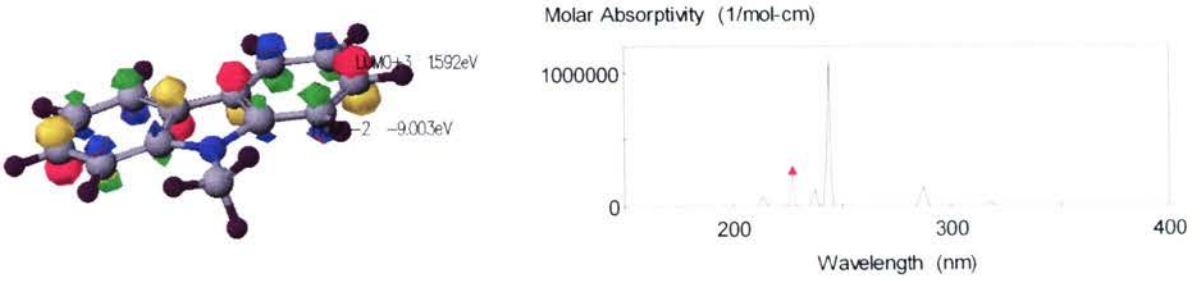

Figure III-6 UV/visible spectrum for N-methyl carbazole and corresponding orbitals

A detailed comparison of modelled and experimental spectroscopic data can be found in section III.6.1.

III.4 Synthesis and analysis of polymers.

III.4.1 Oxidative Chemical polymerisation techniques

The mechanism of polymerisation for aniline has been expressed in various ways and the one shown in Figure III-7 and Figure III-8 is only one of them. The first step shown in Figure III-7 is the formation of the radical cation, then the possible delocalisation of the radical.

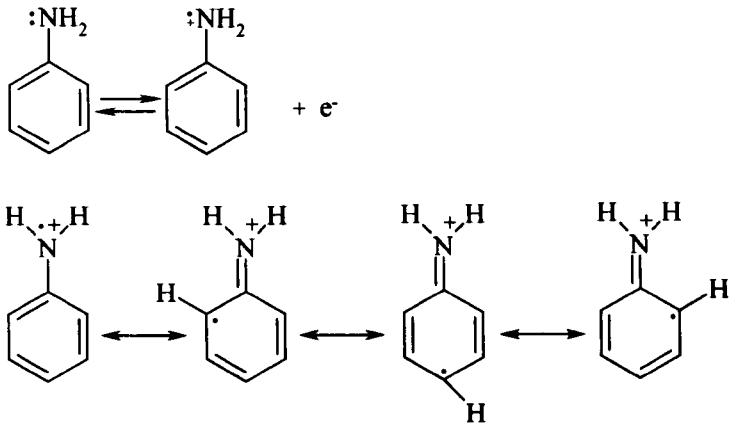

Figure III-7 Radical cation formation and delocalisation in aniline[29]

Figure III-8 shows the polymerisation process itself.

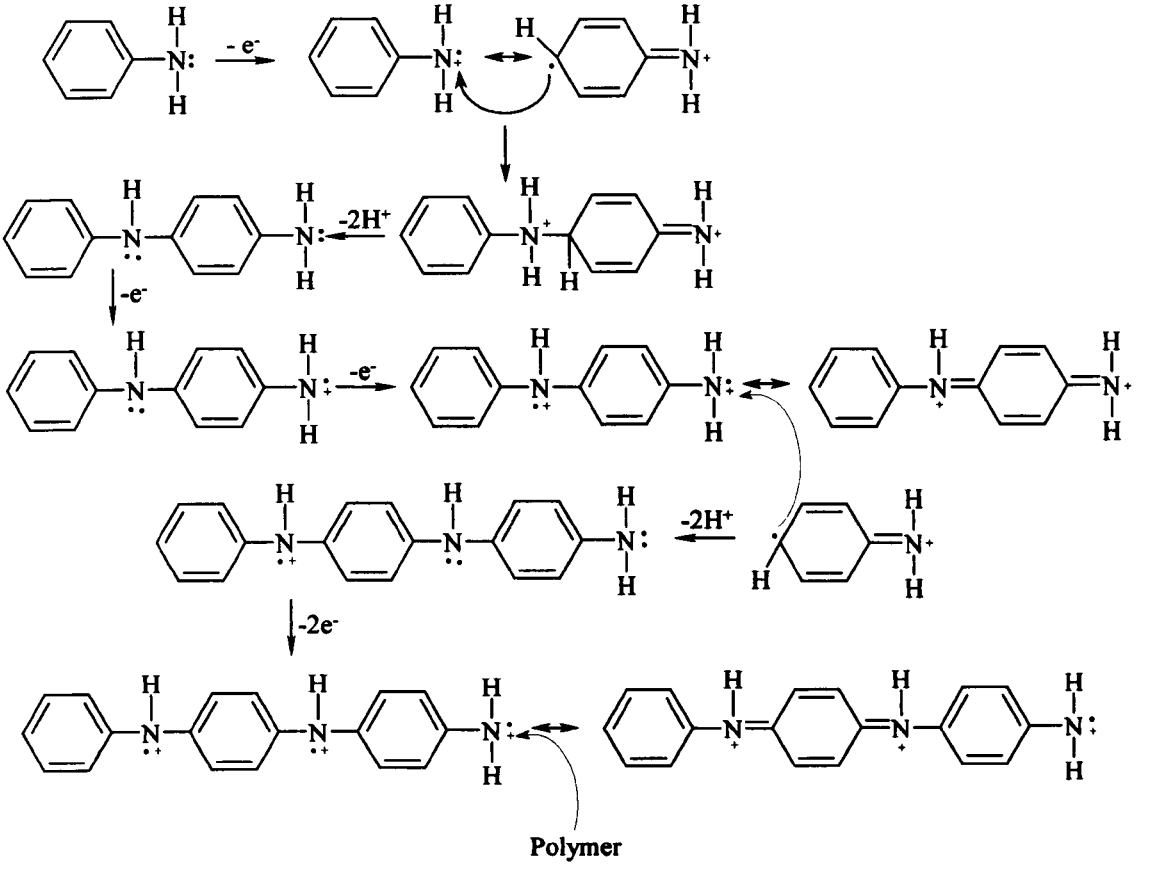

Figure III-8 Mechanism of polymerisation for the formation of polyaniline[29]

III.4.1.1 Emulsion polymerisation

The use of emulsion polymerisation is known from the literature[29, 92] to provide a combination of a good yield together with the ability to produce spherical particles of

fairly even size, thus enabling some control of the rheology of the polymer powder produced.

The method described in previous work used dodecylbenzenesulphonic acid (DBSA) as the surface active agent, which, although it had the advantage to provide an acidic medium and doping agent in itself, was not easy to remove fully from the polymer. The use of a non-ionic surfactant was investigated in the hope that a similarly good yield would be obtained but with an easier recovery and cleaning of the polymer, as the emulsion could easily be broken by the addition of methanol.

For the polymerisation of 2-methoxyaniline using non-ionic surfactant the same route as the one used for the ionic surfactant was first tried but did not yield any polymer. The method used to form poly(2-methoxyaniline) was adapted from the formation of poly(unsubstituted aniline) using a different surfactant, as described by Gan *et al*[92]. Brij 35 (commercial name for polyoxyethylene 23 lauryl ether) was chosen for its chemical similarity as well as for its availability. The use of 3M hydrochloric acid compensated for the absence of the protonating ability of DBSA in the non-ionic experiment. As no further information could be found, the amount of surfactant required in order to obtain a stable emulsion had to be determined before carrying out any other experiment. Compared to unsubstituted aniline, the presence of the methoxy group as an ortho-substituent in the o-anisidine seemed to result in the molecule being less reactive but the use of longer side chains increased the solubility of the resulting polymer without any major change in the reaction time. Different experimental conditions were tried, such as changing the amount of surfactant, which suppressed the reaction at too low a concentration (probably due to the emulsion not being stable enough). Working at lower temperature (around 5°C) was also attempted but the only change noticed was that the particles formed precipitated less easily, presumably because of a decrease in their size. The different attempts are described in Table III-3. This shows that the ratio of

surfactant to monomer which gave the optimum result was the one reported in the experimental procedure: between 1:1 and 1.5:1 surfactant:monomer ratio for each of the starting emulsions. This ensured the stability of the emulsion throughout the experiment but yielded an easily retrieved solid. (The emulsion could be dispersed with no difficulty by excess methanol or water).

The size of the particles formed was observed using TEM on the reaction mixture diluted with excess water. Spherical clusters (diameters 100 to 350 nm) formed of small even spherical particles (average diameter 27 nm) were observed (as illustrated in Figure III-9 and Appendix V.3). The shape as well as the dimensions of the small particles was consistent with the ones described in the literature[92] when a different non-ionic surfactant was used (poly(oxyethylene)$_{5,9}$ nonyl phenol ether), However no mention was made of the clusters.

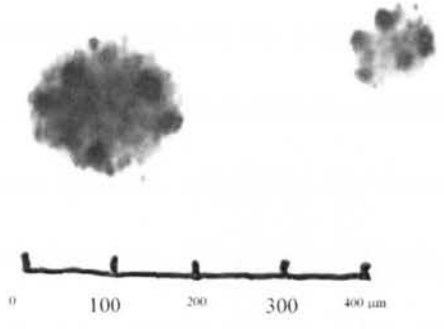

Figure III-9 Detail of TEM scan (magnification x 37,000)

As the distribution of the clusters themselves appeared to be non-uniform throughout the observed sample of the emulsion, it is likely that sonication would have dispersed the particles, preventing the clusters from being observed. The information provided is still valuable as the size of the clusters is believed to be similar to the size of the droplets within the microemulsion. A representation of a typical microemulsion medium can be found in Figure III-10.The species dissolved in those droplets, due to the

dynamic nature of the microemulsion, can mix and react rapidly between the droplets, making this method ideal for the preparation of small spherical particles. The TEM picture in Figure III-9 shows that although assembled as clusters, the particles produced were indeed spherical and of even diameter.

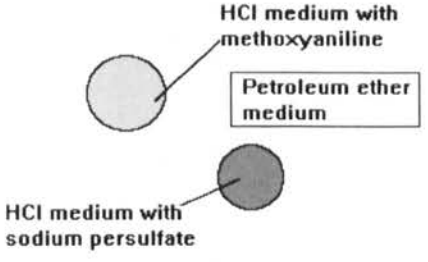

Figure III-10 Microemulsion medium for the polymerisation of methoxyaniline

The two colours observed for the resulting polymer are its protonated (green) and deprotonated (blue) forms. The interconvertibility of those forms can be shown by exposing the deprotonated film to acid vapour (or by immersing it in an acid solution) or (as used in the experimental procedure) by immersing the protonated form of the polymer in a base solution. It is to be noticed that the deprotonated form was stable with time, as it kept its properties (colour, solubility) for several months. The polymers obtained showed a high solubility in chloroform in both their protonated and non-protonated forms, even after a long period of time. After evaporation some of the films of poly-2-methoxyaniline exhibited a metallic foil-like appearance, while having good film-forming ability, which is typical of longer chains of polymers.

Infrared spectra were run from the poly-2-propoxy- and poly-2-butoxy-aniline films and the obtained values (detailed in sections II.3.1.3 and II.3.1.4) confirmed the expected functionalities.

Table III-3 summarises the different emulsion polymerisation experiments and their results.

Table III-3 Emulsion polymerisation results for various aniline derivatives

Aniline monomer	Amount /g	Surfactant /g	Conditions	Solid/ solution	Yield /g	Yield %	Solubility	Deprotonation	Observations
2-methoxy-	0.2200	0.40	None	green/green	0.0355	16.1	No	Yes	Turned to reddish with blue/green precipitate within seconds after mixing
2-methoxy-	0.2035	0.20	$FeCl_3$	green/green	0.0801	39.4	No	Yes	Turned burgundy within seconds, gas formation
2-methoxy-	0.2047	0.20	Ice, $FeCl_3$	green/black	0.1262	61.7	No	Yes	Burgundy in minutes, after a few hours: black particles in suspension.
2-methoxy-	0.5217	0.50	None	green/green	0.2595	49.8	No	Yes	Foam formed on emulsion mixture.
2-methoxy-	0.5080	0.70	None	green/green	0.2860	56.3	No	After ten minutes, blue/green solid on walls of beaker.	
2-methoxy-	0.2042	0.15	None	green/green	0.0335	16.4	No	Green after 24 hrs, rapidly darkened upon mixing.	
2-methoxy-	0.2009	0.30	None	green/green	0.0547	27.2	No	Green after 24 hrs.	
2-methoxy-	0.2005	0.40	None	green/green	0.0523	26.1	No	Green after 18 hrs, green lumps on walls after 5 min.	
2-methoxy-	0.2041	0.60	None	green/brown	0.0398	19.5	No	Dark burgundy after 10 min, TEM	
2-propoxy-	0.2023	0.40	None	green/green	0.0385	19.0	$CHCl_3$	Green after 3hrs	
2-butoxy-	0.2078	0.40	None	green/green	0.0715	34.4	$CHCl_3$	Green after 3h	

Further TEM and rheological studies would enable one to directly link the size of the particles produced to the conditions used, and provide a fuller insight into the optimum

temperature, relative concentrations etc to control the final product while keeping a high yield. The facilities were unavailable at the time to carry out these experiments.

III.4.1.2 Chemical polymerisation of 1-(N-pyrrole)-6-[(4-cyanobiphenyl-4'-yl)oxy]hexane

The polymer formed through chemical oxidation in a hydrochloric acid solution using ferric chloride and 1-(N-pyrrole)-6-[(4-cyanobiphenyl-4'-yl)oxy]hexane softened at quite a low temperature (~90°C) and the liquid crystalline properties would certainly be possible to observe under very slow cooling. Nevertheless the overall yield (<0.01 g) of high molar mass polymeric material was not as good as for the electropolymerisation (section II.3.4), as a lot of non film-forming oligomer was formed. This could probably be overcome by running the reaction for a longer period, or by changing the amount of ferric chloride used, in both cases allowing the polymer chains to grow longer by avoiding premature termination of the chains. With careful handling of the film an infrared spectrum was run, and although the aromatic C-H stretching band was not observed in the 3000/3100 cm^{-1} region due to the shape of the spectrum (broad peak masking that area), the other values (section II.3.3) recorded were consistent with the expected structure.

III.4.1.3 Polymerisation of carbazole derivatives using liquid iodine

The idea of using liquid iodine as a medium for polymerisation came about while looking for papers on electrical properties of polycarbazole derivatives. Papers by Wellinghoff *et al*[102,103] claimed that the use of molten iodine as a solvent for a carbazole derivative would not only induce the polymerisation by oxidation of the monomer to the radical cation, followed by dimerisation and formation of the dication, but also that the

resulting polymer would be stable and of high conductivity. The experiment was replicated in this project using N-methyl carbazole and 1-(N-carbazole)-6-[(4'-bromobiphenyl-4-yl)oxy]hexane in place of the 3,6-diiodocarbazole they had used, and the experiment was performed on the bench-top as well as in an NMR tube so that NMR spectra could be obtained at the same time as the temperature was increased to allow the reaction to be followed. The resulting series of spectra for 1-(N-carbazole)-6-[(4'-bromobiphenyl-4-yl)oxy]hexane can be found in Appendix V.4.

Although the polymerisation did proceed in a satisfactory way, the excess of iodine proved too great to allow full removal from the polymer and gave an apparent yield of about 2000%!. This suggestion was confirmed by the results from elemental analysis performed on polymer samples that were thought to have been thoroughly cleaned (by washing the iodine with solvent and using gentle heating under vacuum to remove the last traces of I_2). The appearances of the NMR spectra were found to be less well defined than that featured in the paper by Wellinghoff, probably due to the different monomer used. It was clear however, that almost all the monomer was used up, even in the case of the model monomer, as the original broad peak of the monomer was observed to disappear during the polymerisation, while new peaks appeared that increased in size as the polymerisation progressed. No further experiments could be performed on the samples because of the lack of processability of the resulting metallic black powder (note: the metallic appearance is thought to be due to the remaining iodine). Although the TMS was present in both samples to provide an internal standard, it did not show in the spectra, as it most probably vaporised in the tube.

In both cases the ^{1}H NMR spectra showed a similar pattern (see Appendix V.4 for the series of spectra obtained for 1-(N-carbazole)-6-[(4'-bromobiphenyl-4-yl)oxy]hexane). The equipment was set to increase the temperature to 435K. The following data refer to the experiment on 1-(N-carbazole)-6-[(4'-bromobiphenyl-4-yl)oxy]hexane. The first

spectrum (V.4.1) was recorded at 370K and showed a very broad peak that was obviously hiding at least 3 sharp peaks or groups of peaks for which the tips could still be seen at 4.80ppm, 7.28ppm and 8.06 ppm. The following spectrum (V.4.2) was recorded at 406K, and showed a noticeable decrease in the previously observed peaks, but the broad overall peak was still present. The following spectrum (V.4.3) was recorded at 435K, after the temperature had been reached for 5 minutes. The disappearance of the broad peak can probably be attributed to the fact that prior to reaching that temperature the sample was not fully liquefied. A large new peak was observed at 5.29ppm with a shoulder at 5.84ppm. Two smaller ones respectively at 2.97ppm and 7.72ppm were also noticeable. Spectrum V.4.4 was recorded after 20 minutes of the temperature being stable at 435K. A medium sized peak had appeared at 10.48ppm. The large peak had disappeared but the previously observed shoulder was now on the right of an even higher peak at 6.24ppm, and another shoulder had appeared at 6.83ppm. The small peak at 2.97ppm was not visible any more but what appeared to be a doublet could be seen at 4.00ppm and 4.23ppm. The temperature was then increased to 440 over 10 minutes. Spectrum V.4.5 was recorded after the temperature had been stable at 440K for 10 minutes. The following peaks were observed: 11.17ppm (medium, broad), 8.73ppm (small, sharp), 7.53 (small, badly defined), 6.89ppm (large, sharp), 5.77ppm (small, sharp), 4.53ppm (large, sharp). When spectrum V.4.6 was recorded, after 35 minutes at 440K, all the peaks looked like they had decreased except for the one at 6.89ppm, which could be observed at 6.99ppm. In spectrum V.4.7, recorded after 50 minutes, all the peaks have smoothed out into a broad peak with shoulders and two summits at 5.85ppm (the highest) and 4.78ppm. After 65minutes, in spectrum V.4.8, the large peak had narrowed down to one summit at 5.35ppm and a noticeable, although low, shoulder at 6.59 ppm. Spectrum V.4.9 was recorded after 80 minutes, and a very sharp peak can be seen at 5.00ppm. A lower but also sharp peak can

be observed at 6.48ppm. In spectrum V.4.10, recorded after 125 minutes, a similar pattern was observed, with a decrease in the peak at 5.00 ppm (observed here at 4.84 ppm). In the following spectrum (V.4.11, recorded after 140 minutes) that originally large peak had decreased even more, and two major peaks were observed at 7.03 and 9.03 ppm, with a minor peak at 7.30 ppm. After a further 15 minutes, spectrum V.4.12 was recorded and an increase was observed in the peak around 7 ppm, while the 4.8 ppm peak had decreased. This trend was confirmed in the following spectrum, V.4.13 recorded after 170 minutes. At this point the cooling process was started as it seemed likely the reaction had reached completion. The experiment was stopped because the time allowed for the reaction was at that point much longer than what had been described in the literature. Spectrum V.4.14 was recorded after 15 minutes of cooling, at a temperature of 347K. The spectrum obtained confirmed that the product of reaction was different from the starting material. Infrared spectroscopy did not allow to verify the structure of the product because of the excess iodine in the sample. Further studies could help to investigate the intermediate species responsible for the peak observed at 11 ppm, which is likely to be due to the formation of the radical cation.

III.4.2 Electro-polymerisation

III.4.2.1 Carbazole derivatives

The shape of the cyclic voltammograms obtained from the experiments (illustrated with N-butylcarbazole in Figure III-11) performed on the carbazole derivatives was in accordance with those for typical polymerisation and redox reactions of conducting polymers and the IR spectrum of the polymer film obtained from N-methyl carbazole confirmed the expected structure.

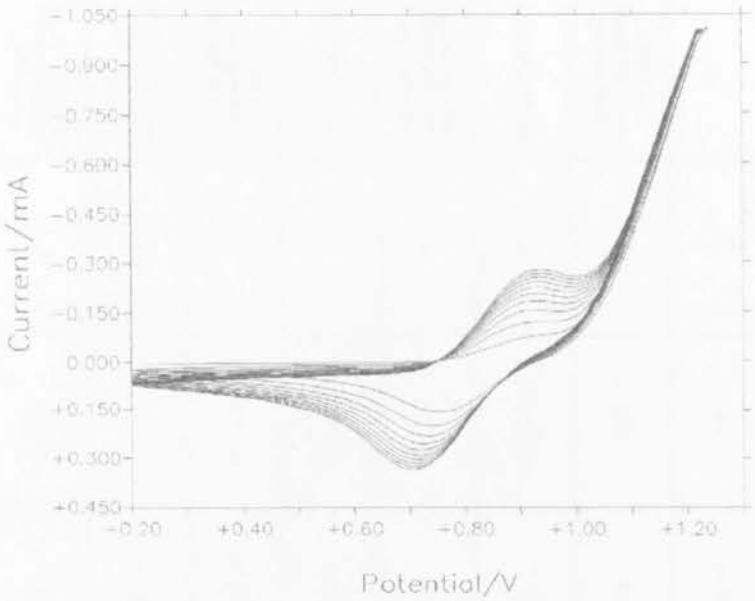

Figure III-11 Cyclic voltammogram for N-butylcarbazole

Further study will be needed to confirm irrefutably that the position of the bond in between monomer units of the polymer backbone is regularly the one predicted. The electrochromic behaviour (dark green at higher positive potentials, yellow at lower potentials) was witnessed every time for the first few cycles after which the dark green colour would persist. Those observations are consistent with those reported in the literature [106,107,108].

The potentials observed for the polymerisation and dedoping of different monomers under different conditions are reported in Table III-4.

Monomer	Specific conditions	Scan range / V	Oxidation potential(s) / V	Reduction potential(s) / V	Film formation	Observations
N-methyl carbazole	Prop. Carb ITO	-0.2 to 1.2	1.0 to 1.2	0.65	✓	Plateau at 0.9V and film growth if cycle = 1.0-1.1V
N-methyl carbazole	Prop. Carb Platinum	-0.2 to 1.2	0.95	0.75	✓	Plateau at 0.9V and film growth if cycle = 1.0-1.1V
N-methyl carbazole	Acetonitrile ITO	-0.2 to 1.6	1.0 to 1.6	0.75	soluble	No plateau effect, but positive slope
N-butyl carbazole 0.05M	Prop. Carb ITO	-0.2 to 1.6	1.07 to 1.2	0.7 to 0.75	×	Not concentrated enough for film growth
Carbazole	Prop. Carb ITO	0.0 to 1.3	1.1 to 1.2	0.77 to 0.82	✓	Plateau from 1.2V
1-(N-carbazole)-6-[(4'-bromobiphenyl-4-yl)oxy]hexane	Acid medium HCl/methanol	0.0 to 1.0	0.9	0.75	×	Plot rather flat, but good sharp slope at 0.8/0.85V
1-(N-carbazole)-6-[(4'-bromobiphenyl-4-yl)oxy]hexane	Prop. Carb ITO	0.0 to 1.3	1.1	0.60 to 0. 77	✓	Plateau from 1.1V
1-(N-carbazole)-6-[(4'-bromobiphenyl-4-yl)oxy]hexane	Methanol/H2SO4 3:1	0.1 to 1.3	1.15	0.65	✓	Steep start, but flattens out almost completely
N-methyl pyrrole	Prop. Carb ITO	-0.3 to 2.0	1.6 to 1.7	1.0	✓	
1-(2-cyanoethyl) pyrrole	Prop. Carb ITO	-0.4 to 1.9	1.6	0.4	✓	Flattens quickly, no obvious dedoping
1-(N-pyrrole)-6-[(4-cyanobiphenyl-4'-yl)oxy]hexane	Prop. Carb ITO	-0.3 to 1.9	1.4	0.6	✓	

Table III-4 Cyclic voltammetry results

The use of acetonitrile suggested in the literature[29] as a solvent for the electrolyte salt did not give satisfactory results since the polymeric material proved to be soluble in acetonitrile, and could not be isolated. The green solid yielded a green solution that turned yellow upon heating. The green colour returned after the solution had been left to cool and stand at room temperature for a few minutes. The acid solution was eventually used as electrolyte because a fairly high concentration of monomer was required in order to produce a film that could be recovered from the acetonitrile solution.

The testing for solubility was studied for N-methyl carbazole in order to determine an appropriate medium for the electro-polymerisation. Typically the procedure for determining the solubility was to try and dissolve a few milligrams of the compound in about 5ml of solvent at room temperature. The sample was left stirring overnight if no immediate dissolution was observed. The system would then be heated to assess the potential solubility in hot solvent. The results of the solubility tests performed on poly(N-methyl carbazole) can be found in Table III-5.

Solvent	Solubility parameter[109]	Cold	Warm
Acetone	9.3	Partially	✓
Acetonitrile	11.9	Partially	✓ (thermochromic)
Chloroform	9.3	✗	✗
Diethyl ether	7.4	✗	✗
Ethyl acetate		✗	✗
Hexane	7.3	✗	✗
IMS		✗	✗
Methanol	14.5	Partially	✓
Petroleum spirit 40-60		✗	✗
Toluene	8.9	✗	✗
Water	9.4	✗	✗

Table III-5 Solubility of poly(N-methylcarbazole)

III.4.2.2 Pyrrole derivatives

The cycles were run between potentials of -300 mV and 1700/1800 mV with a scan speed of 0.1 V/s. The observed potentials for the formation of the polymer films and for the dedoping of the films formed are reported in Table III-4:

The range of potentials used was extended to values up to 2000 mV, but no obvious difference was observed. The voltammogram below shows the typical shape for the electrodeposition of polymer from the model monomer, between -350 mV and 1700 mV (first 5 cycles only shown).

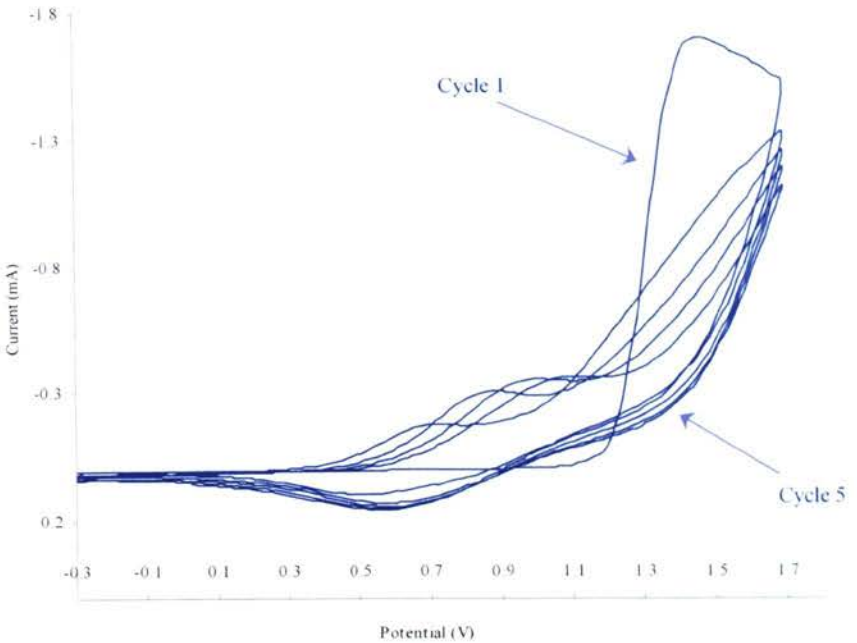

Figure III-12 Cyclic voltammogram for 1-(N-pyrrole)-6-[(4-cyanobiphenyl-4'-yl)oxy]hexane

The formation of the film can be seen where the voltammogram shows a shoulder (at about 1000 mV), and the dedoping of this film occurs at 600 mV (change in sign for the slope indicates the optimum potential for dedoping). The observed shape of the voltammogram is very much the same for all three monomers studied, with the slight variations reported in the above table. The films studied were formed during at least 30 cycles, after which the voltammograms would get 'flat', indicating that the amount of current flowing was getting lower because of the thickness of the film.

III.4.3 Molecular modelling of polymers

Data were obtained for the polymers as well as for the monomers, but because of the computer memory limitations, only oligomers could be modelled. However, as can be seen from the compared spectra in section III.6.1, it gives a good approximation of some of the expected behaviour for larger molecules.

The energy minimisation of molecules provided very encouraging results as the model confirmed the favoured conformations of the carbazole derived molecules, with the substituent pointing alternately up and down, so as to avoid the molecule forming a coil. This can be seen clearly in Figure III-13. If this more extended, linear structure were indeed the favoured one, the potential for electrical conduction would be high, as the delocalisation of electric charges could happen a lot more easily.

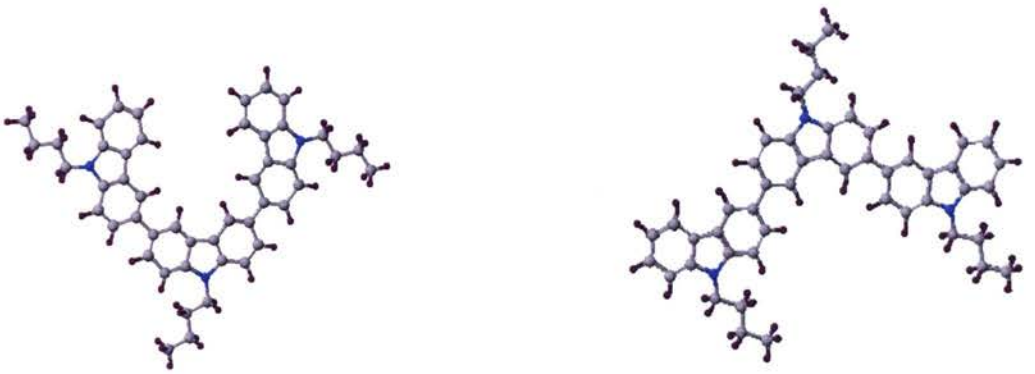

Energy = 1224.62 kJ/mol Energy = 475.03 kJ/mol

Figure III-13 Minimised and un-minimised structures of tri-N-butyl carbazole

Further calculations of the different potential energies were carried out for three different structures of tetra-N-methylcarbazole: coiled, extended, and with random angles between the carbazole units (Figure III-14).

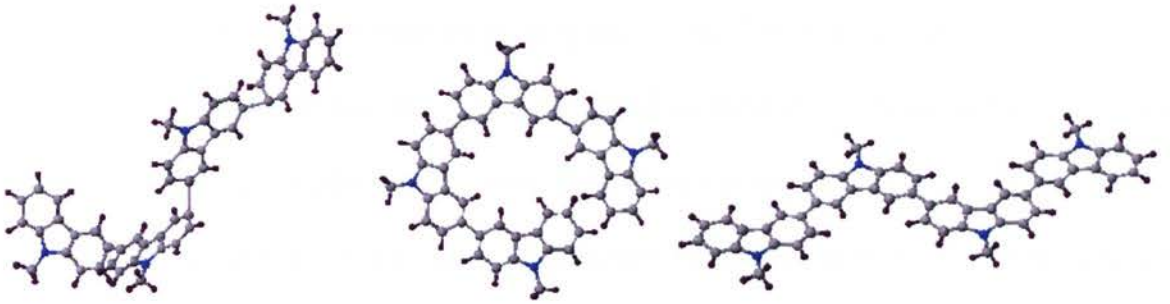

5735.41 kJ/mol 2574.25 kJ/mol 607.30 kJ/mol

Figure III-14 Potential energy of different structure of tetra N-methyl carbazole

The results confirmed what was expected, in that the energy for the 'random' molecule, with arbitrary bond angles, was much greater (5736 kJ/mol) than the one for the coiled molecule (2575 kJ/mol) which in turn had a higher energy than the extended molecule (607 kJ/mol). Those results confirm that, in the case of the computerised molecular model, the elongated structure of poly-carbazole derivatives is favoured. As mentioned before, this property, combined with its redox-active nature, emphasises its potential ability for electrical conduction.

III.4.3.1 Prediction of Various Physical Data using 'Project Leader' Software.

A separate more advanced section of the software package allowed further data to be obtained.

III.4.3.1.1 Specific Polymer data

The polymer models were generated by indicating to the software the linking atoms on the monomer. The software uses the repeat unit as basis for the calculations. Calculations were carried out using the models and equations detailed in J. Bicerano's 'Prediction of Polymer Properties'[110]. The technique is based on experimental property-related data recorded for hundreds of polymers. The data were correlated so as to give rise to a set of semi-empirical models that could be applied to predict properties of new polymers. The techniques use a combination of numerous derived parameters to predict the relevant properties of the modelled polymer from its monomer unit. Although this system is adequate for properties not affected by the chain length, it makes un-mentioned assumptions about properties that are affected by the length of the chain, e.g. Tg.

Although it is not yet part of the molecular modelling package, it is possible that the properties related to liquid crystallinity could be studied for large numbers of molecules and that those data could be correlated to predict liquid crystallinity in different molecules.

At the time of printing, the molecular modelling package cannot give any direct prediction of liquid crystallinity of the molecules modelled. However, by modelling properties potentially related to liquid crystallinity for known available mesogens the prediction of such properties could become possible. Work of this type is under investigation at Kingston University by Dr R. Singer.

III.5 Liquid crystal properties of monomers and polymers

III.5.1 Hot stage microscopy

The first part of this work was carried out on previously produced nitro-compound precursors to the aniline monomers (Figure III-15). The observations resulting from the heating and cooling of those materials, allowed one to check the previously reported textures[29] (Table III-6).

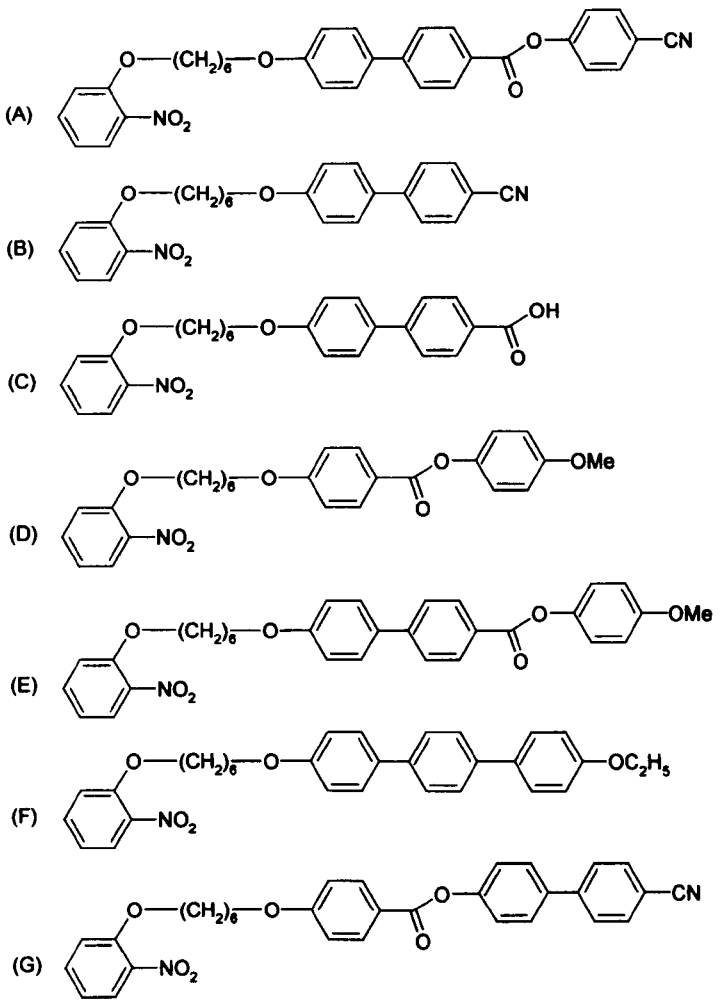

Figure III-15 Nitro-compounds used in the Hot Stage Microscopy experiments

Compound	Experimental LC transition(s) °C	Experimental isotropic melt °C	Literature LC transition(s) °C	Literature isotropic melt °C
A	139.8(N)	192.4	136.0(N)	190.1
B	56.6(N)	96.1	55.3(N)	95.3
C	156.0(S), 173.4(S), 217.5(N)	228.6	157.3(S), 175.7(S), 214.0(N)	227.3
D	56.6(N)	89.1	56.5(N)	88.3
E	75.0(S), 119.6(N)	179.5	72.5(S), 115.2(N)	181.4
F	149.0(N), 221.7(S)	230.0	147.7 (N), 222 (S)	230.3
G	121.2(N)	200.0	124.0 (N)	199.8

Table III-6 Transition temperatures observed using Hot Stage Microscopy for nitro-compounds (N is a nematic phase, S is a smectic phase)

The observation of new materials however was less successful, as the carbazole derivatives proved to be more heat sensitive than their aniline equivalents. As a result, the monomers only exhibited some temperature-dependent changes in the transmission of the polarised light, but no texture was characterised, while the polymers appeared to degrade before any texture could be observed. The use of DSC as well as the prediction of the polymer Tg using the molecular modelling package confirmed that the Tg of the carbazole polymers was higher than that of substituted polyanilines, and hence higher than the liquid crystal transition temperature, which explains why the liquid crystalline textures were not observed.

III.5.2 DSC

The obtained data for various species can be found in Table III-7.

The use of DSC provided data concerning the transition temperatures of the liquid crystals and the polymers as well as the possible thermal degradation of the materials. It was especially useful in cases where the transition temperature of the liquid crystal could not be determined by observation under hot stage microscopy.

The peaks obtained at low temperature are thought to have been due to loss of residual solvent.

The endothermic peaks observed at higher temperatures were typically degradation peaks.

The peak thought to be due to the glass transition temperature of the polymer, and that linked to liquid crystal transitions are featured in Table III-7.

Sample	Gas	Peak type[a]	Peak temp /°C	Peak intensity[b]
Poly(N-butyl carbazole)	Air	Endo.	57	S
		Endo.	220 (Tg)	M/S
		Endo.	317	M/S
		Exo.	335	M/S
	N_2	Endo.	58	S
		Endo.	335	M/S
Poly(N-propyl carbazole)	Air	Endo.	49	S
		Endo.	218 (Tg)	M
		Endo.	318	v.S
	N_2	Endo.	50	S
		Endo.	199	M/S
		Endo.	328	S
polycarbazole	N_2	Endo.	246	VS
		Endo.	293 (Tg)	M/S
Poly(1-(N-carbazole)-6-[(4'-bromobiphenyl-4-yl)oxy]hexane)	Air	Endo.	96	S
		Endo.	118 (Tg)	S
		Endo.	130	S
		Exo.	300	S
	N_2	Endo.	102	M
		Endo.	116	M/S
		Exo.	300	v.S
1-(N-carbazole)-6-[(4-cyanobiphenyl-4'-yl)oxy]hexane	N_2	Endo.	52	S
		Endo.	223/230 (Tg)	S
		Endo.	295/304	S
1-[(aniline-2-yl)oxy]-6-[(1-phenylcarboxylic acid-4-yl)oxy] hexane	Air	Endo.	56	S
		Endo.	155 (LC trans.)	S
		Endo.	203 (m.p.)	S
		Exo.	299	v.S
		Exo.	336	M
	N_2	Endo.	206	v.S
		Endo.	235	M
		Exo.	310	M
1-[(aniline-2-yl)oxy]-6-[(4-biphenylcarboxylic acid-4'-yl)oxy] hexane	Air	Endo.	38	S
		Endo.	158	S
		Endo.	223	S/M
		Exo.	301	v.S
		Exo.	368	S
	N_2	Endo.	155	S
		Endo.	219	M
		Exo.	305	M/S
o-butoxy aniline	N_2	Endo.	69	S/M
		Endo.	131	S
		Endo.	170	M/S
		Exo.	305	S
		Exo.	370	S/M
Poly o-butoxy aniline	N_2	Endo.	95	M
		Endo.	173 (Tg)	M/S
		Exo.	380	M/S
Poly[1-(N-pyrrole)-6-[(4-cyanobiphenyl-4'-yl)oxy]hexane]	Air	Exo.	35.5	S
		Exo.	300	v.S
		Exo.	337	M
	N_2	Endo.	369	S

Table III-7 Peak values obtained from DSC for various monomers and polymers

[a] Exo. is an exothermic peak, Endo. is an endothermic peak

[b] S=strong, M=medium, w=weak, v.=very

III.5.3 Modelled glass transition temperature (Tg)

Despite the flaws of the model when it came to properties dependent on polymer chain length, it nevertheless allowed for reasonable prediction of Tg values. Figure III-16 shows the comparison of predicted Tg with the experimental values for various polymers (Table III-8). Despite the uncertainties, the trend of the prediction definitely appears useful.

Polymer of	Experimental Tg /°C	Predicted Tg /°C
1-(N-pyrrole)-6-[(4-cyanobiphenyl-4'-yl)oxy]hexane	90	99
1-[(aniline-2-yl)oxy]-6-[(4-biphenylcarboxylic acid-4'-yl)oxy] hexane[29]	139	113
1-(N-carbazole)-6-[(4'-bromobiphenyl-4-yl)oxy]hexane	130	179
N-propylcarbazole	219	252
N-butylcarbazole	220	231
1-(N-carbazole)-6-[(4'-cyanobiphenyl-4-yl)oxy]hexane	223	183
carbazole	293	300
N-methylcarbazole	300	309

Table III-8 Prediction of glass transition temperature using CAChe 3.2

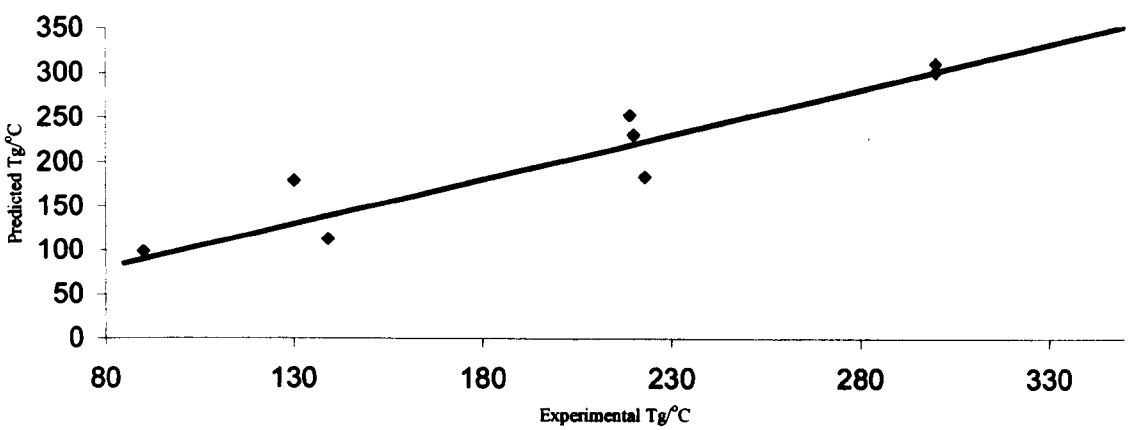

Figure III-16 Predicted Tg versus experimental Tg for various polymers as listed in Table III-8

The accuracy of the prediction of Tg values was confirmed by modelling a series of polymethacrylates (as shown in Figure III-17) with an increasing spacer length, as prepared by Craig and Imrie.[111]

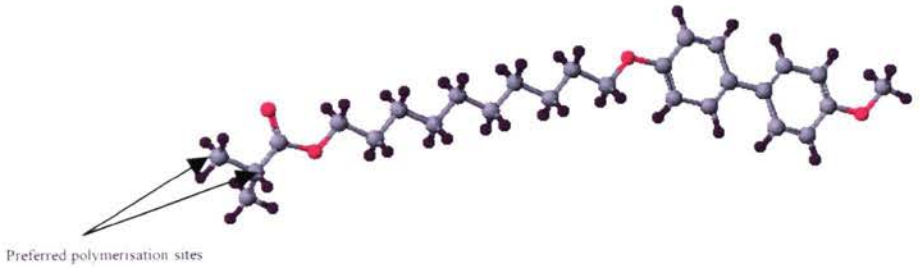

Figure III-17 Monomer of polymethacrylate (n=10)

The predicted results (Figure III-18) showed a steady decrease with the increase in chain length, in good agreement with the experimental data for the smaller chain length. For the greater chain length, the experimental data seem to exhibit a plateau, but this observation may be illusory, as the data published by Nakano *et al* for the same type of polymer were slightly different[112]. However, it is possible that above a given number of spacer units the effect on the Tg may be minimal or non-existent, due to subtle interchain interactions causing a change in the spacer conformation.

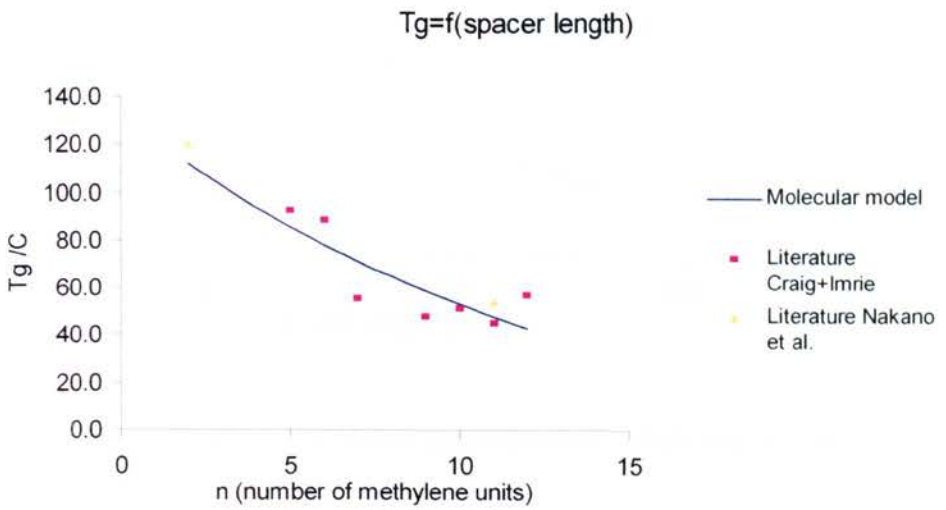

Figure III-18 Dependence of Tg on n, the number of methylene groups as spacer, in LC polymethacrylate series.

III.6 Electronic properties of polymers

III.6.1 Exploitation of UV/visible data

III.6.1.1 UV/Visible spectral data of a liquid crystal N-substituted polypyrrole

The spectrum of a film of polymer cast from chloroform solution onto silica glass (Figure III-19) showed a peak that allowed the determination of the value of the energy gap for that polymer.

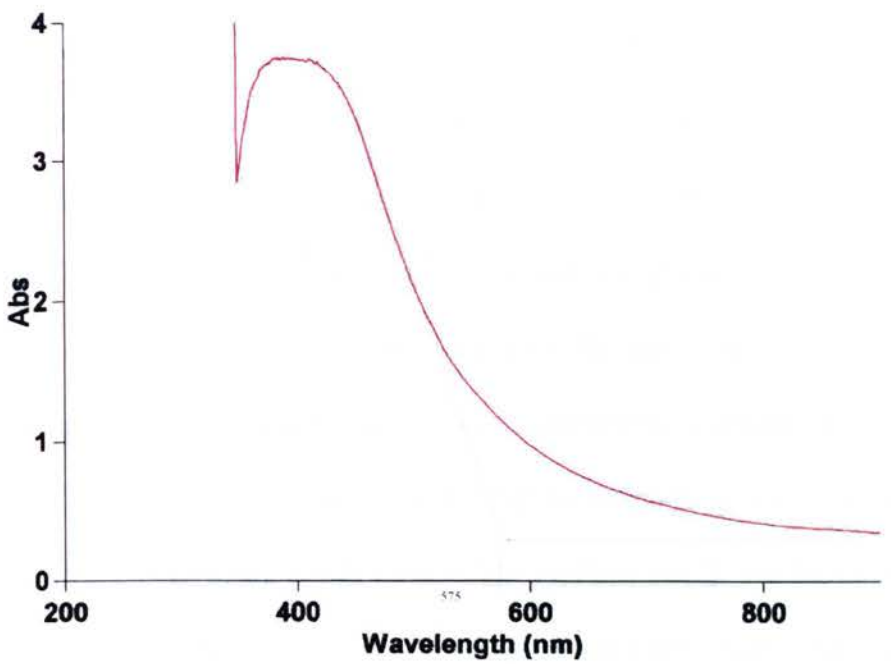

Figure III-19 UV-Visible spectrum of LC substituted polypyrrole

The absorption onset λ (the wavelength of a photon having an energy equal to the band gap Eg) was found to be 575 nm, which could then be put in the formula: $E=hc/\lambda$. (h, Planck's constant = 4.13×10^{-15}eV.s, c the speed of light = $3\times10^{8}ms^{-1}$)

The value of the energy gap was thereby calculated to be 2.16 eV. This value is smaller than that obtained for protonated poly-N-methylcarbazole (2.25 eV, section III.3.2), and also smaller than that reported for polyaniline bearing a similar type liquid crystal substituent[66] (3.1 eV for the protonated form).

III.6.1.2 Computer prediction of Infrared and UV/visible spectra for polymers

As mentioned for the monomers, predictions of the spectroscopic data for polymers were obtained by use of Quantum CAChe 3.2.

A good likeness of general features was obtained for both IR and UV spectra, as can be seen by comparing Figure III-21 with Figure III-22 and Figure III-23.

The five experimental peaks in the UV/Visible spectrum (250, 260, 295, 340, and 350nm) can be related to the five main peaks in the predicted UV/Visible spectrum (220, 240, 270, 290, and 315nm). Although the predicted peaks were shifted towards lower wavelength, the overall distribution of the peaks was very similar.

In a similar manner main peaks in the experimental infrared spectrum (peaks at 3426, 1463, 1174, 1070, 857, and 575 cm^{-1}) can be matched to peaks in the predicted infrared spectrum (3300, 1750, 1600, 1450, 1200, and 850 cm^{-1}). As for the UV/Visible spectra, although the values for the predicted spectrum were shifted, the overall shapes of the spectra were found to be very similar.

However it is important to note that the predicted spectra do not give an accurate numerical prediction of wavelengths, and that the IR spectra of polymers are in reality a good deal less sharp than the predicted spectra.

The prediction of infrared spectra however served a different purpose. Until that time we had not identified the polymerisation pattern for the carbazole units. By simply comparing the predicted infrared spectra for the two different types of polymers shown

in Figure III-20 and Figure III-21 with the experimental spectra, it is clear that the polymerisation occurs at the 3,6-positions. The UV/visible spectrum exhibits a number of peaks too great (5) to match the 3 predicted in the case of a 2,7-link, but it fits almost perfectly the 5 major peaks of the modelled 3,6-link. The infrared spectra can be compared simply by their general shape, for which the 3,6-model is again a very good match to the experimental spectrum, while the 2,7-model exhibits a strong peak at about 1800 cm^{-1}. In addition to this predicted peak that does not exist in the experimental spectrum, the pattern of the rest of the modelled infrared for the 2,7-poly(N-methylcarbazole) quite clearly does not correlate with the experimental data.

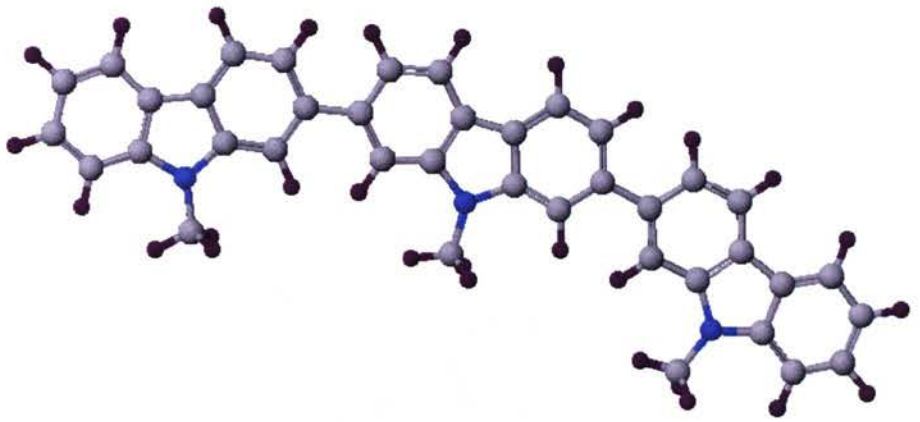

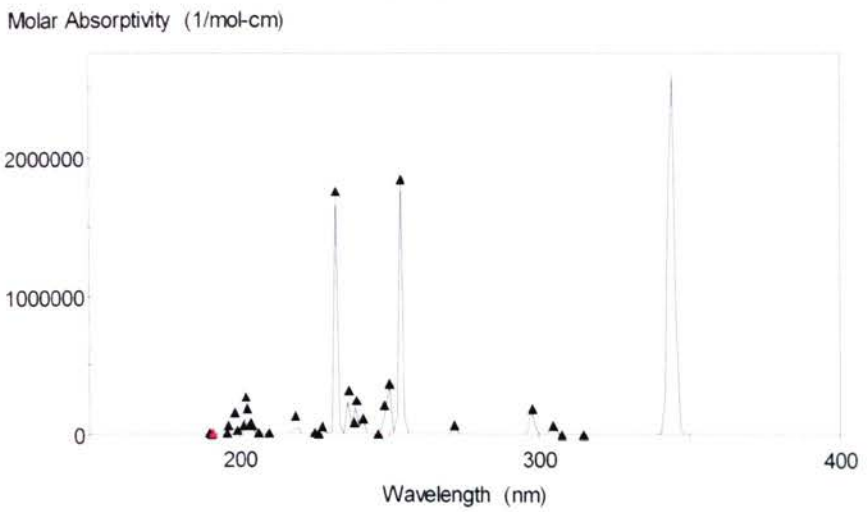

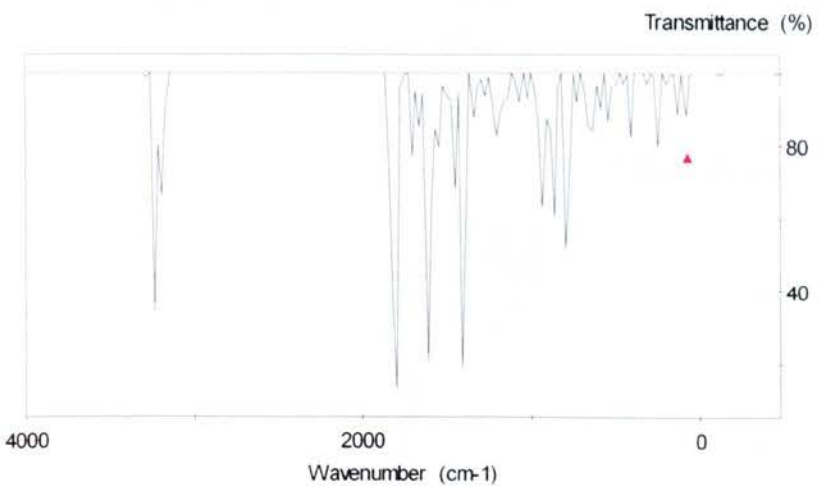

Figure III-20 Predicted UV-visible and Infrared spectra for poly(N-methylcarbazole) linked at position 3

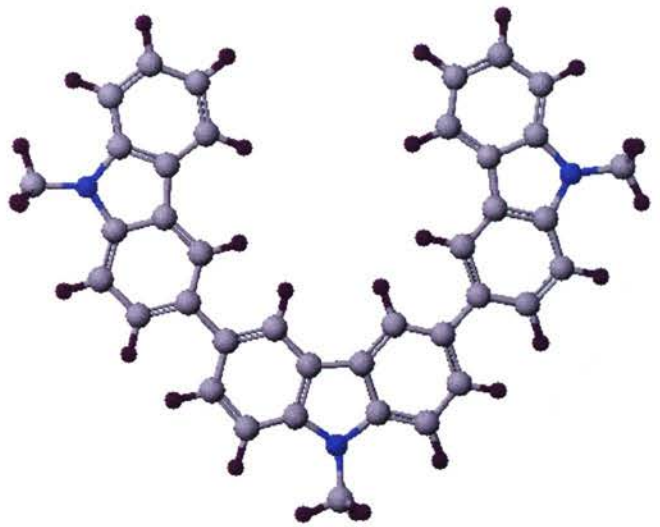

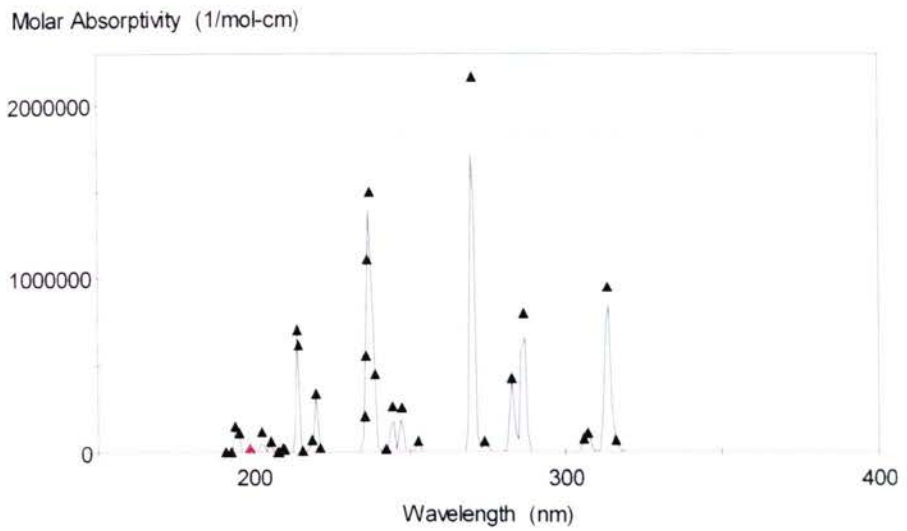

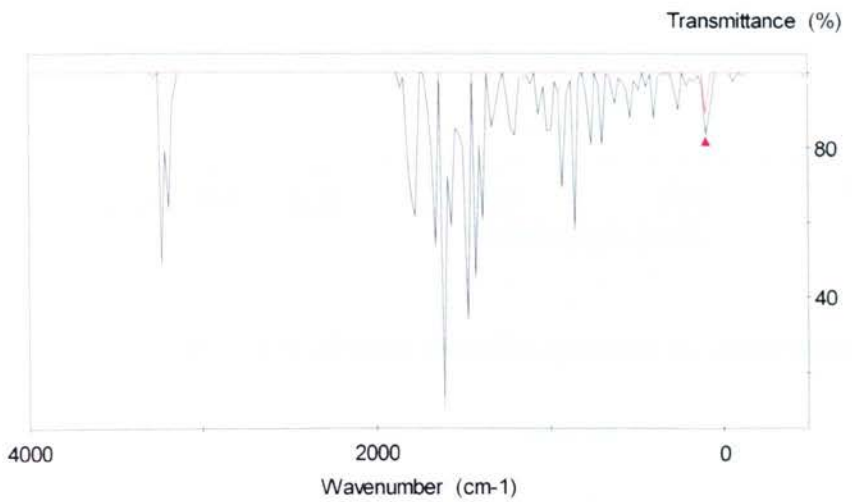

Figure III-21 Predicted UV-visible and Infrared spectra for poly(N-methylcarbazole) linked at position 4

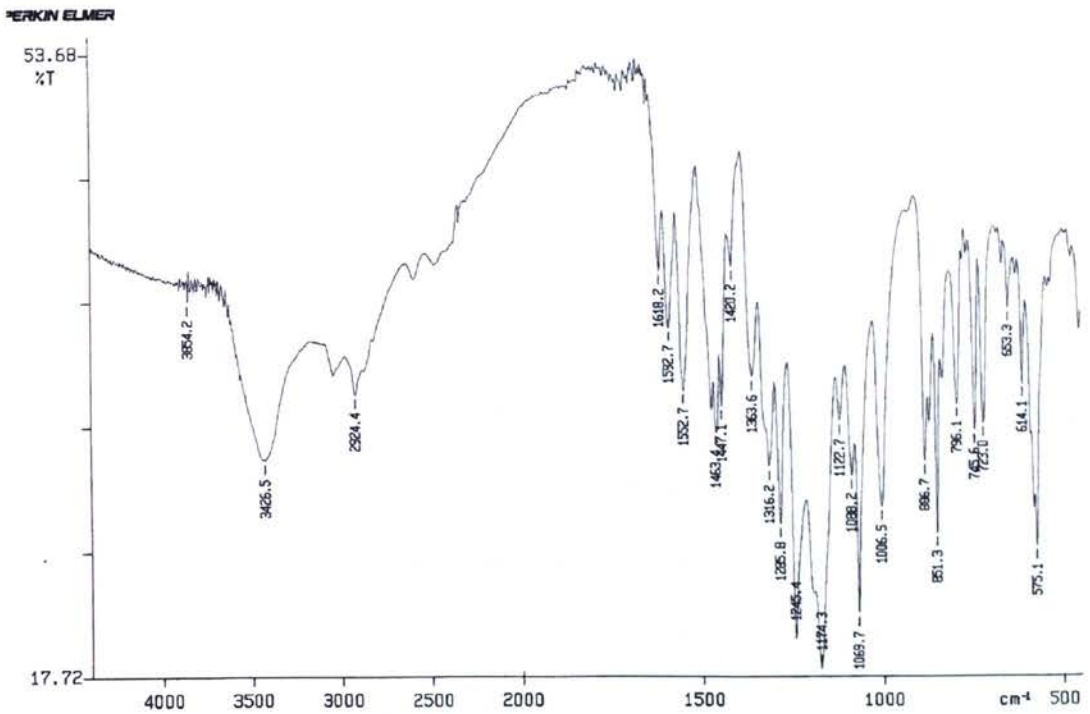

Figure III-22 Experimental Infrared Spectrum for poly(N-methylcarbazole)

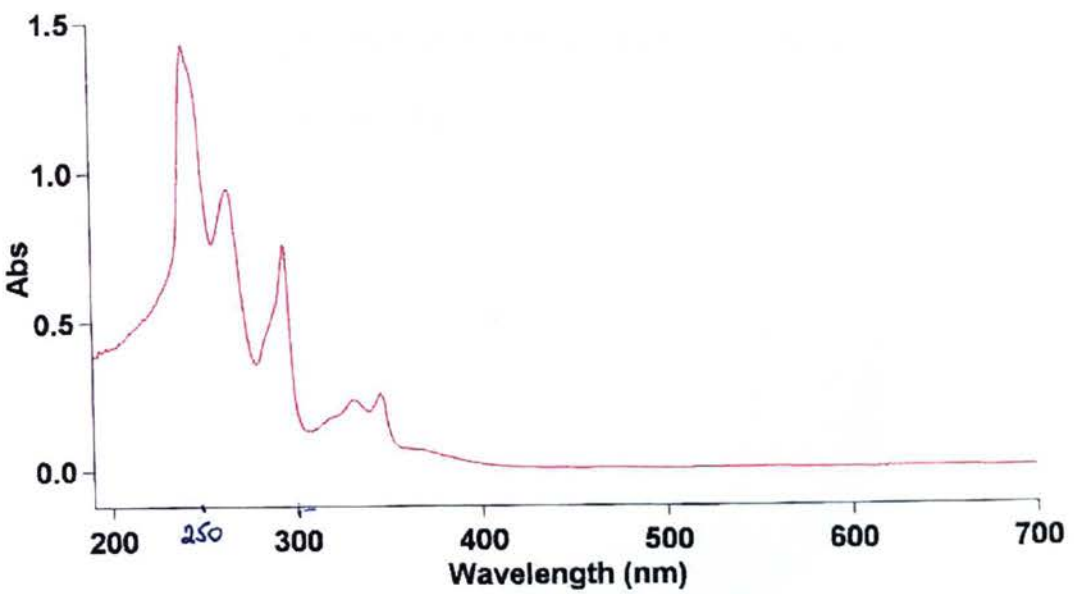

Figure III-23 Experimental UV/visible spectrum for poly(N-methylcarbazole)

III.6.2 Cyclic voltammetry

The use of cyclic voltammetry to produce polymers also provides information such as doping and dedoping potentials for the polymeric material as the film grows on the electrode.

III.6.2.1 Polypyrroles Derivatives

The voltammograms (an example of which can be found as Figure III-24 for 1-(N-pyrrole)-6- [(4-cyanobiphenyl-4'-yl)oxy]hexane) showed an increase in both the apparent formation and the dedoping potentials as the films thickened, probably due to the increase in resistance induced by the thickness of the films. As the cycle speed was quite fast (100mV/min), the film thickness may have slowed the diffusion process enabling the polymeric material to be fully dedoped in each cycle. As this would in turn somewhat inhibit further polymerisation, this could be the reason for the observed plateau in film formation and dedoping.

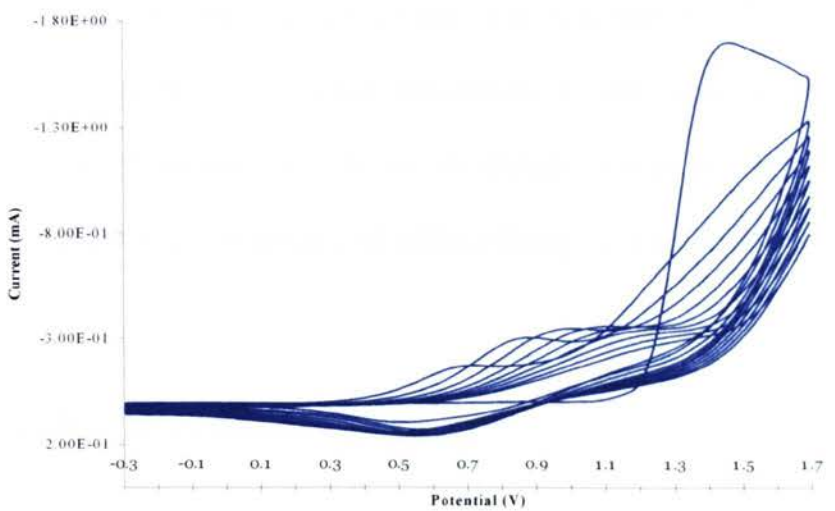

Figure III-24 Cyclic voltammogram for 1-(N-pyrrole)-6- [(4-cyanobiphenyl-4'-yl)oxy]hexane

A yellowish colour was observed, which became darker as the films were getting thicker (after ~30 cycles).

The films produced from 1-(N-pyrrole)-6- [(4-cyanobiphenyl-4'-yl)oxy]hexane were observed under the hot stage microscope but the liquid crystalline behaviour described in the literature[2] was not observed. In general, electrochemically grown polymers are less regular than chemically grown ones, and the resulting disorder probably prevented the liquid crystallinity from being observed.

III.6.2.2 Carbazole Derivatives

The shape of the CV obtained from the experiments performed on the carbazole derivatives was typical of a conducting polymer with the deposition of polymer followed by doping and dedoping processes and the IR spectrum of the polymer film obtained from N-methyl carbazole did tend to confirm the expected structure (see section II.3.4.2.1.2 for infrared data). The electrochromic phenomenon (dark green at higher positive potentials, yellow at lower potentials) was witnessed every time for the first few cycles, after which the dark green colour would persist. These observations are consistent with those reported for polycarbazole in the literature [40-42].

Since a fairly high concentration of monomer was required in order to produce a film that could be recovered, a different electrolyte system was successfully adopted involving the use of an acid solution as electrolyte (a mixture of aqueous acid and methanol) which led to the formation of a film of polymeric material.

III.6.3 Effect of potential cycling.

The use of cyclic voltammetry to obtain polymers also provides useful information about the potential for conductivity of the polymer as well as about the type of polymer formation observed. N-butylcarbazole provides a very good example for the study of electropolymerisation, and redox mechanisms (Figure III-25).

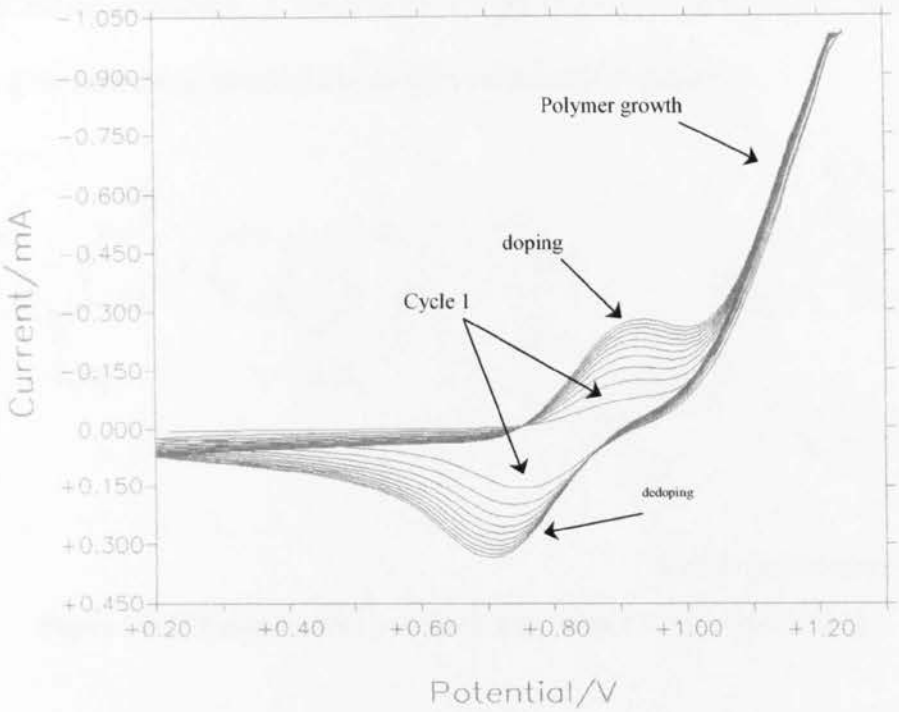

Figure III-25 Cyclic Voltamogram for N-butylcarbazole

The formation of the radical cation for N-butylcarbazole, and the delocalisation of the radical are illustrated in Figure III-26.

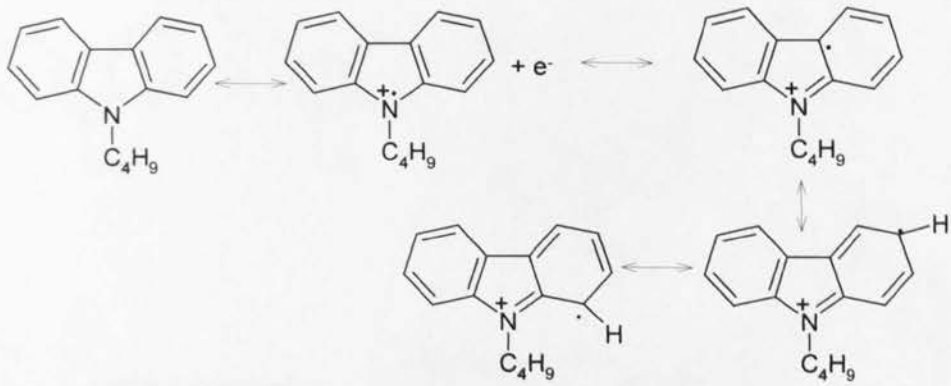

Figure III-26 Formation of the radical cation for N-butylcarbazole and delocalisation of the radical (note: the radical cation delocalises onto the same sites)

The mechanism for the polymerisation itself can be represented in a variety of ways, but the literature[98] suggests the electrochemical oxidation initially produces the 3-3'-dicarbazolyl radical cation (Figure III-27). As this species is more easily oxidised than

the corresponding monomer, it undergoes further oxidation at the same potential and couples to give polymeric products with the elimination of protons.

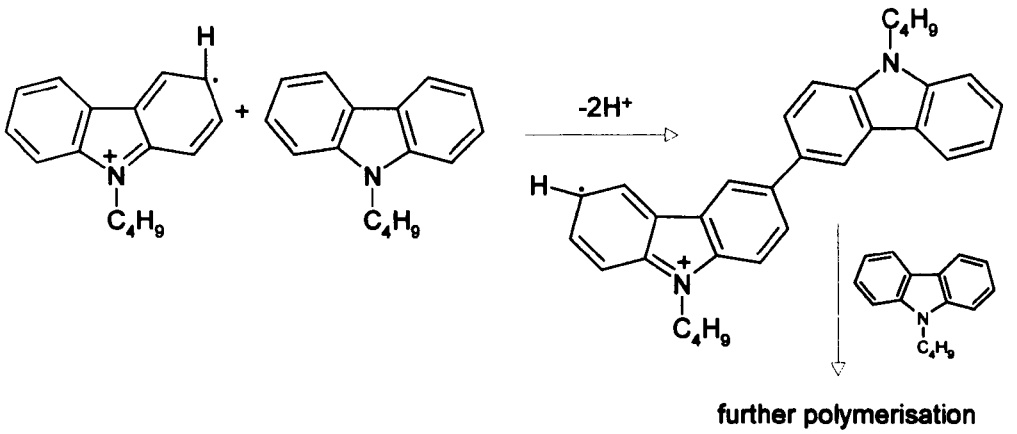

Figure III-27 Radical cation polymerisation route for N-butylcarbazole

Another possibility is that the polymerisation process may be similar to that of polypyrrole[33], with firstly the coupling of two radical monomers followed by the loss of two H^+. The dimer is then oxidised again to form a new radical cation that can react in a similar way (Figure III-28).

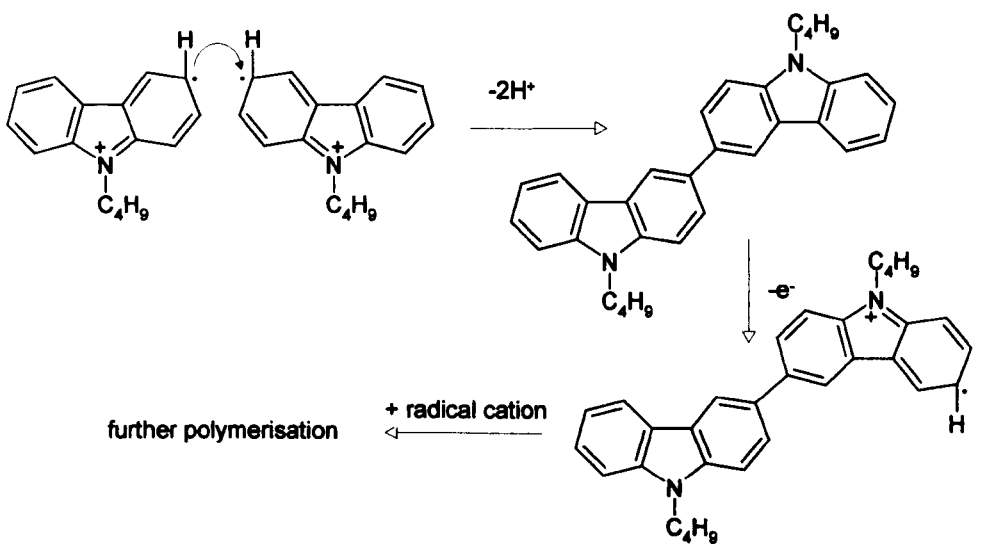

Figure III-28 'Pyrrole-type' polymerisation route for N-butylcarbazole

Even though the voltammogram exhibits an apparent plateau at 1 mA due to the limitations of the machine, on the first cycle it can clearly be seen that the first oxidation step has an onset at about 1.0V. This corresponds to the oxidative formation of

positively charged species (bearing one or two positive charges), and leads to the formation of oligomers. As the cycle carries on, the lower part of the voltammogram exhibits a peak (at around 0.75V) indicating a reduction process. In the following cycles an additional matching oxidation process can be observed (onset around 0.75V). These values are comparable to those observed in the case of carbazole but they are lower than that obtained for N-methylpyrrole (Table III-4).

The following cycles also provide information on the formation of the polymer. The fact that the area within the cycle is increasing indicates an even growth of conductive film, as opposed to a growth occurring as localised spots. The polymer forms on the layer(s) of polymer formed in the previous cycles. If the polymer had not been conductive, the coverage of the conducting layer on the ITO glass by polymeric material would have inhibited further growth of the polymer. The oxidation/reduction potentials of polycarbazole are associated with different colours for the bulk material: the reduced form of the polymer is yellow and the oxidised form is green.

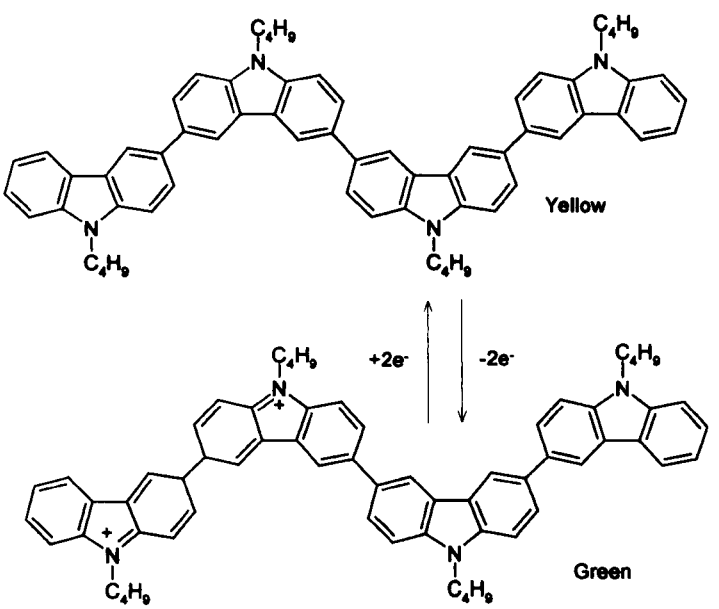

Figure III-29 Redox mechanism for poly-N-butylcarbazole[98]

The change in colour was only observed for the first few cycles, probably owing to the subsequent thickening of the material. As the thickness increased, the reduction process did not occur throughout the material due to diffusion limitations, and the polymer appeared green at all stages of the cycle. The other phenomenon that can be noticed in the voltammogram is a shift of the potentials to lower values. When attempting to make conducting polymers, this observation is an indication of an increase in the conjugation of the species present, therefore confirming the growth of a polymer with the possibility to delocalise charge effectively.

The combination for speed/film-forming of the cycling was found to be optimal at 100mV/s, but speeds between 50mV/s and 150mV/s yielded similar voltammograms.

III.7 Electrical Conductivity

III.7.1 Protonated/deprotonated

Because of its good solubility in chloroform in both protonated and deprotonated forms, poly *o*-methoxyaniline was a good model compound for the investigation of the influence of protonation of polyaniline samples on the conductivity. While the current-voltage plot for the deprotonated sample showed fluctuations and a great lack of linearity, the one for the reprotonated samples was strictly linear, as is illustrated in Figure III-30.

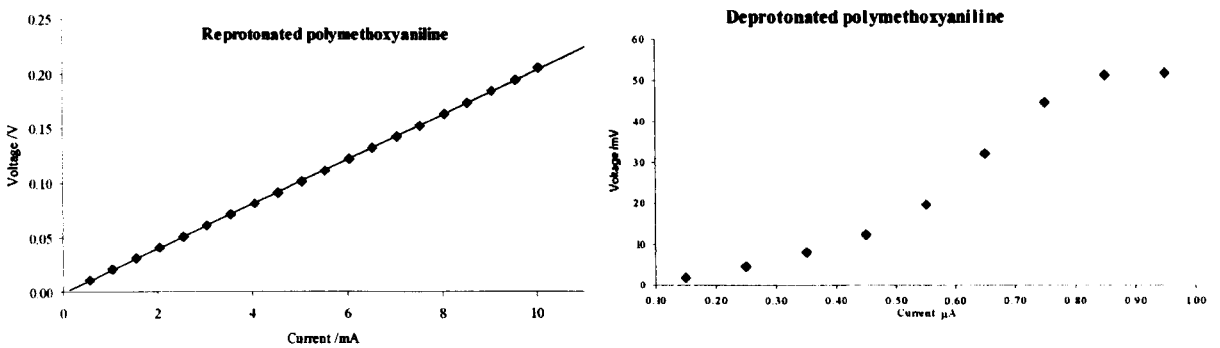

Figure III-30 Voltage vs current plot for deprotonated and reprotonated polymethoxyaniline

The reprotonated sample was found to be much more conductive than the deprotonated one, probably due to the H_2SO_4 acting as a strong doping agent. No value was obtained for the 'original' polymer as the sample used was prepared using the microemulsion method, and the deprotonated blue form was extracted from chloroform. Despite several rinses, the polymer did remained stable in this form, and yielded a free standing metallic-looking film.

III.7.2 Dopant exposure effect

The effect of exposure to dopant was measured on samples of liquid crystalline substituted polypyrrole film cast onto commercially available electrode substrates, as described in section II.1.5.2 and Figure II-1. The doping medium used was a solution of ferric chloride in methanol. The samples were repeatedly dipped in the saturated solution of ferric chloride for determined amounts of time and the conductivity was measured as described in the Experimental section, after the sample had been rinsed or not with clean methanol. The results of the experiments can be found in Table III-9 and Figure III-31.

Exposure time /min	Slope of V=f(I), rinsed sample (Ω)	Slope of V=f(I), unrinsed sample (Ω)
0	$8x10^8$	$5x10^8$
5	10^7	
10	$5x10^7$	
20	$3x10^6$	$4x10^6$
30	$3x10^7$	
40	$5x10^6$	$9.4x10^6$
60	$8.5x10^6$	10^8
120		$2x10^6$
180		$3x10^6$

Table III-9 Conductivity depending on dopant exposure for liquid crystal substituted polypyrrole

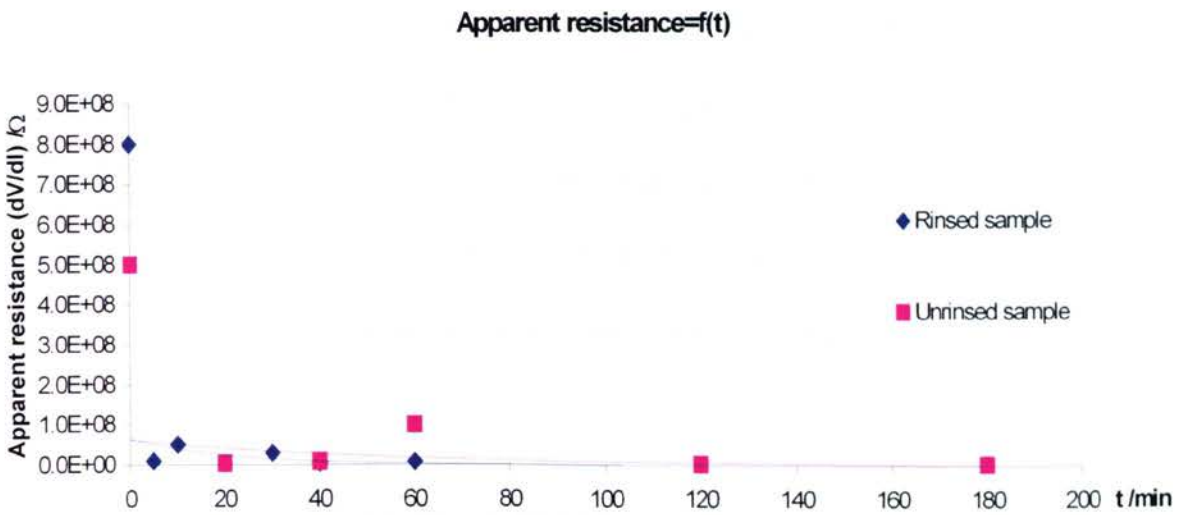

Figure III-31 Apparent resistance depending on dopant exposure time for liquid crystal polypyrrole

Although the plot is not very clear, it can be observed that the resistance dropped dramatically after a very short exposure time (a few minutes). The increase in conductivity could be attributed to the residual ferric chloride on the surface for the unrinsed samples, but since a similar effect was observed for the rinsed samples, it is more likely that the doping ions had already diffused into the polymeric material.

After the initial drop in resistance, the measured values did not decrease much further, as can be seen on the plot in Figure III-31.

After 20 minutes, the readings for the rinsed sample started to become unstable, making the plots less linear and more difficult to interpret. After 60 minutes when the readings

were deteriorating further, it became quite obvious from observing the sample itself that the amount of polymeric material had decreased, eventually yielding a patchy film on the substrate. It is in fact likely that the polymer was somewhat soluble in methanol, an effect worsened by the repeated rinsing of the sample. The un-rinsed sample was less affected, probably because the saturated solution of ferric chloride did not provide as much solubilising potential. However the sample showed evidence of slight degradation by the solution (thinner edges) after 3 hours. By looking at the results it is quite obvious that no real increase in the conductivity occurred in the last hour of exposing the sample. Therefore it is possible to dope the polymer to a satisfactory level without losing any significant amount of material. In both rinsed and un-rinsed cases it can be observed that the trend lines in Figure III-31 show a plateau, which confirms that the polymer reached maximum potential dopant concentration.

III.7.3 Temperature dependence

The measurements were recorded as described in chapter II.1.5.2.2. Figure III-32 shows the evolution of the resistance as the temperature increased.

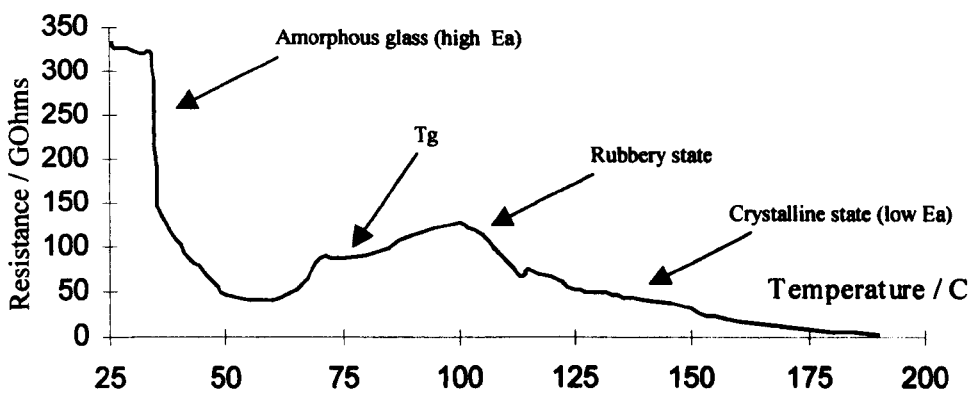

Figure III-32 Resistance versus temperature for deprotonated poly *o*-methoxyaniline, with suggested states and transition for the bulk material (Ea the activation energy)

As expected, it started quite high at room temperature but quickly started to decrease. However between 65°C and 100°C the trend was reversed and the resistance increased again. This could not be matched to a DSC transition as the obtained plot did not show any peak. When the temperature increased further, the expected decreasing trend was observed again, and at higher temperatures its evolution was simply activated. The trend was confirmed by the complete linearity of the plot of Ln σ=f(1/T) in the higher temperature region (illustrated in Figure III-33).

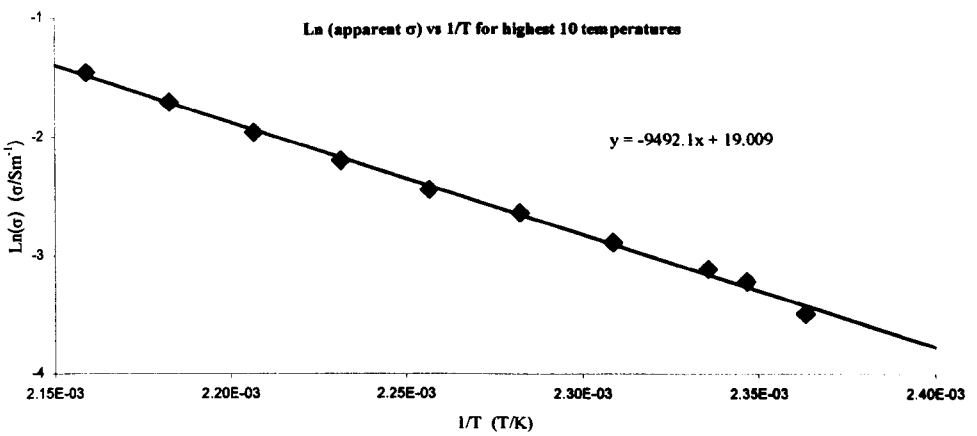

Figure III-33 Ln (apparent σ) vs 1/T for highest 10 temperatures

This behaviour is of the type that would normally be observed in inorganic semiconductors. The lowest recorded value for the apparent resistance was 4.3Ω, which corresponds to an apparent conductivity of 0.23Scm^{-1} for the sample (note: the sample was not heated further so as to avoid possible degradation).

A similar experiment was run using a thin film (0.1mm thick, 0.4mm^2 surface area) of polymer of 1-(N-pyrrole)-6- [(4-cyanobiphenyl-4'-yl)oxy]hexane (PYLC), slightly doped with $FeCl_3$. A plot of the results is illustrated in Figure III-34.

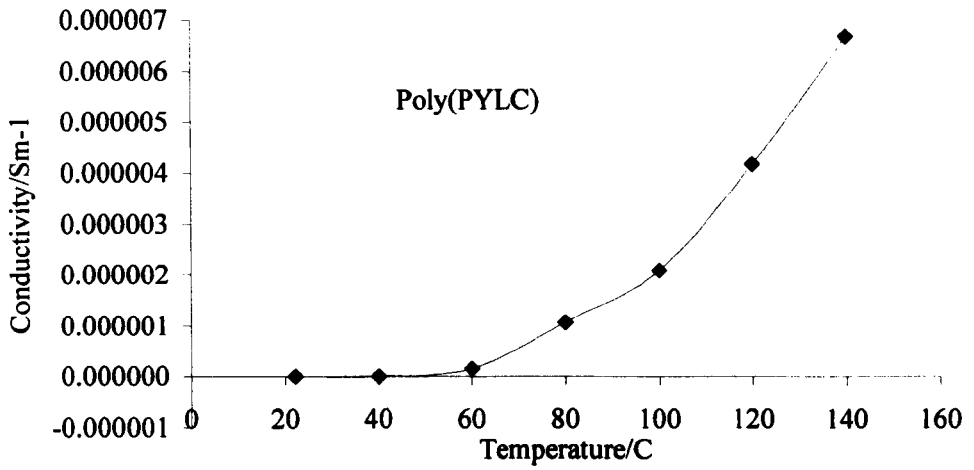

Figure III-34 Temperature dependence of conductivity for PYLC

The change in slope observed around 73°C (from intersect of trend lines in figure) probably corresponds with the development of the liquid crystalline (nematic) texture. The change in activation energy was obtained from the plot of Lnσ vs 1/T (Figure III-35), and was found to decrease from 1.43eV to 0.39eV after the transition temperature. This indicates that a change occurred that rendered the material more conductive, most likely linked to an improvement in the linearity of the polymer backbone. This was confirmed by the fact that by leaving the liquid crystal texture to develop, the conductivity could be improved even further.

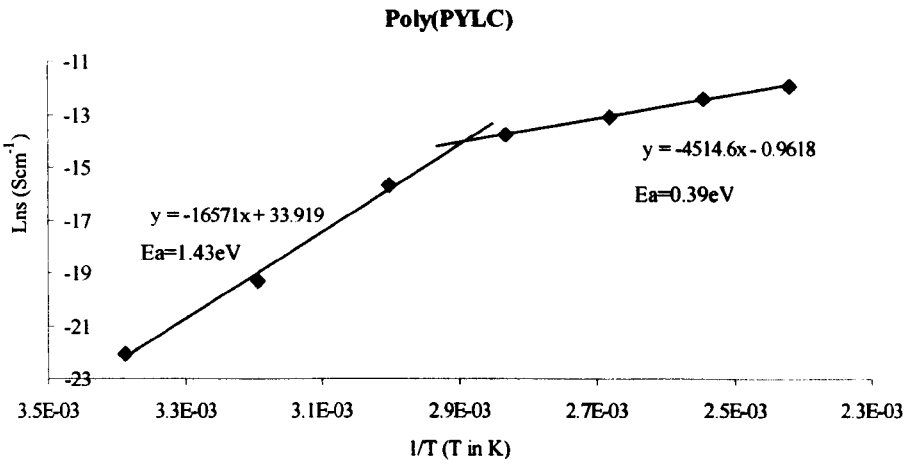

Figure III-35 Lnσ vs 1/T for poly(PYLC) (Ea is the calculated activation energy)

This behaviour was unusual as the expected phenomenon in the case of a conventional (non-liquid crystal) conducting polymer would have been a sharper increase in the activation energy as the polymer becomes less ordered after reaching its Tg.

Although a nematic transition was reported by Ibison at 49.8°C[2], this was observed in the process of cooling from the isotropic melt. The predicted Tg for the pyrrole polymer using CAChe 3.2 was found to be around 99°C. An isotropic transition was recently reported at 90°C for this polymer by Hasegawa *et al*[113, 69]. From previous work by Ibison *et al*[2], it is very likely that the transition at 90°C is in fact the Tg. If this is the case, then although no transition was optically detected upon heating, the material would probably have softened enough at 73°C to allow the liquid crystal texture to develop.

A DSC scan showed a small, broad transition at 60°C, followed by a small but sharp transition at 70°C. This could indicate that the polymer started softening at the first transition. At the second transition the medium would have attained a low enough viscosity, while still being in the nematic range, to allow the liquid crystal texture to develop.

III.8 Laser alignment of liquid crystal conducting polymers

III.8.1 Theory

Since their discovery, the organisation of liquid crystal polymers has been somewhat of a challenge for scientists. The phenomenon seemed to be limited to polymers with saturated backbones[114,115,116,117]. For the reasons discussed in chapter I.3, an organised backbone is potentially useful for increasing the conductivity of conjugated polymers.

Lasers have been used extensively for technological applications in recent years, and the fields of liquid crystals as well as that of conducting polymers have been affected by this. Typically for polymer lithography the laser has been used to cross-link a specific (unrequired) area of conducting polymer[118] or to locally photo-polymerise a film of monomer[119]. Other photolithographic methods using lasers have also included the specific removal of conductive polymer film, followed[120] or not[121] by re-coating using a cladding layer, and metal thin film transfer[122]. In all cases the processes were irreversible and/or did not lead to an improvement of the conductivity (in the case of the cross-linked conducting polymer the treated area becomes less conductive than the untreated material). The use of a laser on previously organised liquid crystals would typically result in local melting and disorganisation along the track. Early work[116,117] on laser micro-lithography of insulating liquid crystal polymers used a laser beam to alter locally the organisation of smectic films, and the liquid crystal moieties were found to reorganise perpendicularly to the laser track, yielding a track of high optical anisotropy.

The idea behind laser alignment for liquid crystal conducting polymers was directly derived at Kingston and Greenwich Universities[2, 66, 70, 116, 117] from the expected properties of the novel materials produced. With a Tg lower than the liquid crystal

transition temperature(s), it was expected that if the polymer was heated up it would allow the liquid crystal behaviour to show itself. Because the polymer at that temperature would be above its softening point, the self-organisation of the liquid crystalline moiety would be able to affect the polymer backbone, forcing it to be more regular. Combining this effect with that of the directional freezing, the backbone might also be expected to become more aligned and linear. As explained previously a more aligned backbone would yield a better electrical conductivity as it allows for greater electron mobility (both along the polymer chain and between different chains) as well as improved delocalisation. By using a focussed laser beam to heat up the polymer very locally, the idea could be taken a step further: a fine conductive track might perhaps be drawn on an otherwise non-conductive amorphous background. The use of the laser beam as the means for heating allows one to work on a microscopic scale, and by modifying the intensity and/or the wavelength of the beam the temperature can be varied to suit the investigated sample. Evidently such a process requires the polymer sample to be thermally stable.

The efficiency of such a method is expected to be greatly dependent on the symmetry and the regularity of the repeat unit in the polymer conjugated backbone. Unless the mesogenic group is attached so that the repeat unit is 'reversible' (where the favoured polymerisation sites are not distinguished one from the other, and the monomer unit exhibits a plane of symmetry) the maximum alignment will only be obtained if the polymer has been prepared following a regio-specific route.

III.8.2 The Samples

Most of the following work was done in collaboration with Dr. P. Ibison, using the facilities kindly provided by Greenwich University.

Three types of liquid crystal substituted conjugated polymer backbones (Figure III-36) were considered and prepared[2, 29, 66, 70] for these trials: polypyrrole (P1), polythiophene (P2) and polyaniline (P3).

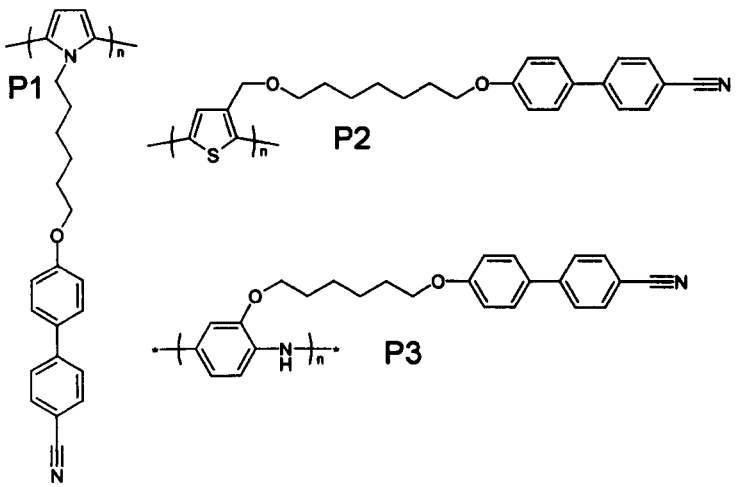

Figure III-36 Structure of the liquid crystalline polymers investigated for laser alignment.

The experimental procedure was similar for all the samples. A polymer film of thickness up to about 150 μm was cast from a solution of the polymer in chloroform on a borosilicate microscope glass slide. Thinner films (0.2-1 μm) were obtained using a spin-coating technique. All the films were amorphous, as can be seen in the background of Figure III-37, with only tiny areas of organised material. No peaks were observed for them when studied by X-ray diffractometry. A fixed laser beam was focussed using plano-convex lenses so it would just melt the film on a diameter 1-20μm (typically 5μm). The laser used was helium-neon based, providing 20mW at 632.8nm wavelength. The sample was moved steadily (0.5cm per second) perpendicularly to the beam using an X-Y translation stage to form a series of parallel tracks. As soon as the beam moved away from the spot that had been melted, the polymer would cool down and solidify. The experiment produced regular track patterns as can be seen in Figure III-37. On a 1x1cm sample, 50 tracks 1cm long were written, typically up to 10μm wide and 9μm deep.

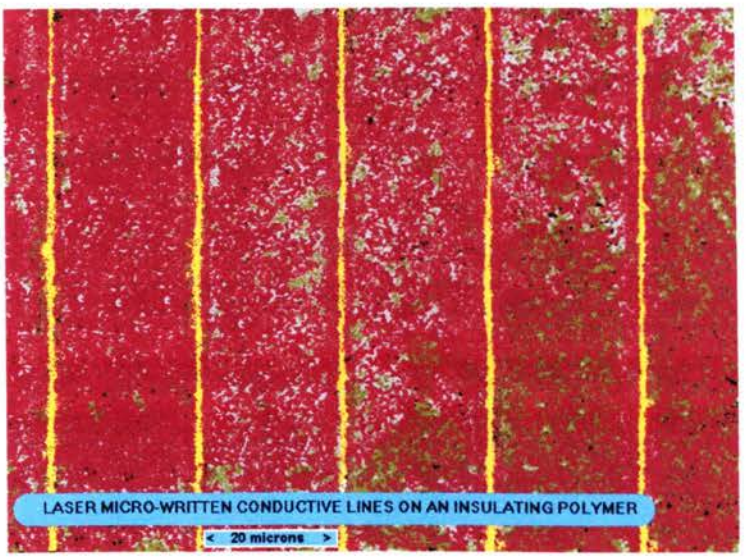

Figure III-37 Organised tracks on amorphous polymer backbone seen under crossed-polarisers

The tracks were investigated using oil-immersion optical microscopy in order to get a better idea of the appearance of the track (Figure III-38).

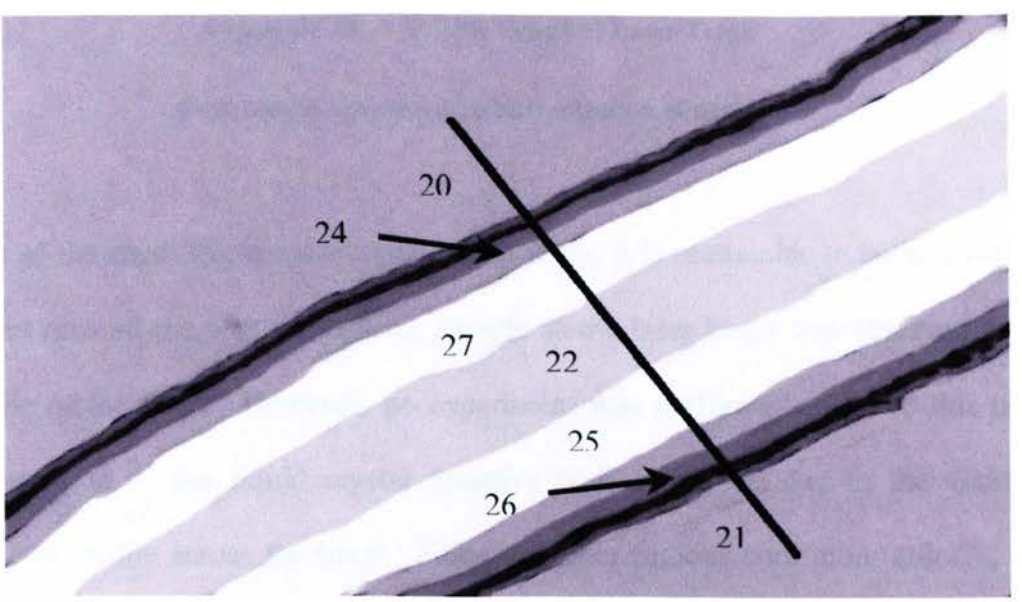

Figure III-38 Oil-Immersion Optical Micrograph of a Laser Track

(Contour map shows profile section, numbers indicate relative concentration of dopant)

A profile graph was obtained (Figure III-39), which allowed one to determine the shape of the groove produced from the melting and the depth of the track.

The process that created the observed channel probably had two origins. The edges of the track are slightly raised compared to the bulk, so some of the material might have

been displaced or 'pushed up' during the writing of the tracks. However the most likely reason is that the laser action creates more organised material which is denser than the bulk, hence occupying less volume.

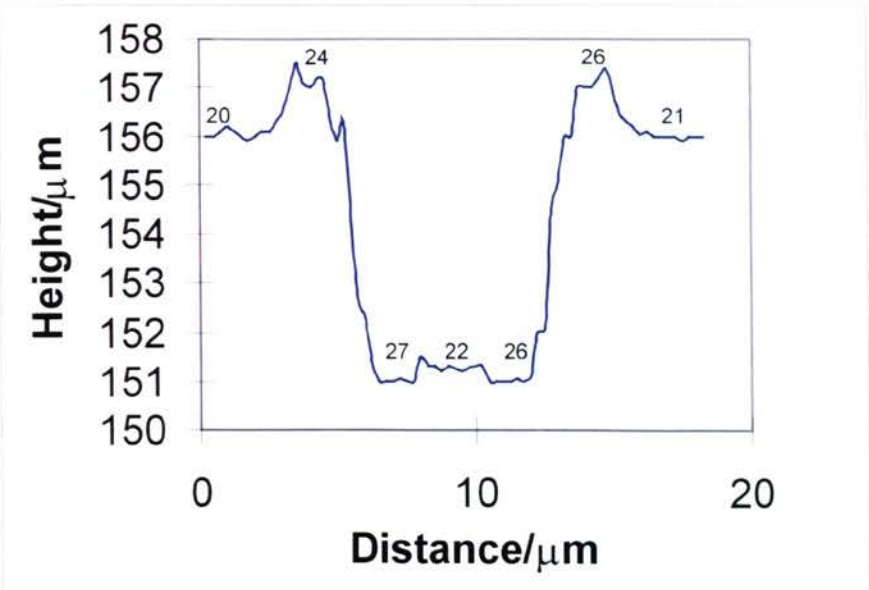

Figure III-39 Profile Graph of Laser Track

(Numbers indicate relative concentration of dopant)

Because of the small thickness of some of the films, it is reasonable to believe that the alignment runs all the way through the sample as the laser beam was observed on the other side of the films. However, no experiment was performed to prove this point. The orientation of the liquid crystal moieties is likely to be due to the Gaussian temperature profile across the track. Since the outer regions cool more quickly, they undergo an isotropic-to-nematic transition. This in turn induces alignment of the hotter material at the centre. The density change causes the material to flow towards the region of highest temperature. This means the material tends to flow in the direction of the scan during the writing process. Also, because of the reduced viscosity in those areas, the flow effect is greater in the centre of the beam. Experiments on non-conductive liquid-crystal polymers have shown a visible flow effect under high-

magnification when a laser track was written in an otherwise smectic phase with a dye present[116].

In order to prove that the laser had induced a greater ordering within the material, the optical anisotropy of the tracks was studied.

III.8.3 Anisotropy

The tracks were observed under a polarising optical microscope. Two types of polarised light were used to investigate the effect of the localised melting on the alignment of the backbone and the organisation of the liquid crystal moieties.

By using crossed-polars, as pictured in Figure III-37, the change in the organisation of the liquid crystals in the tracks compared to the bulk was shown. The bright yellow colour contrasts with the dark red of the background due to the induced optical anisotropy, indicating that the orientation of the LC inside the tracks is consistent and different from the patchy amorphous background. The laser beam had increased the organisation of the liquid crystal moieties. (note: the yellow track is in fact 'underlined' by a thin red track each side, and the pattern of dark-light-dark could be reversed by rotating the crossed polars together: the sample was birefringent)

The use of simple polarised light also allowed visualisation of the effect on the polymer backbone. By aligning the polarisation direction of the light with that of the track, it was observed that a lot less light was transmitted in the region of the track, than in the background. The absorption of light by the material in the track was anisotropic because of an alignment of the polymer chains which induced a previously non-existent specific direction for the π-π^* electronic transition. Because the direction of polarisation was parallel to the track, and the polymer backbones were preferentially aligned along the same direction, little to no light could be transmitted (if the

polarisation ran perpendicular to the track, an increase in the light transmission would be observed).

Infrared spectra of thin films of the polymers remained the same before and after laser-treatment, and the solubility of the samples remained complete. The stability of the polymers was such that the tracks could be erased by heating the samples to their isotropic temperature or by re-dissolving them and re-casting new films repeatedly without any apparent degradation in their aligning ability, as they could be laser-aligned with equal success after recasting the films.

Since the optical anisotropy of the sample indicated that the material was indeed more ordered within the tracks, the electrical anisotropy of the sample was investigated to see whether the polymer backbone planarity had benefited from this treatment.

III.8.4 Conductimetric Data and Analysis

Using identically treated square samples of liquid crystal polymer films lightly doped by ferric chloride, linear electrodes of silver paint were applied (Figure III-40). The resistances were measured parallel and perpendicular to the direction of the laser tracks.

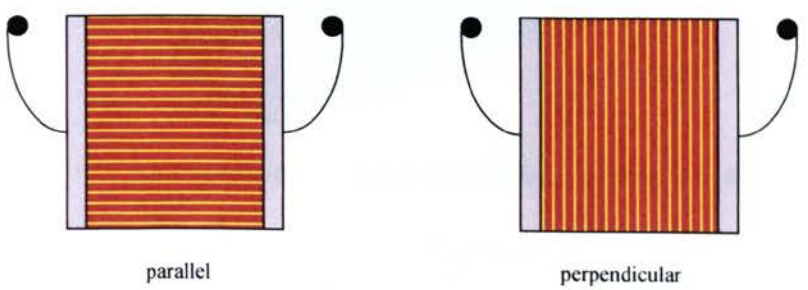

Figure III-40 Set-up of electrical contacts for conductivity measurements on laser-aligned material, parallel and perpendicular to the laser tracks

Knowing the film thickness, comparative values were obtained for the apparent film conductivity in both directions. As shown in **Error! Reference source not found.** for

each polymer (structures illustrated in Figure III-36) an increased conductivity along the tracks was observed, which is consistent with the alignment of the polymer backbone in this direction.

It is important to notice at this point that the overall proportion of aligned material represents less than 1% of the bulk. An estimate of the aligned volume was obtained from the profile experiment. It suggested for P1 that the local improvement of the conductivity was 50,000 to 100,000 times that of the original value.

Sample	$\sigma_{\perp}$ (Sm^{-1})	$\sigma_{/\!/}$ (Sm^{-1})	Anisotropy
P1	1.3 E-6	4.0 E-5	31
P2	5.7 E-7	1.7 E-6	3
P3	2.0 E-5	4.0 E-5	2

Table III-10 Conductivity of various polymers after laser alignment

The conductivity along the tracks was then measured directly as pictured in Figure III-41 using a 4-probe system.

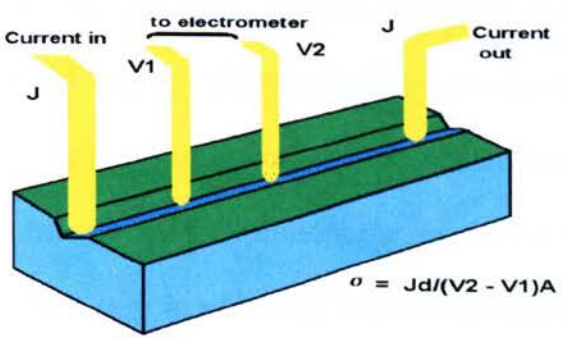

Figure III-41 Track Conductivity Measurement

The conductivity of the undoped material, as well as the electron mobility of polymer P2 for aligned and unaligned material was recorded (Table III-11). The measurement of the mobility was obtained using the Shockley-Haynes method. A charge (electrons) was injected at one extremity of the sample and the signal was picked up by an oscilloscope at the other extremity. The peak recorded on the oscilloscope gave a

measurement of the time required for the charge to travel a known distance along the sample, and thus the electron mobility. The mobility was improved by over 1500 times! As predicted, the electron mobility was immensely improved along the track, supporting again the hypothesis of an improvement in the alignment of the backbone.

Polymer	Electron mobility ($cm^2/V.s$)	'Undoped' p-type conductivity (Scm^{-1})
P2 (unaligned)	7.4 E-5	4.8 E-7
P2 (laser aligned)	2.2 E-1	1.2 E-3

Table III-11 Electron mobility and conductivity for aligned and un-aligned material

It is so far unclear what the exact mechanism of the alignment is, and it seems very likely to be due to flow as well as liquid crystal influence. However, in experiments using non-liquid crystalline poly(3-dodecylthiophene), no laser alignment effects were observed, which confirms that the presence of a liquid crystal moiety is a pre-requisite. The liquid crystal moieties would be expected to take the direction of flow as their director. However, since the polymer backbone has been shown to be aligned along the track, or flow direction, it suggests that the liquid crystal moieties are at an angle with respect to the track. This may come from two phenomena: either the influence of the flow is greater than the effect of the mesophase, or the mesophase produced by the substituted polymer is of a type in which the LC units are tilted, or angled with respect to the director, such as smectic C.

From looking at the drawn structure of substituted polyaniline and polythiophene, it is just possible that the chosen spacer might allow for the liquid crystal moiety to lie parallel to the polymer backbone. Molecular modelling would be able to predict if indeed this conformation would be favourable. This will be studied in more detail in section III.8.6.

However the increase in the conductivity of the doped samples may have had another cause, which is a possible concentration of doping agent molecules within the laser-treated regions.

The distribution of dopant iron atoms (e.g. in $FeCl_4^-$) in the samples was monitored by SEM-EDXA (Energy-dispersive X-ray analysis), using a low-intensity electron beam and low accelerating voltage. This work was carried out by the University of Brighton EM unit.

When the track bearing polymer film was doped using $FeCl_3$ (for P1 and P2) or dilute sulphuric acid (for P3), it was observed that the concentration of dopant was slightly greater (about 20% greater) in the tracks than in the bulk. The relative values for Fe atom concentration in P2 can be found in both Figure III-38 and Figure III-39, and it can be observed that the concentrations were the greatest on the 'walls' of the track, i.e. the region of greater alignment of the material.

This observation was not what was expected, since the thickness under the track is smaller than that of the bulk (8-10% smaller), but mostly because more aligned, hence more ordered materials, are typically reluctant to accept dopant molecules. This comes from the denser packing of the molecules reducing the available sites for the dopant molecules. However the observed behaviour might be due to the fact that within the tracks the energetic availability of electrons is much improved, as the energy gap is smaller, which makes it a more attractive site for acceptor dopant molecules.

Either way, the slightly greater concentration of dopant in the track increased further the conductivity of the already improved material, so this was an unexpected bonus coming indirectly from the ordering of the polymer backbone.

III.8.5 XRD

Samples of both aligned and unaligned polymer of liquid crystal N-substituted pyrrole were sent for XRD. Whereas the unaligned samples did not give any peak, the aligned sample did exhibit two peaks: a sharp peak corresponding to a spacing of 8.8 Å with an angle of around 10°, and a 3.7 Å strong broad peak for 24°.

III.8.6 Molecular modelling

Molecular modelling was used again, in order to provide some insight into what may have happened during the process of laser alignment.

The positioning of the various parts of the molecule in the case of liquid crystal polymers is yet to be fully understood. The following section is an attempt to discuss the possible molecular re-arrangements that take place in the material when it is subjected to a laser beam.

When it comes to liquid crystal polymers, the literature suggests various positioning and directions for the mesogenic groups. Some authors [58] describe the monomer units as being all oriented the same way, so that the mesogens position along one direction, generally perpendicular to the polymer backbone (Figure III-42a). Because the structure of the polymer backbone does not usually provide a big enough spacing between the links to individual mesogens, these will tend to hinder each other, rendering this particular structure rather unlikely.

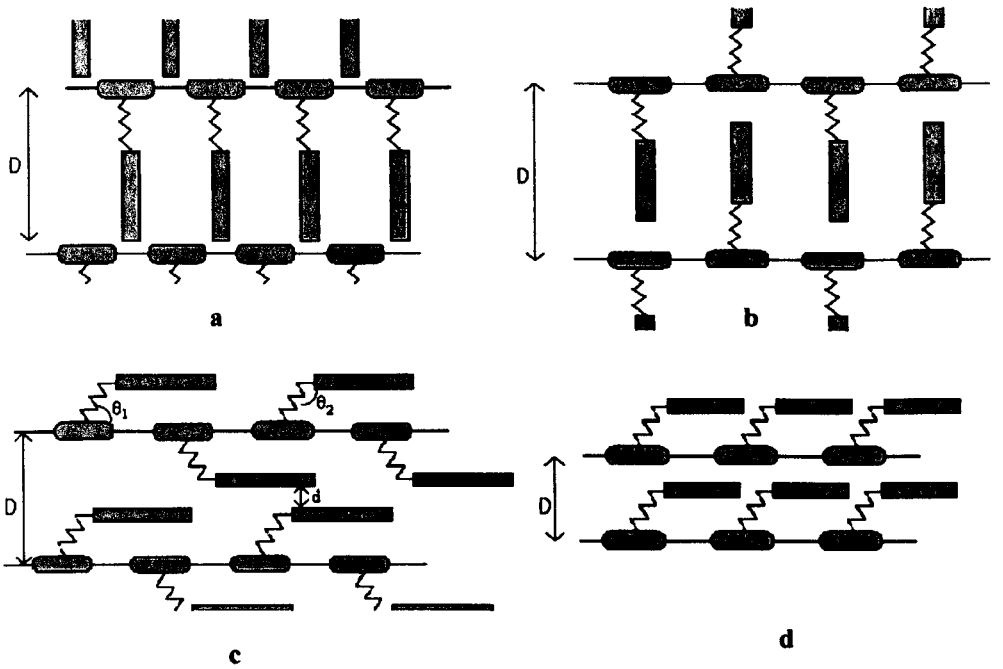

Figure III-42 Possible conformations of the side-chain liquid crystal polymer

The model shown in Figure III-42-a is a good illustration of a monolayer type arrangement, where the distance (D) between the polymer chains is almost equal to the length of a fully expanded substituent. If we refer to the latter as D_l, it enables us to compare the distances between polymer chains for the various possible conformations. Hence in Figure III-42-a we have $D=D_l$.

The molecular model confirmed the possible steric hindrance from the substituents, but some caution is required due the fact that in the case of aromatic backbone, the positions of the double bonds drawn in the model will influence the resulting 'optimised' conformation. This was discussed in the chapter covering molecular modelling.

Another possible configuration, which now appears more likely, shows the moieties with alternating directions (Figure III-42-b). In that case we have $D \geq D_l$, due to 'intermeshing' of the liquid crystals (However D could even be greater than $2 \times D_l$).

This is nearer to the conformation most favoured in the computer simulation, where the model usually featured a slight twist in the backbone to accommodate the steric repulsion between substituents.

The other aspect to consider is the positioning of the liquid crystal moieties with respect to the polymer backbone. Although most papers [59, 76] suggest a fairly perpendicular direction of the liquid crystal when the material is force-aligned, newer publications actually favour the possibility that the mesogens could lie parallel to the backbone. In the description of their work on liquid crystal substituted poly (p-phenylene) and poly (p-phenylenevinylene)[123], Oguma *et al* suggested that the orientation direction of main and side chain crucially depend on the site and the number of substituents linked with the phenylene moiety, rather than the kind of polymer. Their analysis of XRD patterns and of polarised absorption and fluorescence revealed that in the case of mono-substituted polymers, the alignment of both the main chain and the side chain was parallel to the magnetic field.

The feasibility of this arrangement depends greatly on the length of the spacer. As discussed before, too short a spacer would not allow enough freedom for the mesogen to sit in its preferred position, and too long a spacer would not allow the aligning effect of the mesogen to act on the backbone. The case depicted in Figure III-42-d is only possible with a twist in the backbone to allow the LC moieties to coexist so close to each other. In that case D would be expected to be found a lot smaller than D_1, as this theoretical model allows for the closest packing.

In the case shown in Figure III-42-c, the substituents adopt an arrowhead conformation, with the mesogens parallel to the backbone. In that case the value of D will depend on the packing ability of the material, directly linked to the minimum tolerable distance (d) between moieties from adjacent chains, and the minimum possible values for the angles θ_1 and θ_2.

Although the previous studies carried out at Kingston University have proposed that laser alignment results in the liquid crystal chains sitting perpendicular to the backbone, other factors may have to be considered. First there is the possibility that the liquid crystal mesophase may not be smectic S_A (as usually suggested in the literature for liquid crystal polymers[30]), but smectic S_C, or even a nematic phase[2]. As described in the Introduction, a smectic S_C would result in the favoured direction of the mesogens being tilted with respect to the director, not parallel. More importantly in our case, the effect of forced or induced alignment using techniques such as shear stress, magnetic field or laser alignment may result in the expected alignment of the mesogens in the same direction as the applied force, field or flow, but with the unusual effect of the backbone becoming aligned along the same direction.

As an example, a liquid crystal monomer of aniline was modelled, and the likelihood for the mesogen to sit parallel to the chain axis was assessed by rotating the linking bond. Although the resulting minimum was not a structure with the liquid crystal coplanar, and in the same direction as the chain axis, several similar structures with a slight twist between the phenyl rings were found to have low energy (Figure III-43)..

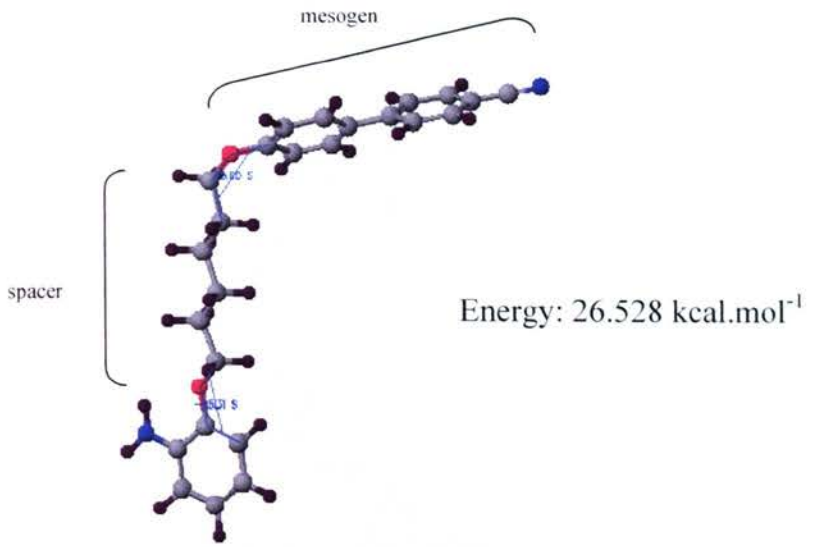

Figure III-43: Liquid crystal aniline monomer

When a model of the liquid crystal polypyrrole (4 repeat units) was subjected to the optimisation process of the software, it resulted in the structure shown in Figure III-44. The lower half of the optimised structure supports the likelihood of an even distribution of the mesogens, oriented parallel to the chain axis. Oddly enough, the upper part did not. The effect of the rotation of the bond linking the liquid crystal moiety to the polymer backbone was studied. Although the perfectly planar polymer structure actually corresponded to an energy maximum, structures where the monomers were twisted at a slight angle to one another were amongst the lower energy configurations.

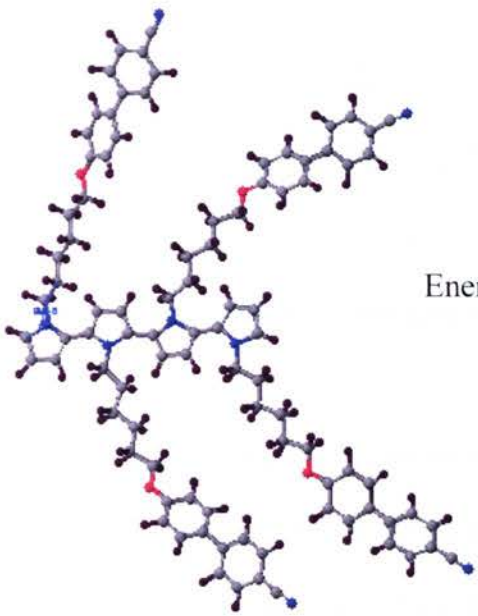

Energy: 198.55 kcal.mol^{-1}

Figure III-44 Tetramer of liquid crystal substituted pyrrole

The software being limited by the number of bonds that could be considered and altered for a single molecule (only a maximum of 2 bonds simultaneously, for a simple molecule), it was not possible to run the same 'rotation of the mesogen' experiment in this case: the molecule was too large, and the calculations could not be processed. It is however reasonable to suggest from the previous experiments that should the polypyrrole chain be longer, the chances of a natural order would be greater. This was supported by modelling oligomers of N-hexylpyrrole, for which again only the last substituent was not positioned like the others.

Altogether the combination of results from the models suggests that a structure which would combine an even distribution and direction of the spacers with a parallel direction of the liquid crystal to the backbone would exhibit a rather low energy, and therefore a good stability.

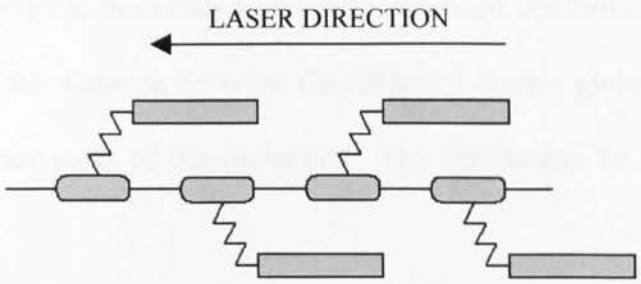

Figure III-45 Schematisation of expected structure

In the case of laser alignment this new description could mean that instead of sitting perpendicular to the flow, the liquid crystals would now be parallel to it. They would also tend to align the polymer chain parallel to the flow, as observed in practice. In addition, the liquid crystal moieties would then be in a position that would allow the development of nematic or smectic optical textures.

It does however remain unclear which direction with respect to the flow ('positive', with the flow, or 'negative', against the flow) the liquid crystals adopt. From the model and intuition it seems more likely that the mesogens would adopt an arrow-head shape, pointing against the direction of the flow.

Such an arrangement differs from the results obtained for other side-chain liquid crystal conducting polymers by Goto *et al*[124] and Kijima *et al*[69], in which the distances between the backbones were reported to be respectively 0.7 and 1 times the length of the fully extended substituent, as is illustrated in Figure III-42-c.

In order to support this theory, powder XRD data for aligned and unaligned films was obtained (section III.8.5), in order to indicate the angle or the bending that can be expected to occur between the polymer, the spacer, and the mesogen. Distinct spacing patterns were observed, parallel (3.7Å) and perpendicular (8.8Å) to the backbone.

By modelling the pyrrole monomer in its most extended conformation, CAChe 3.2 was used to determine the distance between the different atoms, giving a good estimate of the length of various parts of the molecule. The results can be found represented in Figure III-46.

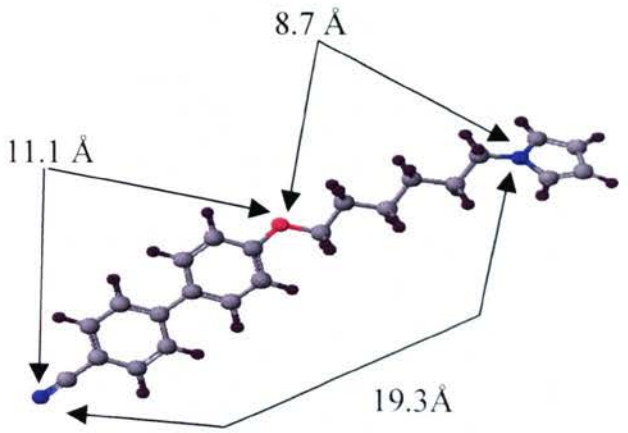

Figure III-46 Modelling of distances between atoms in the pyrrole monomer

By comparing the experimental data (sharp 8.8 Å peak) with the distances obtained from the model, it is possible to see that the peak observed is most likely to correspond to the length of the extended spacer. This seem to indicate a conformation such as the one in Figure III-43 (shown for an aniline monomer). As far as organisation affects the molecule, we can propose that the liquid crystalline moiety may force the organisation of the backbone not by pulling it perpendicularly as suggested before, but by adopting an arrow-head shape that pulls the backbone along. The other alternative, which would also allow a spacing of 8.8 Å to exist between the polymer backbone layers, involves the spacer sitting at an angle with respect to the backbone, as illustrated in Figure III-47. In this example, the layers are represented with a spacing of 3 Å between them, allowing for the van der Waals repulsion forces between adjacent atoms.

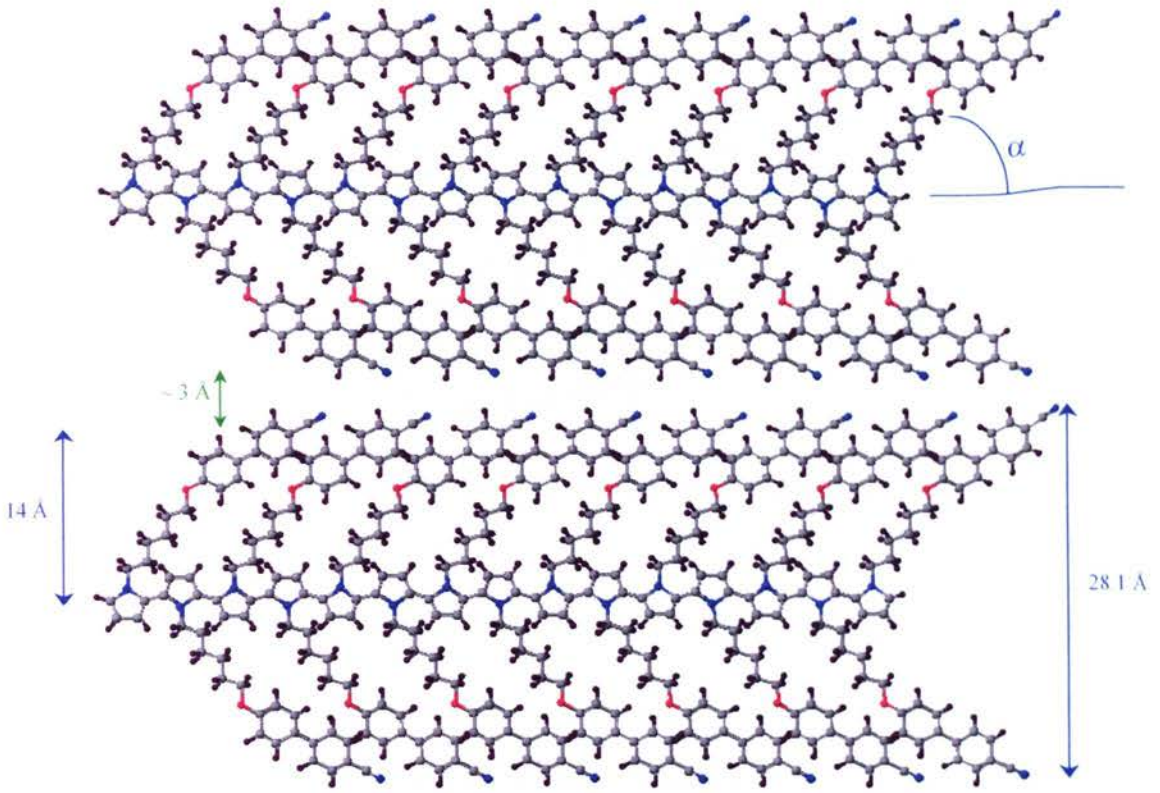

Figure III-47 Angled conformation for the liquid crystal polymer

An approximation of the angle required to create a layer 8.8 Å thick can be calculated by assuming that all the parts of the molecule can be represented by straight lines. By doing so, we can reduce the backbone and the angled moiety to a right-angled triangle, and the angle α can be obtained using the equation: sin α = spacing/length of moiety. Rearranging the equation using the value obtained from Figure III-46 for the length of the side-chain and 8.8 Å for the spacing yielded a value for alpha of 25.7°. This very small angle seems unlikely, as it would create a big steric hindrance between the backbone and the spacer. This result indicates that the most likely conformation for the aligned polymer would be that of the bent structure (Figure III-48).

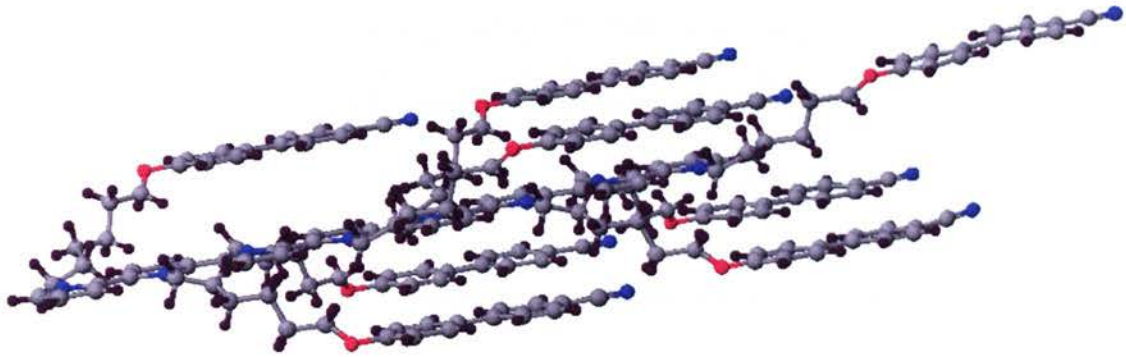

Figure III-48 Proposed (idealised) conformation for aligned liquid crystal polypyrrole

This conformation would result in a maximum planarity and alignment of the backbone. This is illustrated in Figure III-49 and the same representation enables one to see that the mesogens are all pointing in the same direction. This could favour either a smectic or a nematic mesophase, but in view of the types of mesogen used, it seems more likely that there is a lower degree of order, yielding a nematic structure.

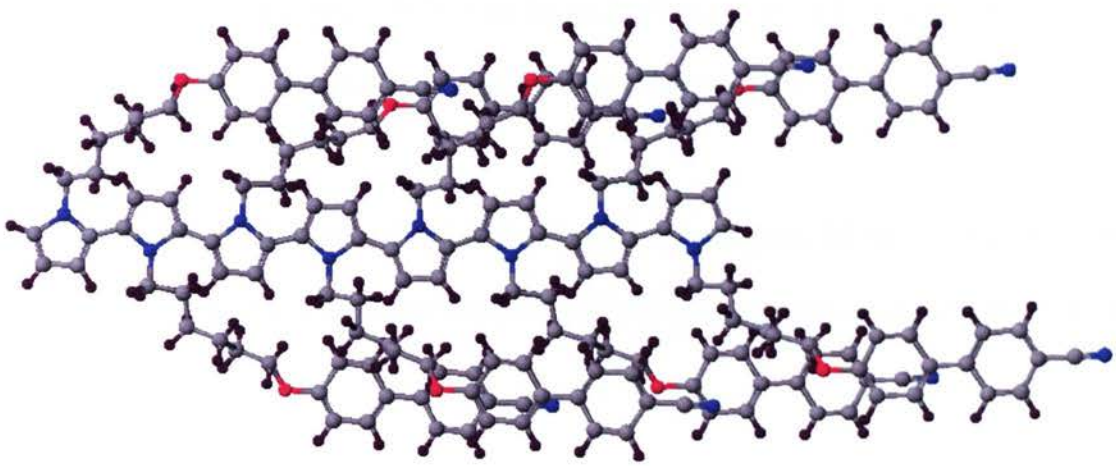

Figure III-49 Proposed (idealised) conformation for aligned liquid crystal polypyrrole (viewed from above)

The spacing of 8.8 Å was found to correspond to the thickness of the long molecule formed, as illustrated in Figure III-50.

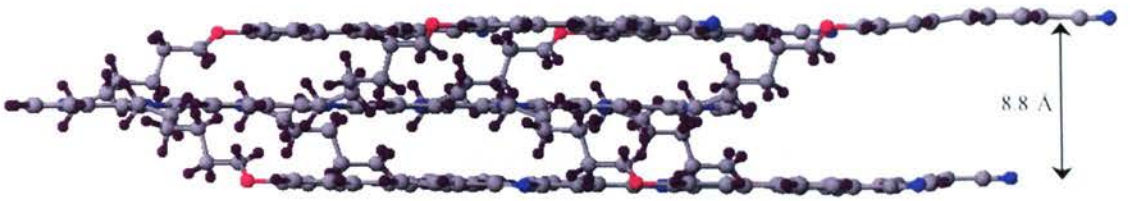

Figure III-50 Proposed (idealised) conformation for aligned liquid crystal polypyrrole (viewed from side)

By modelling an oligomer of the liquid crystal substituted pyrrole, it was possible to assess that the value of 3.7 Å corresponded almost exactly to the distance 'centre to centre' between two consecutive pyrroles.

As the XRD results support the compact structure shown in Figure III-45, the closer packing of the molecules in the material would account for the observed decrease in volume from laser alignment. With such an arrangement for the polymer molecules, there is the possibility for one chain to pack very closely with the next one. This could be verified by heating the whole sample and aligning it with a magnetic field and comparing the final thickness (volume) with the original data.

An illustration of the possible packing is shown in Figure III-51. This front view highlights the space available on both sides of the polymer chain as well as above and below.

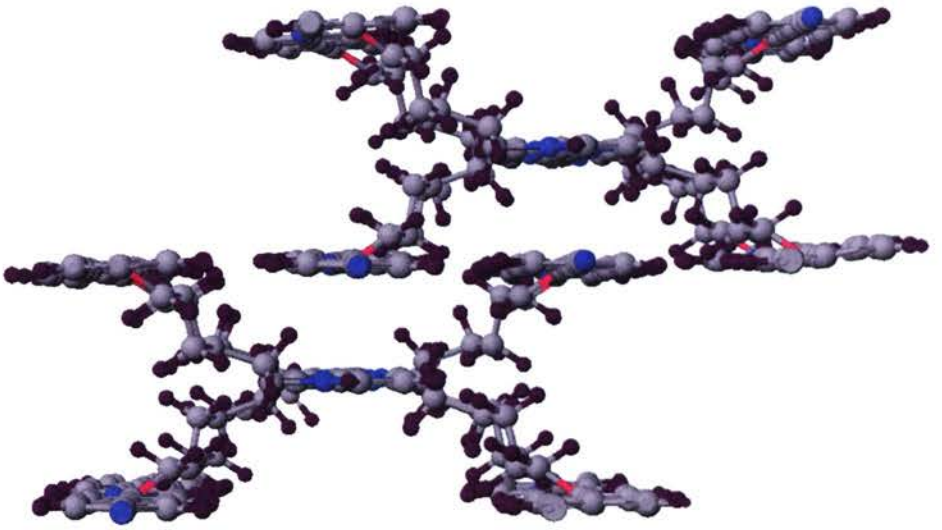

Figure III-51 Possible packing of aligned LC polypyrrole molecules (front view)

The possibility of interlocking the neighbouring chains is made more favourable by the fact that it could allow the mesogens to position themselves so that the –CN group is next to an O. This 'coupling' of electron rich and electron poor groups forms a makeshift bond (Figure III-52).

Figure III-52 Interactions between mesogens from neighbouring chains

IV CONCLUSION AND FUTURE WORK

The work carried out during this project was divided into small inter-related modules.

The first step was to get familiar with the techniques involved in the study of liquid crystals. For this reason, hot stage microscopy of liquid crystalline materials prepared by a previous research student was studied. The next step was to study the polymerisation techniques involved. The emulsion polymerisation of aniline derivatives was studied, and the ionic surfactant originally used was quickly replaced with an a non-ionic one that proved just as efficient but was much easier to separate from the polymeric product. An ideal concentration of surfactant was experimentally determined to optimise the yield, and satisfactory results were obtained.

A different method of polymerisation was chosen for the pyrrole and carbazole derivatives. Electropolymerisation using cyclic voltammetry allowed one easily to get a clean film of polymer that could be characterised as well as providing some useful information about the polymer itself. The potentials at which the polymerisation and the dedoping process occurred were compared with the ones found in the literature. The pyrrole monomers chosen were commercial N-alkyl substituted ones at first, after which some monomers and intermediates bearing liquid crystal or liquid crystal-like pendant groups were studied. This work provided an excellent basis for the polymerisation of liquid crystal monomers. The polymerisation of simple commercial N-alkyl-derivatives of carbazole was performed using the same method. Both polymerisation techniques yielded products that were easily retrieved from the reaction medium and were of high apparent molar mass, as they exhibited very good film forming ability.

The last synthetic part of the project was the preparation of carbazole N-derivatives, substituted with alkyl chains at first and subsequently with a liquid crystal like substituent. The synthetic route using a crown ether proved successful, but the small yields limited the number of tests which could be carried out afterwards. Electropolymerisation of N-butyl carbazole was successfully performed, and film formation could be observed, but again the amount of polymeric material was small. The chemical polymerisation in aqueous solution of the carbazole monomers could also probably be improved even further. Much more promising was the use of liquid iodine as a medium, despite the difficulty of removing the excess iodine. Despite the lack of processability of the carbazole polymers produced, they still appear to be materials worthy of further investigation, as the extended system of rings should further stabilise any applied charge. Hopefully future research will succeed in producing larger amounts of processible material. One way of encouraging a more favourable structure may involve changing the liquid crystal moiety in order to decrease the Tg, and/or increase the LC transition temperature. A terphenyl equivalent, for example might be considered. In the case of nitrobenzene substituted with a terphenylethoxy based mesogen (section III.5.1) it was found that the liquid crystal transition was increased to 220°C instead of the 60-150°C usual range for liquid crystal anilines. The molecular modelling of such a molecule should provide some indication as to the improvement obtained from the addition of a phenyl group to the monomer originally prepared.

Conductivity measurements versus temperature for a liquid crystal pyrrole provided a good estimate of the thermal activation behaviour of the conductivity. It exhibited a change from high activation energy at low temperatures to a low activation energy at higher temperatures. This unusual change in trend coincided with the reported nematic liquid crystal transition.

In the later part of the project the use of molecular modelling package was introduced to provide a simulation of the behaviour of the monomers and polymers at the molecular level as well as properties of the bulk material. This provided useful clues and information as to what may be happening to the materials throughout the experiments. Furthermore, the model enabled a new proposal to be made, supported by XRD data, in an attempt to explain the phenomena involved in the laser alignment of liquid crystal polymers. This novel alignment technique was shown greatly to improve the conductivity of liquid crystal conducting polymers, through an increase in the backbone alignment. Optical data from microscopy (using cross-polarised light) confirmed the anisotropy resulting from the laser treatment of the polymers.

The use of laser alignment as a means to improve the planarity and the electrical conductivity of polymeric materials could have many industrial applications. This is enhanced by the fact that provided the heating process did not damage the polymer, the tracks could be wiped out using for example exposure to infrared heating, and re-written at will[70]. The already very small width of the tracks is probably only limited by the focussing of the beam. Even greater ordering of the liquid crystal, and hence of the backbone might be obtained if a magnetic or electric field was applied to the sample during the laser-track writing. Even if no further improvement of the conductivity was observed, it would most certainly affect the orientation of the liquid crystal moieties with respect to the track, resulting in different optical absorption, and maybe offering possibilities for optical data storage.

A new field of investigation for the use of laser alignment is the growing range of potential light-emitting polymers. A recent publication[125] reported that some polymers derived from carbazole could show light-emitting properties. By slightly modifying such a polymer and substituting it with a liquid crystal moiety, it might be possible to produce a material for which the luminescence in the laser-aligned tracks

would be different from that of the background. Furthermore, the switching voltage required to operate the device would be lower for the laser aligned polymer due to a smaller energy-gap. But the main direct advantage of laser-induced alignment is that micron-scale tracks can be produced, in any required pattern on a material that does not have to be rigid and incorporates the liquid crystals as part of its structure. Most flexible liquid crystal displays (such as the one in Figure IV-1) rely on the liquid crystal being sandwiched between thin polymer sheets.

Conducting polymers are already used for applications such as backlighting for liquid crystal displays, and also for sensors. The latter would greatly benefit from being able to produce microscopic patterns of conductive material, allowing very small-scale devices to be produced, cheaply and efficiently.

There was great anticipation that the carbazole polymers would yield themselves to a similar treatment with similar results, which will only be verified by producing soluble polycarbazoles with low glass-transition temperatures. This would require alternative methods of polymerisation as the polymers obtained from carbazole derivatives in this project were found not to be easily processible.

Another area that would benefit from being investigated would be the preparation of co-polymers of the liquid crystal moieties with unsubstituted monomers, or with monomer units bearing a pendant group such as an alkyl chain to help lower the glass transition temperature of the polymer. By producing a symmetrical trimer first with the liquid crystalline unit in the centre, it would ensure that a regular copolymer is produced, the study of which would hopefully show that the aligning properties did remain. The study of regular and non regular co-polymers with increasing ratios of non-mesogenic units should allow the determination of the optimum composition to ensure a low Tg while retaining the aligning properties. Such polymers, especially non-regular ones would be more likely to find industrial applications, thanks to their lower cost.

To complete the work on conducting properties discussed in this thesis, further experiments measuring the evolution of conductivity with temperature would need to be carried out, with slower rates and a series of measurements carried out in upon cooling as well as upon heating. This would provide information on the effect of the thermotropic liquid crystal transition on the charge carrier mobility, by allowing the determination of the activation energy. The use of dielectric thermal analysis (DETA) measurements might help clarify the nature of the transition observed in the 'conductivity versus temperature' experiment.

As for the aligning itself, further study will be needed to fully understand the nature of the phenomenon. The use of a moving heating source that could melt a specific section of the sample (as in the case of zone refining) should enable the simulation of laser alignment on a whole sample, allowing further investigation of the

---

[1] Picture from the UNIAX website.

molecular orientation using x-ray diffraction. Together with this experiment a study of the effect of the width of the laser track on the alignment could be carried out.

The investigation of the effect of a magnetic field applied at the same time as the laser or the gradual heating might lead to the development of improved techniques for further enhancement of the conducting properties by increasing even more the planarity of the backbone.

In the meantime this project has contributed a little to the creation of new materials and -maybe- to better understanding of others, and that, I feel, was the original aim of it all.

V APPENDICES

V.1 Lexicon and List of Abbreviations

b.p.	boiling point
BuLi	butyl lithium
CB	conduction band
conc.	concentrated
DBSA	dodecylbenzenesulphonic acid
DSC	differential scanning calorimetry
DMF	N,N-dimethylformamide
DMSO	dimethylsulphoxide
Endo.	endothermic
Et	ethyl
Et_4NBF_4	tetraethylammonium tetrafluoroborate
Exo.	exothermic
FTIR	Fourier transform infrared
GPC	gel permeation chromatography
h	hours
HPLC	high performance liquid chromatography
I	isotropic
IMS	industrial methylated spirit
LC	liquid crystal
LCD	liquid crystal display
LCP	liquid crystalline polymer
m.p.	melting point
MCLCP	main-chain liquid crystalline polymer
Me	methyl
min	minutes
MS	mass spectrometry
MW	molar mass
N	nematic
NMC	N-methyl carbazole

NMR	nuclear magnetic resonance
OMe	methoxy
PA	polyacetylene
PANI	polyaniline
Ph	phenyl
PPO	poly(*p*-phenyleneoxide)
PPP	poly(*p*-phenylene)
PPy	polypyrrole
PYLC	liquid crystal substituted polypyrrole
S	smectic
SCLCP	side-chain liquid crystalline polymer
TGA	thermogavimetry analysis
THF	tetrahydrofuran
TLC	thin layer chromatography
TMA	thermomechanical analysis
UV	ultra-violet
VB	valence band
Vs	versus

V.2 Elemental Analysis Data

Compound	Formula	RMM	C%	H%	N%	O%	Br%	Exp C%	Exp H%	Exp N%	Exp O%	Exp Br%	Comments
1-(N-carbazole)-6-[(4-cyanobiphenyl-4'-yl)oxy]hexane	C31H28N2O	444	83.78	6.31	6.31	3.60	0.00	0.12	0.10	0.00	0.00	0.00	Sample too small
N-propylcarbazole	C15H15N	209	86.12	7.18	6.70	0.00	0.00	84.16	5.24	7.91	2.69	0.00	Carbazole present
N-butylcarbazole	C16H17N	223	86.10	7.62	6.28	0.00	0.00	85.81	7.67	6.23	0.29	0.00	
								85.96	7.69	6.25	0.10	0.00	
1-(N-carbazole)-6-[(4'-bromobiphenyl-4-yl)oxy]hexane	C30H28NOBr	498	72.29	5.62	2.81	3.21	16.06	74.69	6.03	3.28	1.54	14.46	
1-bromo-6-[(4-cyanobiphenyl-4'-yl)oxy]hexane	C19H20NOBr	358	63.69	5.59	3.91	4.47	22.35	34.27	4.67	0.51	52.03	8.52	H2O plus product has decomposed
								34.00	4.80	0.51	52.30	8.39	
poly[1-(N-carbazole)-6-[(4'-bromobiphenyl-4-yl)oxy]hexane]	poly C30H28NOBr	498	72.29	5.62	2.81	3.21	16.06	45.64	5.07	0.00	49.29	0.00	Too much iodine from polymerisation
								45.61	5.08	0.00	49.31	0.00	
poly(N-methylcarbazole)	poly C13H11N	181	86.19	6.08	7.73	0.00	0.00	45.99	5.04	0.11	48.86	0.00	Too much iodine from polymerisation
								46.20	5.08	0.10	48.62	0.00	

V.3 TEM scan of the emulsion polymerisation medium for polymethoxyaniline

V.4 ^{1}H NMR from the polymerisation of 1-(N-carbazole)-6-[(4'-bromobiphenyl-4-yl)oxy]hexane in liquid iodine

V.4.1 T=370K (heating)

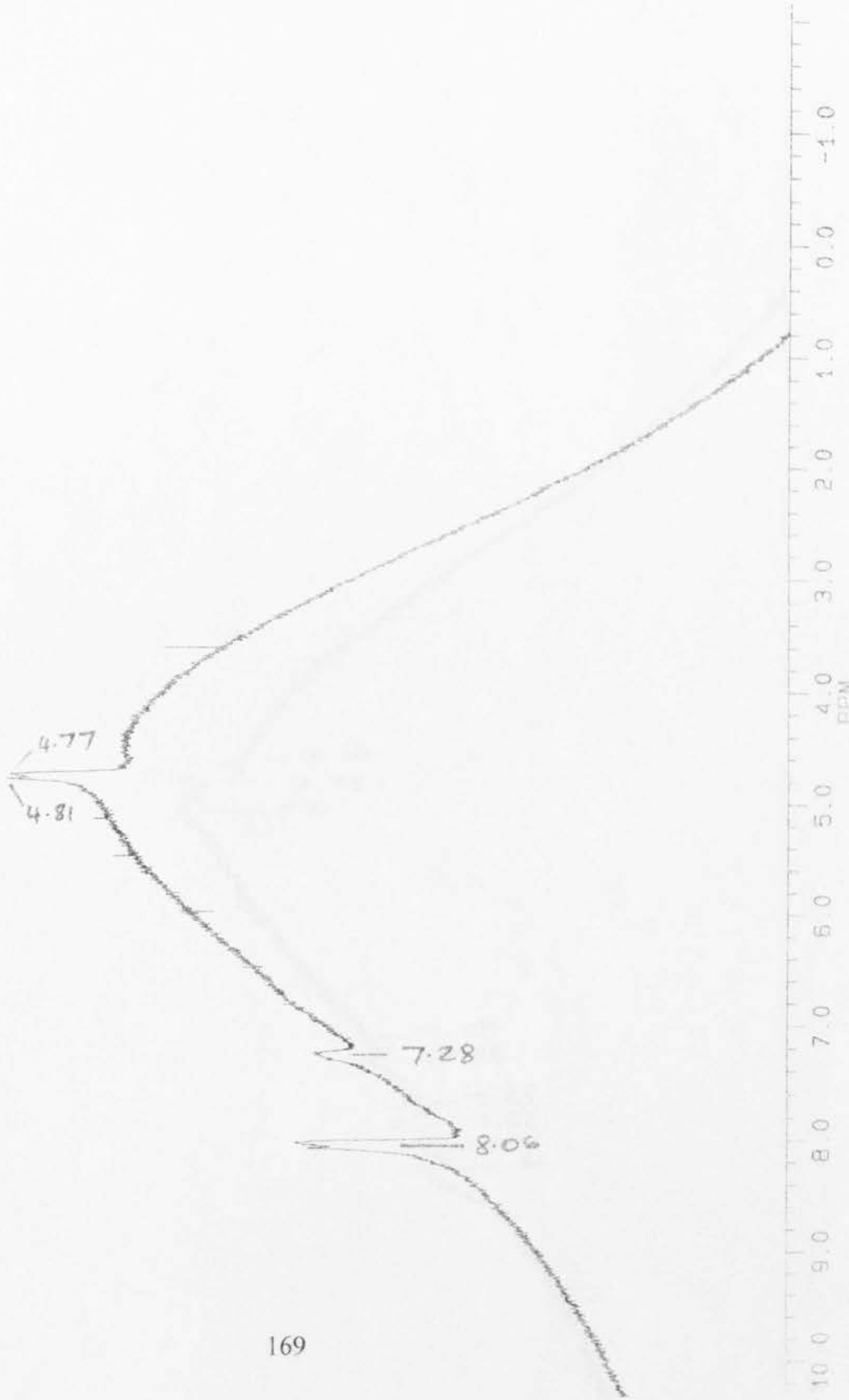

V.4.2 T=406K (heating)

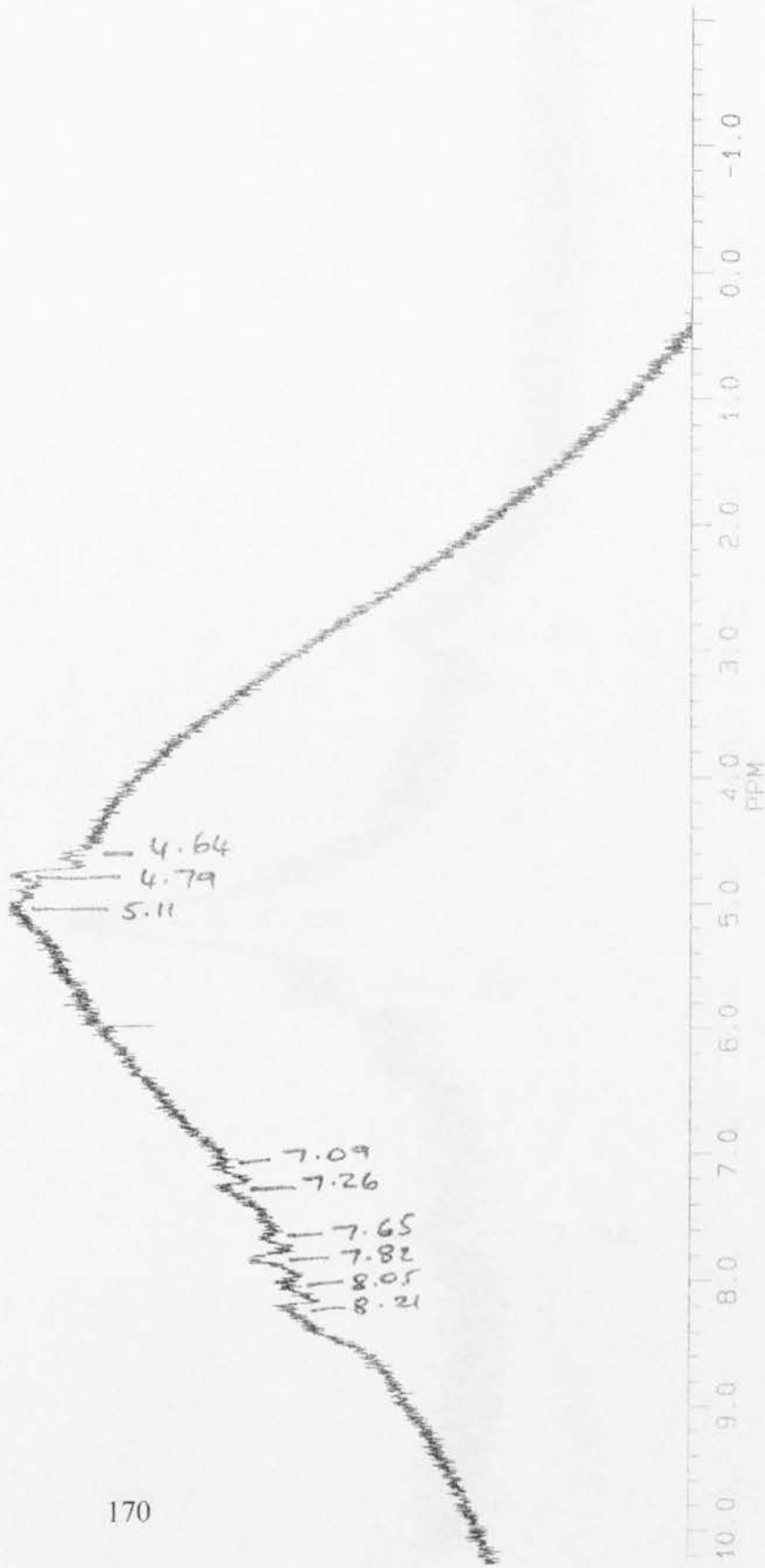

V.4.3 T=435K (stabilised, t=5min)

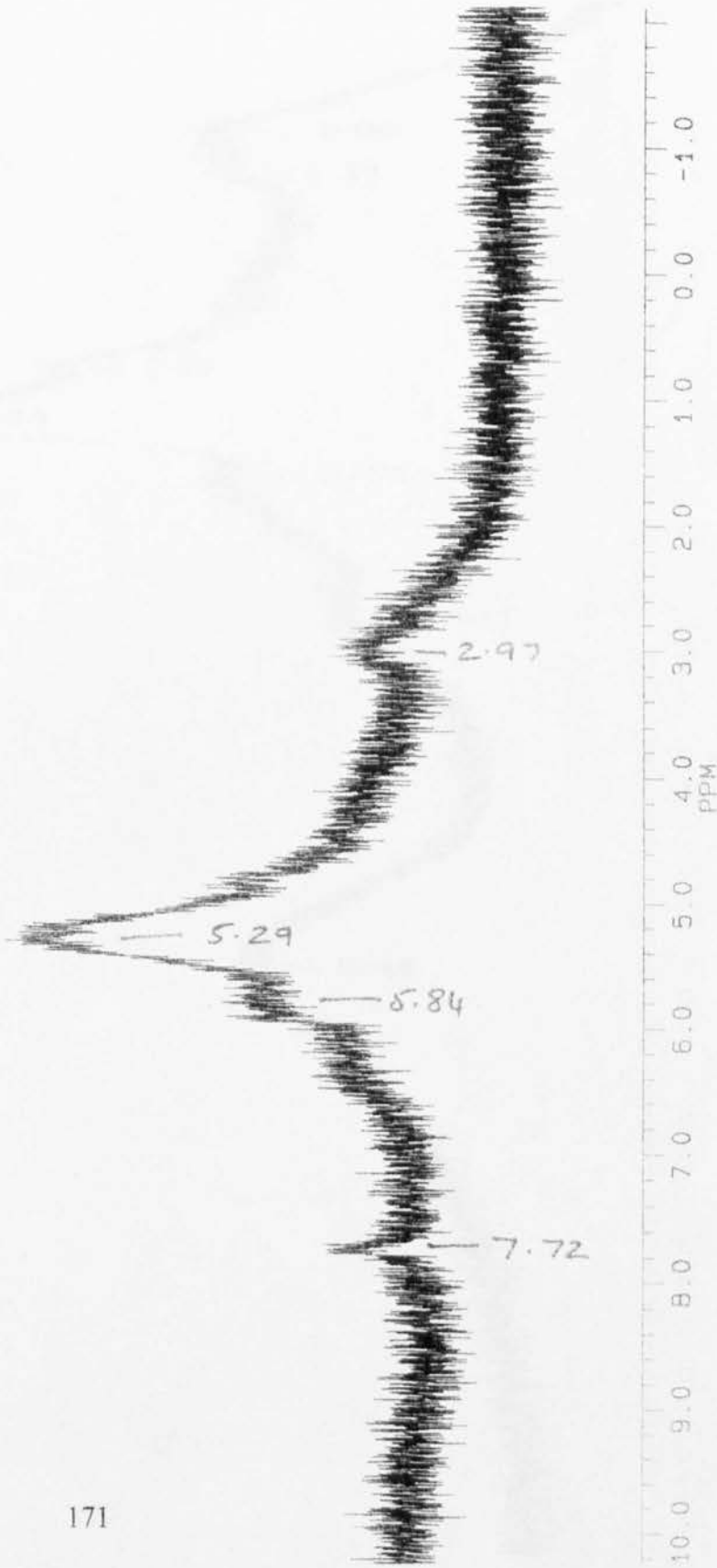

V.4.4 T=435K (stabilised, t=20min)

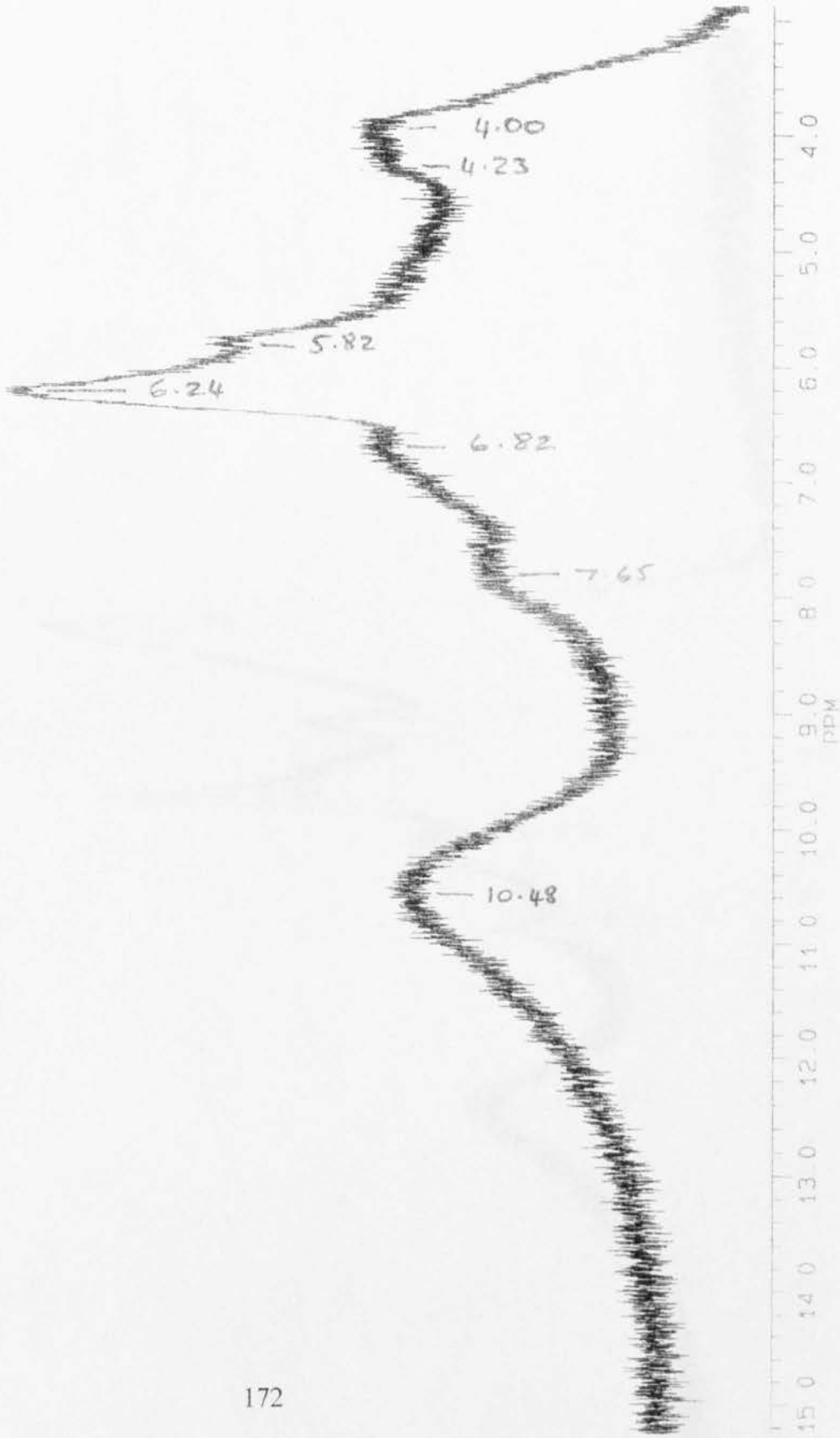

V.4.5 T=440K (stabilised, t=40min). [T increased at t=30min.]

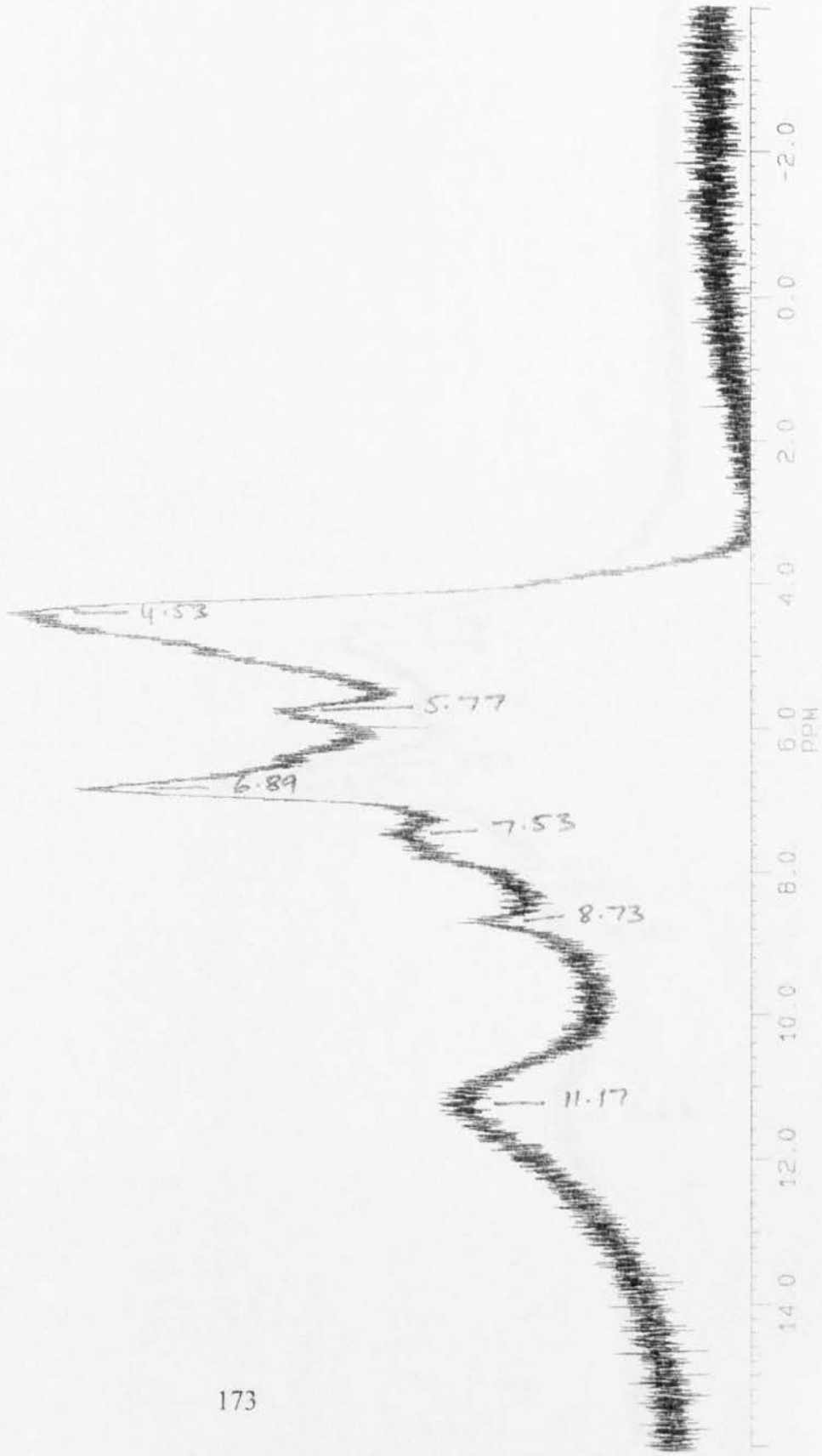

V.4.6 T=440K (stabilised, t=65min)

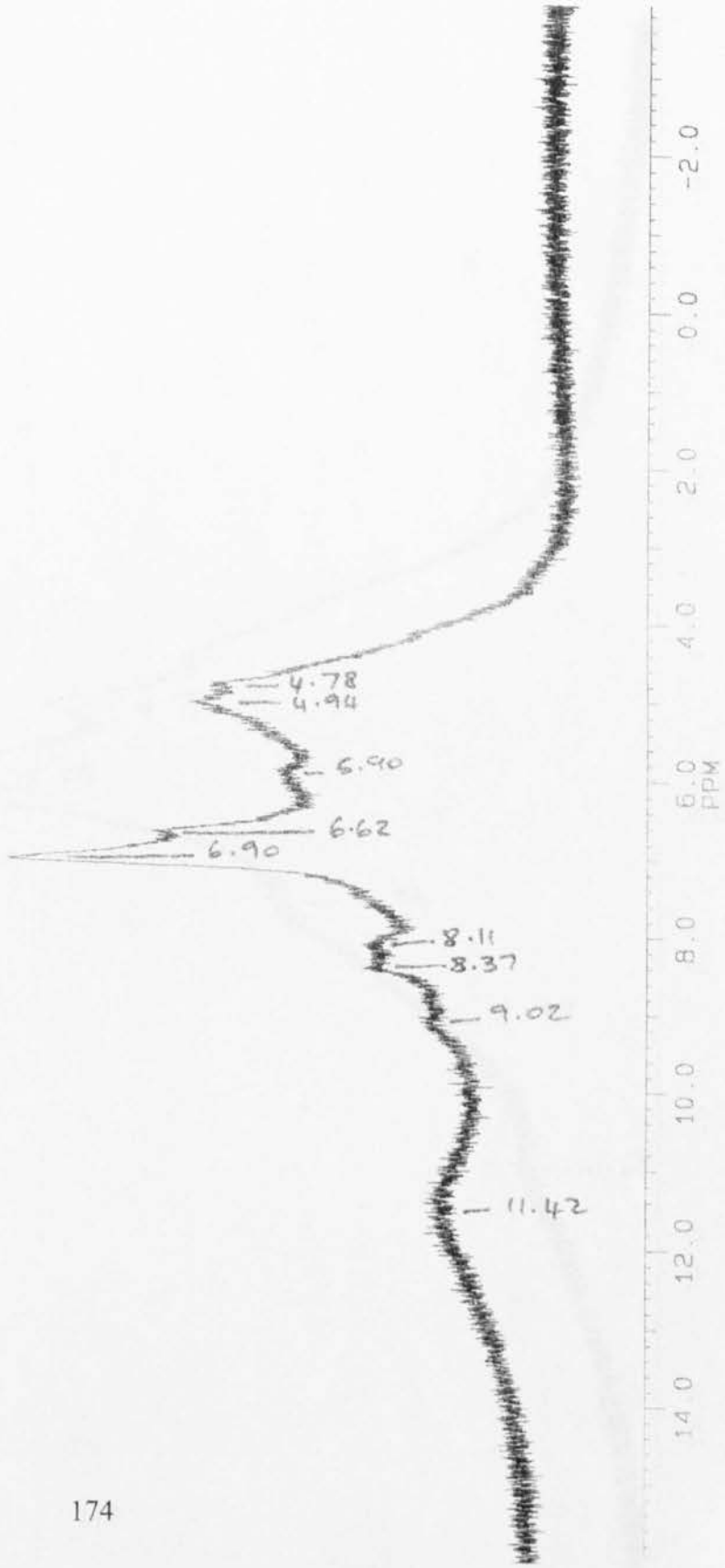

V.4.7 T=440K (stabilised, t=80min)

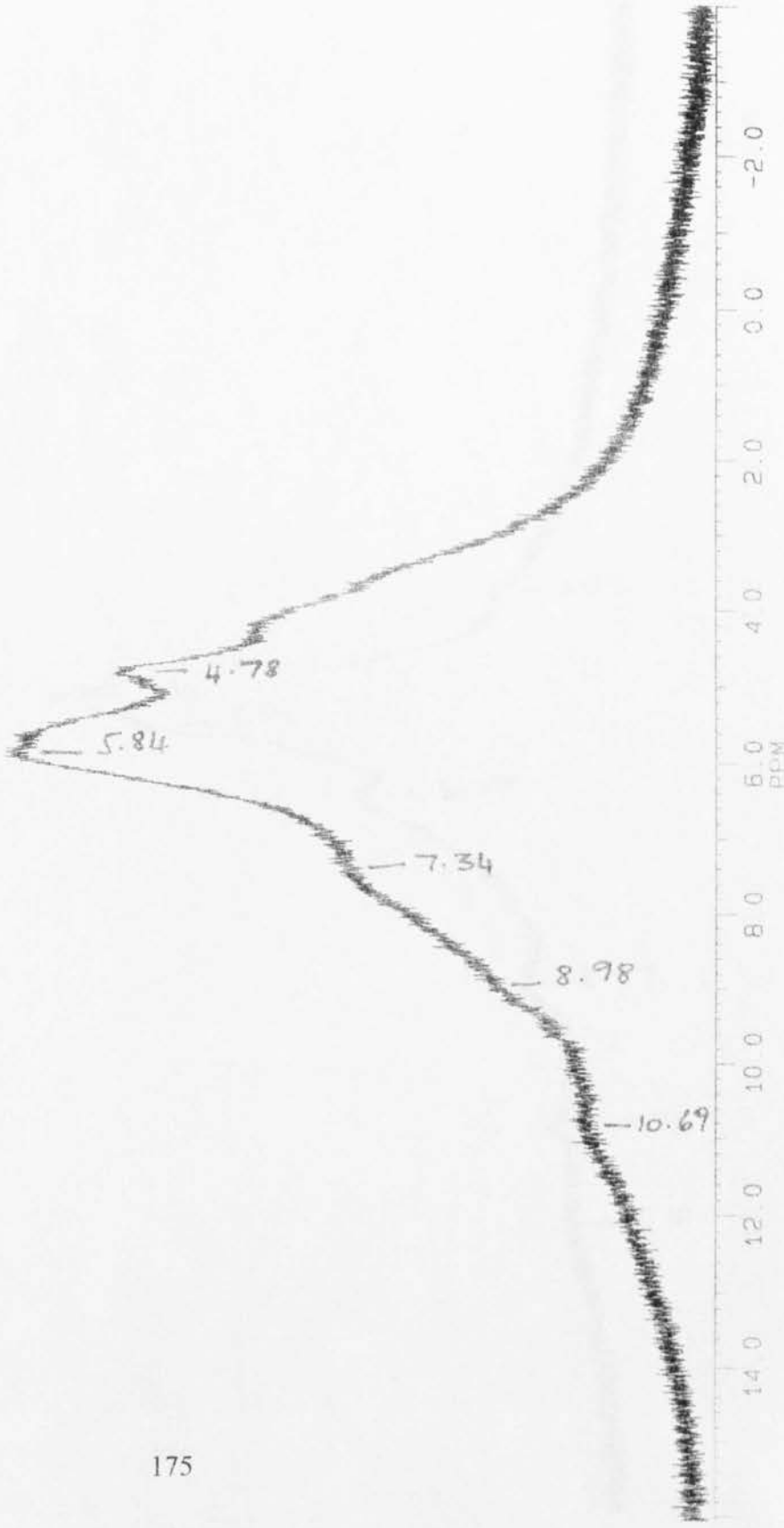

V.4.8 T=440K (stabilised, t=95min)

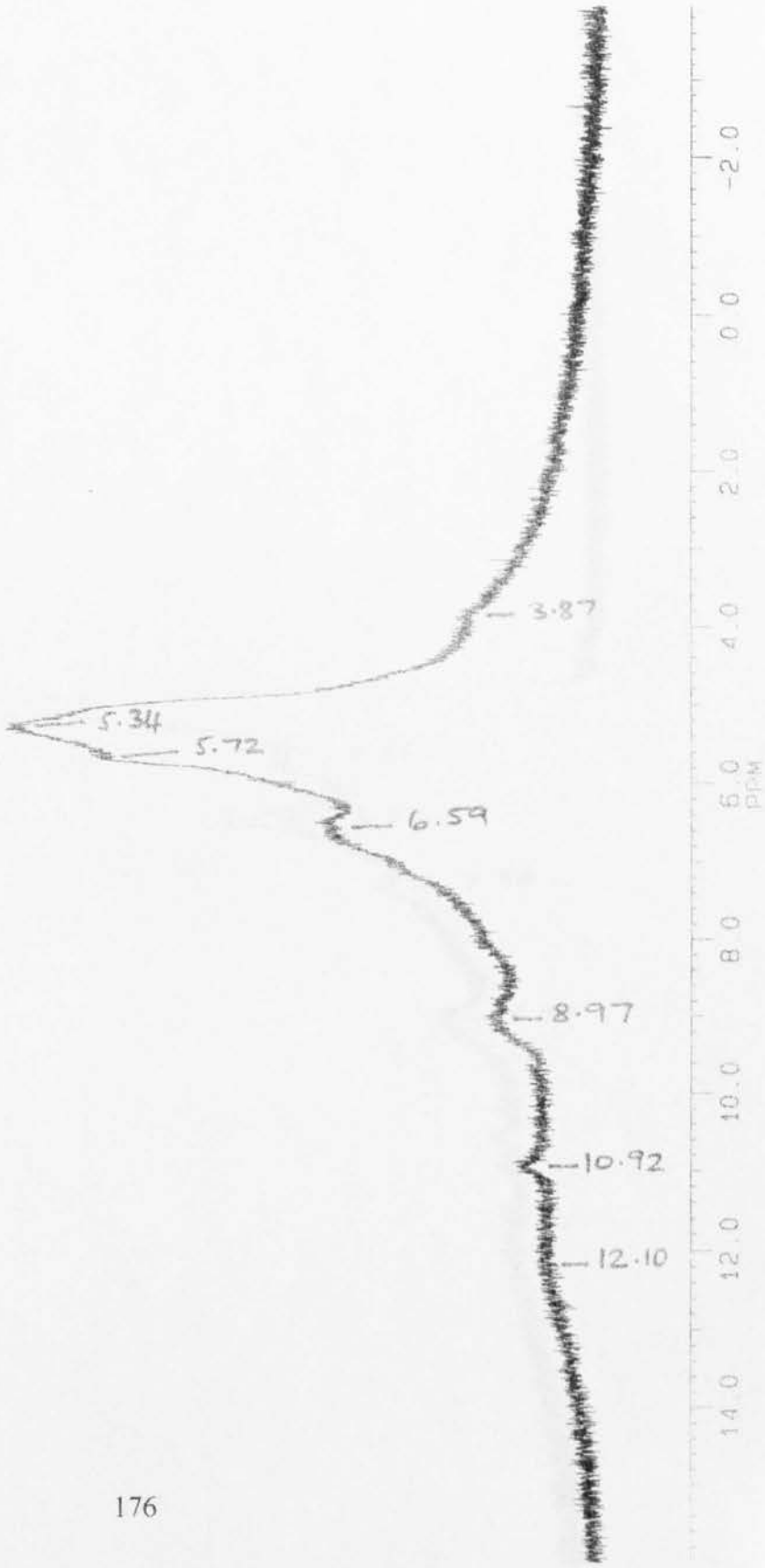

V.4.9 T=440K (stabilised, t=110min)

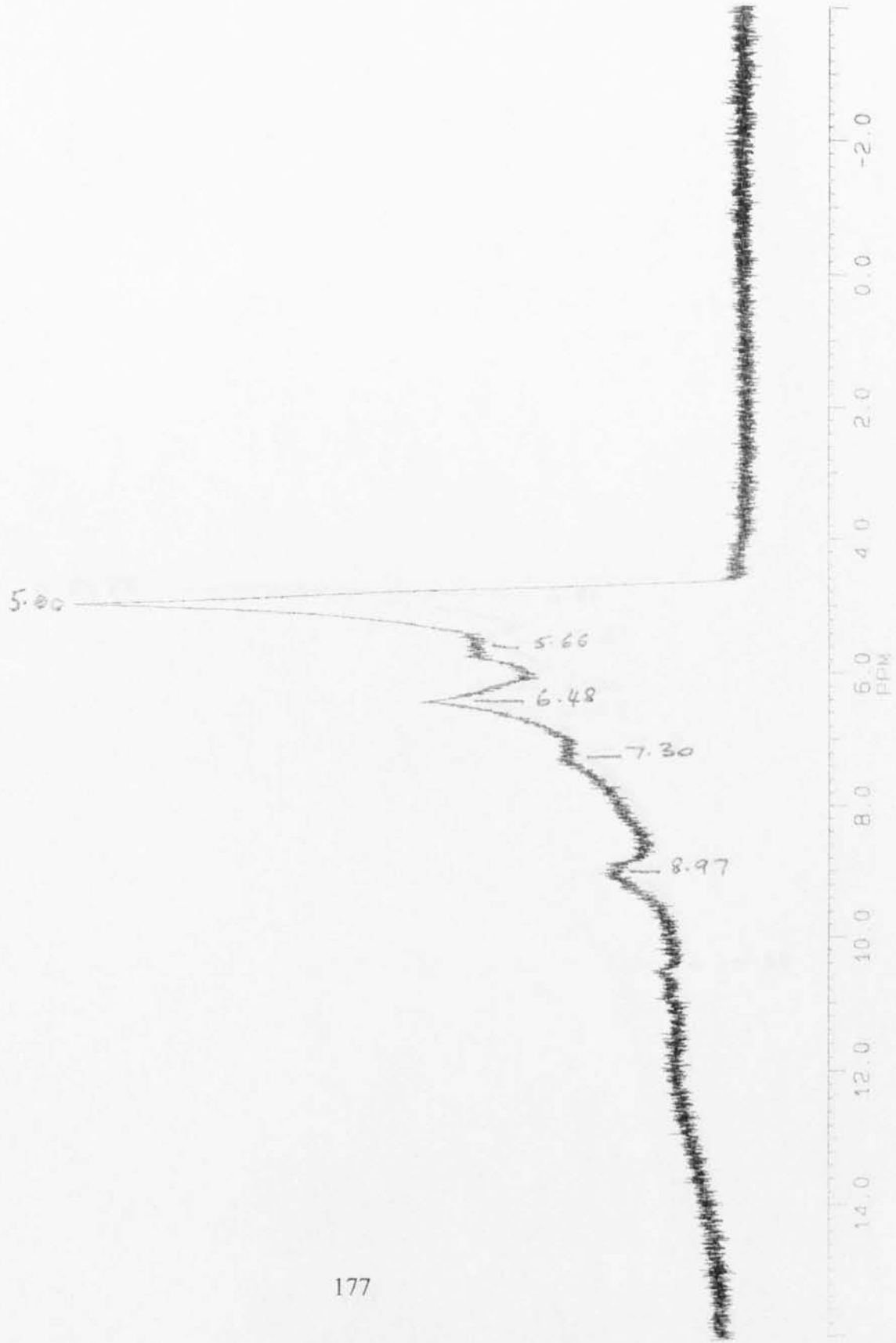

V.4.10 T=440K (stabilised, t=125min)

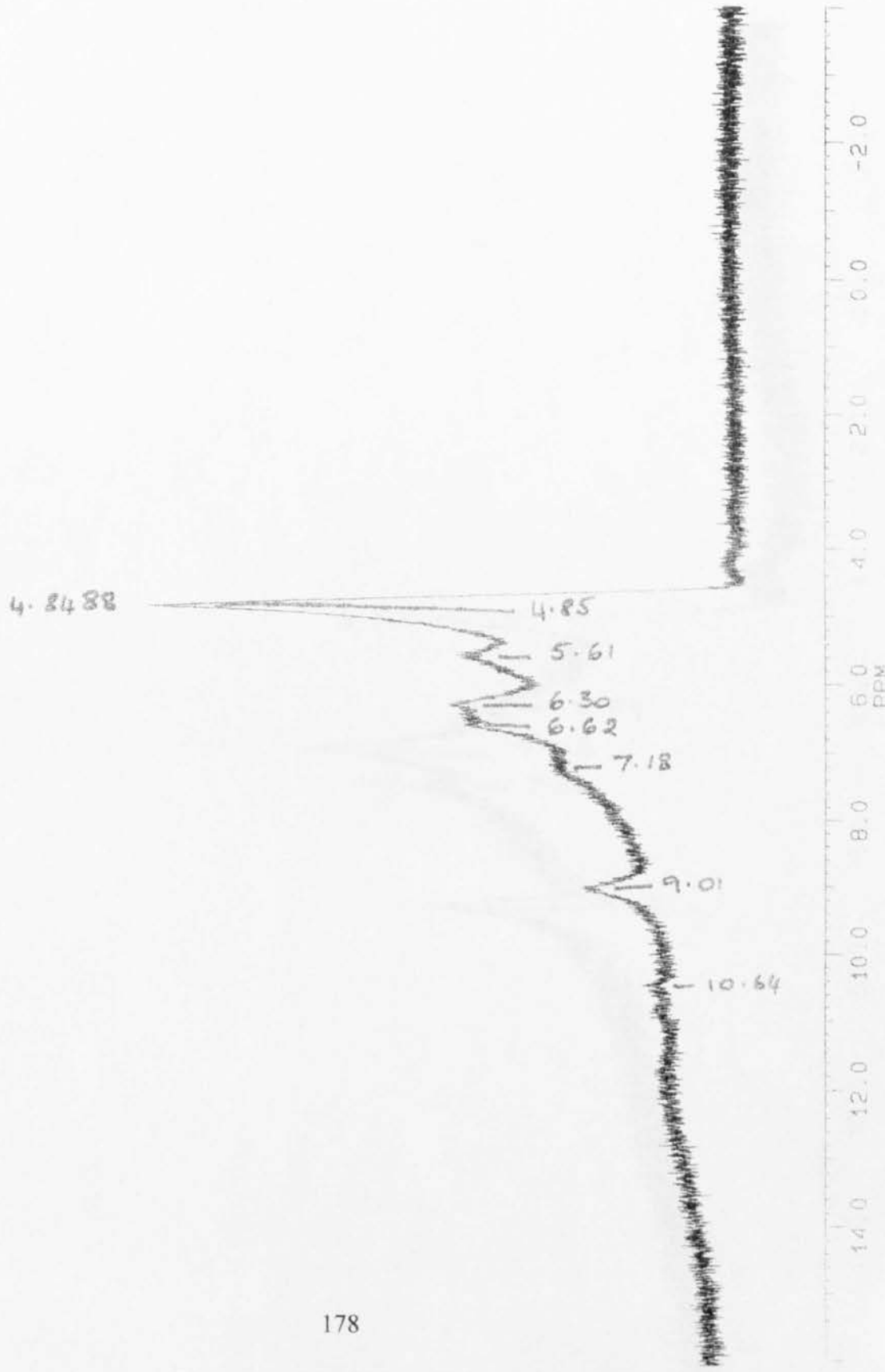

V.4.11 T=440K (stabilised, t=140min)

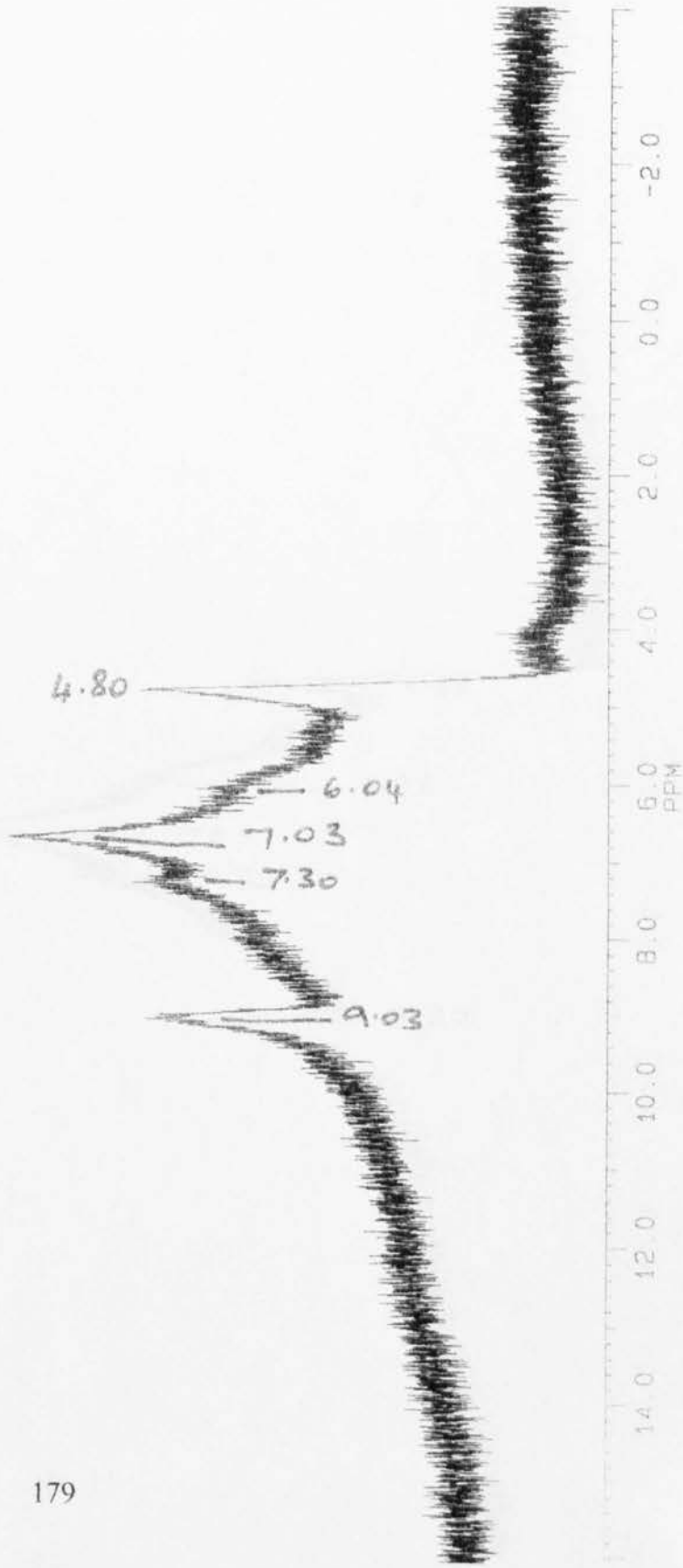

V.4.12 T=440K (stabilised, t=155min)

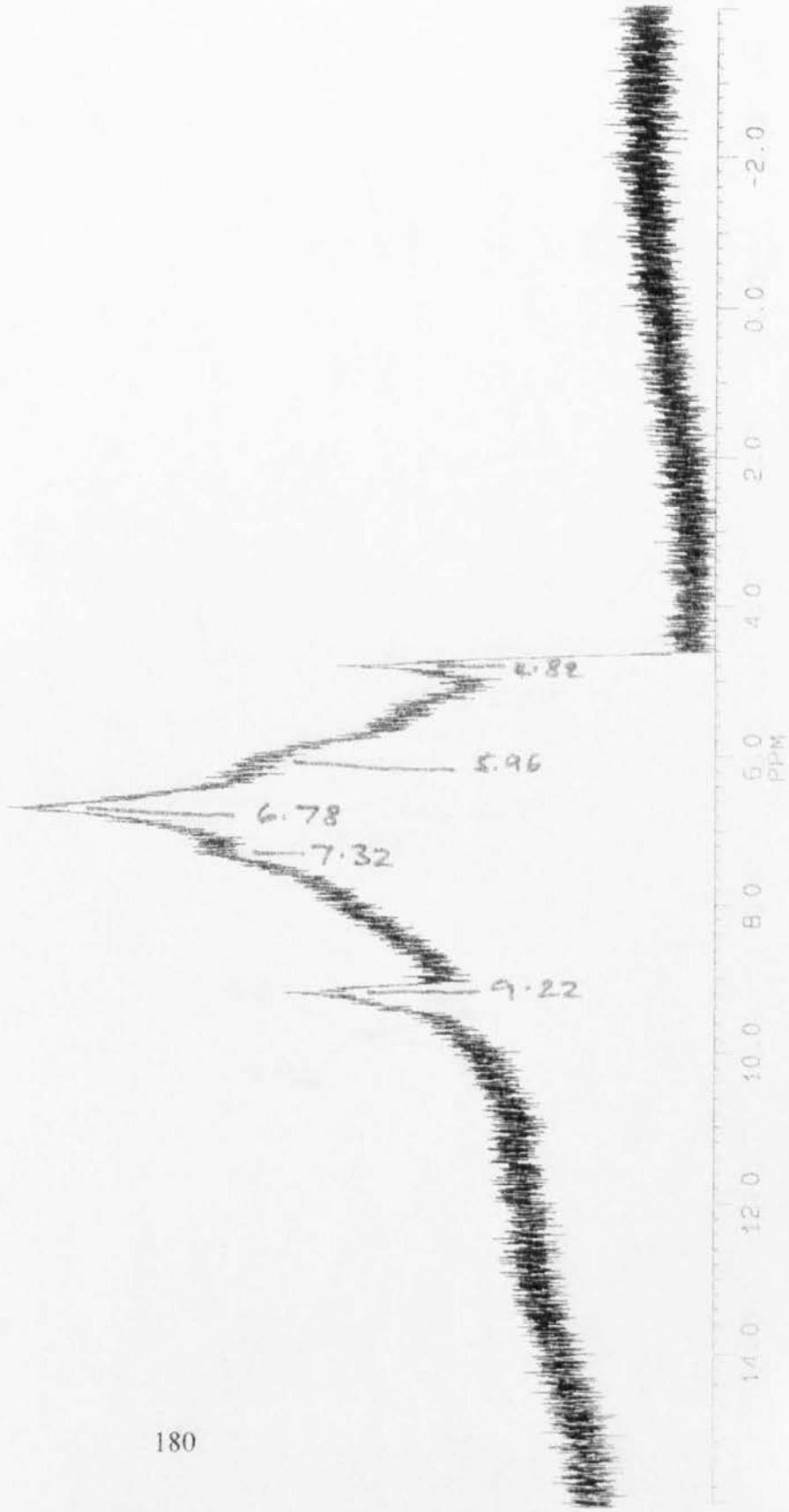

V.4.13 T=440K (start of cooling, t=170min)

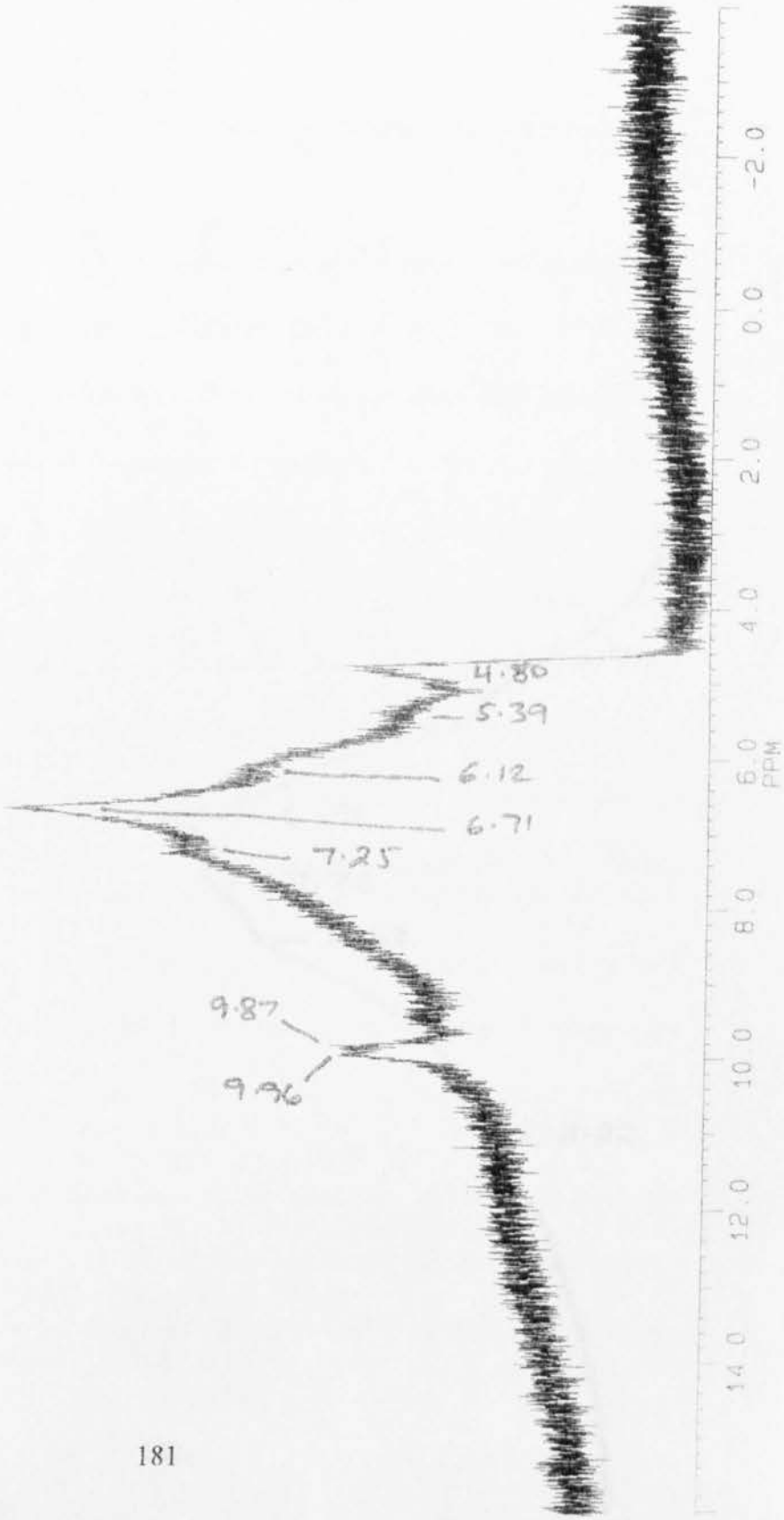

V.4.14 T=347K (cooling, t=185min)

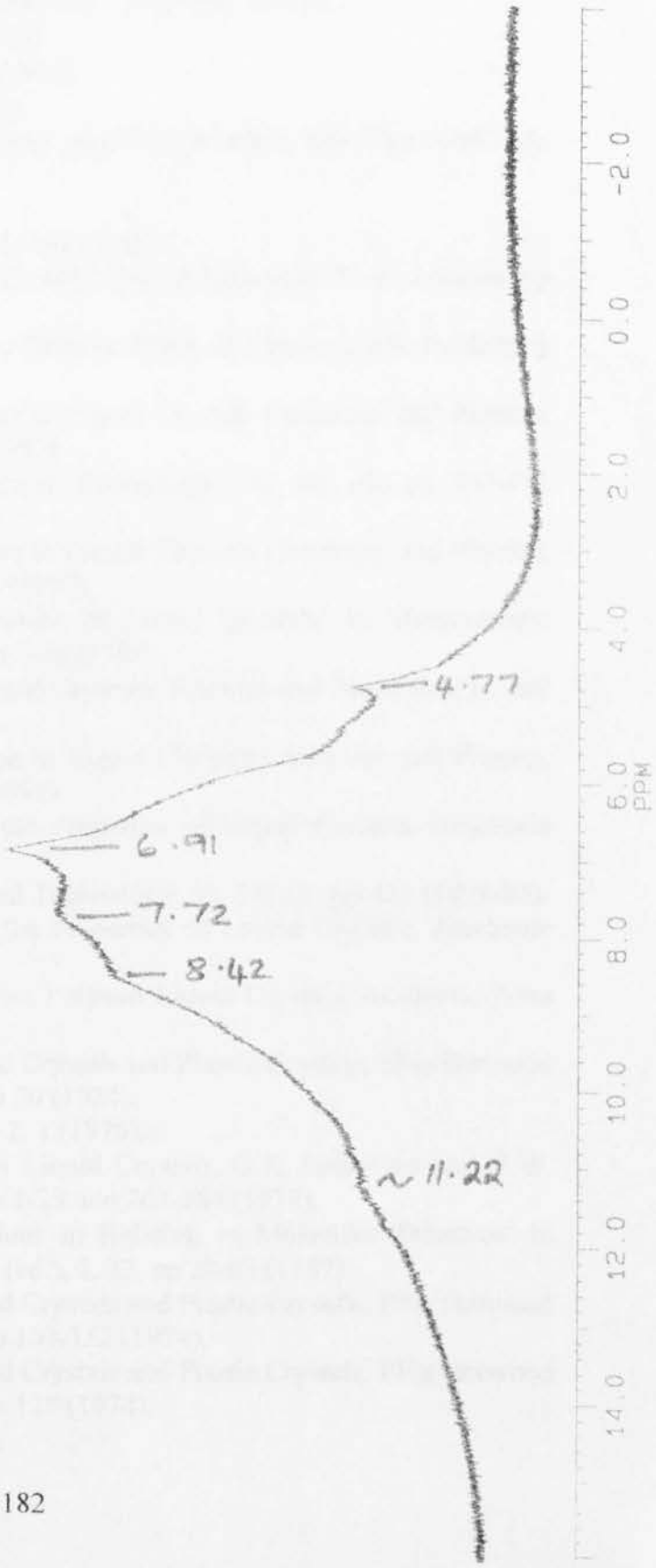

VI REFERENCES

1 F. Vollrath, and D.P. Knight, Nature, 410, 6828 (2001) 541-548
2 P. Ibison, P.J. Foot, and J.W. Brown, Synth. Met., 76 (1994) 297-300
3 F. Reinitzer, Monatsh. Chem., 9, 421 (1888)
4 R. Virchow, Virchows Archives, 6, 571 (1854)
5 O.Z. Lehman, Phys. Chem., 4, 462 (1889)
6 Liquid Crystals Plastic Crystals, G.W. Gray, and P.A. Windsor, Ellis Horwood Ltd., ix-xiv (1974)
7 G. Friedel, Ann. Phys., 18, 273 (1922)
8 A. Saupe, G. Englert, Phys. Rev. Lett., 11, 462 (1963).
9 P.G. de Gennes, The Physics of Liquid Crystals, Oxford University Press, London, pp 23-56 (1974).
10 P.J. Collings, Liquid Crystals: Nature's Delicate Phase of Matter, I.O.P. Publishing Ltd, pp 7-9 (1990).
11 P.J. Collings, and M. Hird, Introduction to Liquid Crystals Chemistry and Physics, Taylor and Francis (publisher) pp 79-92 (1997)
12 Kirk-Othmer Encyclopaedia of Chemical Technology, 14, 3rd ed., pp 397-411 (1978-84).
13 P.J. Collings, and M. Hird, Introduction to Liquid Crystals Chemistry and Physics, Taylor and Francis (publisher) pp 133-146 (1997)
14 A.J. Leadbetter, 'Structural Classification of Liquid Crystals' in Thermotropic Liquid Crystals, G.W. Gray (ed.), 22, 1, pp 1-20 (1987)
15 G.W. Gray, J.W. Goodby, Smectic Liquid Crystals, Textures and Structures, L. Hill (publisher), (1984)
16 P.J. Collings, and M. Hird, Introduction to Liquid Crystals Chemistry and Physics, Taylor and Francis (publisher) pp 43-77 (1997)
17 G.W. Gray, Molecular Structure and the Properties of Liquid Crystals, Academic Press Inc., New York, pp 138 (1962).
18 Kirk-Othmer Encyclopaedia of Chemical Technology, 14, 3rd ed., pp 411 (1978-84).
19 G.W. Gray, Molecular Structure and the Properties of Liquid Crystals, Academic Press Inc., New York, pp 138 (1962).
20 K.A. Ciferri, W.R.Krigbaum, R.B.Meyer, Polymer Liquid Crystals, Academic Press Inc., pp 5-22 (1982).
21 G.W. Gray, P.A. Windsor (eds.), Liquid Crystals and Plastic Crystals, Ellis Horwood Ltd (publisher), Chichester, England, 1, pp 30 (1974).
22 G.W. Gray, Advanced Liquid Crystals, 2, 1 (1976).
23 G.W. Gray, The Molecular Physics of Liquid Crystals, G.R. Luckhurst and G.W. Gray Eds., Academic Press, New York, pp 1-29 and 263-284 (1979).
24 K.J. Toyme, 'Liquid Crystal Behaviour in Relation to Molecular Structure' in Thermotropic Liquid Crystals, G.W. Gray (ed.), 2, 22, pp 28-63 (1987).
25 G.W. Gray, P.A. Windsor (eds.), Liquid Crystals and Plastic Crystals, Ellis Horwood Ltd (publisher), Chichester, England, 1, pp 103-152 (1974).
26 G.W. Gray, P.A. Windsor (eds.), Liquid Crystals and Plastic Crystals, Ellis Horwood Ltd (publisher), Chichester, England, 1, pp 125 (1974).

27 G.W. Gray, Molecular Structure and the Properties of Liquid Crystals, Academic Press Inc., New York, pp 138 (1962).
28 Kirk-Othmer Encyclopaedia of Chemical Technology, 14, 3rd ed., pp 397-411 (1978-84).
29 L. Gabaston, PhD thesis, Kingston University, 1995.
30 H. Finkelmann, 'Liquid Crystal Polymers' in Thermotropic Liquid Crystals, G.W. Gray (ed.), 2, 22, pp 162-164 (1987).
31 M.Yamamoto, Y.Hatano, and Y.Nishijima, Chemistry Letters (1976) 351-354.
32 N. Ohta *et al*, J.Phys.Chem, 100 (1996) 19295-19302
33 John Wiley & Sons, Encyclopaedia of Polymer Science and Engineering 2nd Ed., , Wiley-Interscience Publication. (1985)
34 T. Ito, H. Shirakawa, and S. Ikeda, J. Polym. Sci. Polym. Chem. Ed., 12 (1974)11
35 H. Shirakawa, E.J. Louis, A.G. MacDiarmuid, C.K. Chiang, and A.J. Heeger, JCS. Chem. Commun., (1977) 578.
36 L.W. Shacklette, R.L. Elsenbaumer, R.R. Chance, J.M. Sowa, D.M. Ivory, G.G. Miller, and R.H. Baughman, J. Chem. Soc., Chem. Commun., 361 (1982)
37 D. Bloor, Chemistry in Britain, 31, 5, 1995.
38 K. Akagi, S. Katayama, H. Shirakawa, K. Araya, A. Mukoh, and T. Narahara, Synth. Met., 17 ,1-3 (1987)241-246
39 N. Coustel, N. Foxoneet, J.L. Ribet, P. Bernier, J.E. Fisher, Macromolecules, 24, 21 (1991) 5867-5873
40 W. Torres, M.A. Fox, Chem. of Mat. 4, 3 (1992) 583-588
41 G. Tourillon and F. Garnier, J.Polym. Sci.- Polym. Phys., 22 (1984) 33
42 Tsibouklis *et al*, Liquid Crystals, 3,10 (1988) 1393-1400
43 J LeMoigne *et al*, Liquid Crystals, 6, 6 (1989) 627-639
44 M.R. Bryce *et al*, Synth. Met., 39 (1991) 397-400
45 S.H. Jin *et al*, Macromolecules, 24, 22 (1991) 6050-6052
46 K.Yoshino *et al*, Jpn. J. Appl. Phys., 32 (1993) L1673-L1676
47 Z. Bao, R. Cai, and L. Yu, Abs.Pap. Amer. Chem. Soc., 206 (1993) 296
48 P.J. Langley, F.J.Davis, and G.R.Mitchell, Mol.Cryst. Liq. Cryst., 236 (1993) 225-230
49 H. Awaji, J.Takad, and M Koshioka, Jpn. Kokai Tokkyo Koho, JP 05,320,322 [93,320,322] Dec. 1993
50 H. Awaji, J.Takad, and M Koshioka, Jpn. Kokai Tokkyo Koho, JP 05,279,457 [93,279,457] Oct. 1993
51 H. Awaji, J.Takad, and M Koshioka, Jpn. Kokai Tokkyo Koho, JP 05,331,266 [93,331,266] Dec. 1993
52 F. Vicentini, M. Mauzac, and R. Laversanne, Liquid Crystals, 16, 5 (1994)721-733
53 F. Vicentini *et al*, Liquid Crystals, 19, 2 (1995)235-240
54 C. Thobie-Gautier *et al*, Adv. Mater., 6, 2 (1994) 138-142
55 D. Melamed, C. Nuckols, and M.A. Fox, Tetrahedron Letters, 35, 45 (1994) 8239-8332
56 Yoshino *et al*, Mol. Cryst. Liq. Cryst., 261 (1995) 637-647
57 K. Akagi *et al*, Mol. Cryst. Liq. Cryst., 267 (1995) 277-282
58 K. Akagi *et al*, Synth. Met., 69 (1995) 13-16
59 K. Akagi *et al*, Synth. Met., 69 (1995) 33-34
60 K. Yoshino *et al*, Synth. Met., 69 (1995) 399-400
61 Koide, Naoyuoki (Nippon Soda Corp.), Jpn. Kokai Tokkyo Koho, JP 06,321,935 [06,321,935] 1995
62 F. Vicentini *et al*, unpublished conference paper

63 F. Vicentini *et al*, Liquid Crystals, 19, 2 (1995) 235-240
64 F. Vicentini *et al*, Europhysics Letters, 32, 8 (1995) 657-662
65 K. Akagi, and H. Shirakawa, Macromol. Symp., 104 (1996) 137-158
66 L.I. Gabaston, P.J.S. Foot, and J.W. Brown, Chem. Commun., 429 (1996)
67 K. Akagi, H. Goto, and H. Shirakawa, Synth. Met., 84 (1997) 313-316
68 H. Goto, K. Akagi, and H. Shirakawa, Synth. Met., 84 (1997) 385-386
69 M. Kijima, H. Hasegawa, and H. Shirakawa, J. Polym. Sci. Part A: Polym. Chem., 36 (1998) 2691-2698
70 P.J.S. Foot, J.W. Brown, P. Ibison, and R. Simon, UK patent, GB2318119-B (2000)
71 I. Rabias, I. Hamerton, B.J. Howlin, and P.J.S. Foot, Comput. Theor. Polym. Sci., 8 (3-4) (1998) 265-271
72 V. Percec *et al*, Macromolecules, 32 (1999) 2597-2604
73 R. Kiebooms, H. Goto, and K. Akagi, Synth. Met., 119 (2001) 117-118
74 X.M. Dai *et al*, Synth. Met., 119 (2001) 397-398
75 S. Abe, M. Kijima, and H. Shirakawa, Synth. Met., 119 (2001) 421-422
76 I. Osaka, H. Goto, K. Itoh, and K. Akagi, Synth. Met., 119 (2001) 541-542
77 L.M. Gan, C.H. Chew, H.S.O. Chan and L. Ma, Polym. Bulletin, 31 (1993) 347.
78 G. Bischoff, and W.F. Schmidt, Die Angewandte Makromolekulare Chemie, 208 (1993) 151.
79 T.S.Stevens, and S.H.Tucker, (1931).
80 W.C.Guida, and D.J.Mathre, J.Org.Chem, 45 (1980) 3172-3176.
81 S.H.Hosseini, A.Entezami, Eur.Polym.J., 31 (1995) 7 635-641.
82 D.H. Evans, K.M. O'Connell, R.A. Petersen, and M.J. Kelly, J. Chem. Educ., 60 (1983) 4 291.
83 T.E.Roland, and M.B.Jones, J. of Polymer Science Part C, 24 (1986) 233-239.
84 M.M.Verghese, M.K.Ram, H.Vardhan, B.D.Malhotra, and S.M.Ashraf, Adv. Mat. For Optics and Electronics, 6 (1996) 399-402.
85 K.S.V. Santhanam, N.S. Sundaresan, Indian J. of Tech., 24, 7 (1986) 417-422
86 V. Rani, K.S.V. Santhanam J. of Sol. St. Electron., 2, 2 (1998) 99-101
87 R. Prakash, R.C. Srivastava, P.K. Seth, Polym. Bullet., 46, 6 (2001) 487-490
88 N. Ohta *et al*, J.Phys.Chem, 100 (1996) 19295-19302
89 T.S.Stevens, and S.H.Tucker, (1931).
90 W.C.Guida, and D.J.Mathre, J.Org.Chem, 45 (1980) 3172-3176.
91 S.H.Hosseini, A.Entezami, Eur.Polym.J., 31 (1995) 7 635-641.
92 L.M. Gan, C.H. Chew, S.O. Hardy and L. Ma, Polym. Bullet., 31 (1993) 347-350
93 G. Mengoli, M. M. Musiani, B. Schreck and S. Zecchin, J. of Electroanal. Chem., 246, 1 (1988) 73-86
94 P. S. Abthagir, K. Dhanalakshmi and R. Saraswathi, Synth. Met., 93, 1 (1998),1-7
95 H. Taoudi, J. C. Bernede, A. Bonnet, M. Morsli and A. Godoy, Thin Solid Films, 304, 1-2 (1997) 48-55
96 A. Entezami and S. H. Hosseini, Euro. Poly. J., 31, 7 (1995) 635-641
97 D.H. Evans, K.M. O'Connell, R.A. Petersen, and M.J. Kelly, J. Chem. Educ., 60 (1983) 4 291.
98 M.M.Verghese, N.S.Sundaresant, T.Basu, and B.D.Malhotra, J of Mat. Sc. Letters, 14 (1995) 401-404
99 S.H. Hosseini, A. Entezami, Eur. Polym. J., 31 (1995) 7 635-641.
100 M.M. Verghese, M.K. Ram, H. Vardhan, B.D. Malhotra, and S.M. Ashraf, Polymer, 38 7 (1997) 1625-1629.
101 G. Mengoli, M.M. Musiani, B. Schreck, and S. Zecchin, J. Electroanal. Chem., 246 (1988) 73-86.

102 S.T. Wellinghoff, D. Zhi, T.J. Kedrowski, *et al*, Mol. Cryst. Liq. Cryst., 106 , 3-4 (1984) 289-304
103 S.T. Wellinghoff, Z. Deng, J.F. Reed, *et al*, Mol. Cryst. Liq. Cryst., 118, 1-4, (1985) 403-412
104 CAChe 3.2 User Manual
105 www.chem.uni-potsdam.de/tools/index.html
106 T.E.Roland, and M.B.Jones, J. of Polymer Science Part C, 24 (1986) 233-239.
107 M.M.Verghese, M.K.Ram, H.Vardhan, B.D.Malhotra, and S.M.Ashraf, Adv. Mat. For Optics and Electronics, 6 (1996) 399-402.
108 M.M.Verghese, M.K.Ram, H.Vardhan, B.D.Malhotra, and S.M.Ashraf, Polymer, 38 (1997) 7 1625-1629.
109 R.C. Weast, Handbook of Chemistry and Physics, 69th edition, CRC Press (1988)
110 Prediction of Polymer Properties, J. Bicerano, Marcel Dekker Inc., (1993)
111 A.A. Craig and C.T. Imrie, J. Mater. Chem., 4, 11 (1994) 1705-1714
112 T. Nakano, T. Hasegawa and Y. Okamoto, Macromolecules, 26 (1993) 5494
113 H. Hasegawa, M. Kijima, and H. Shirakawa, Synth. Met., 84 (1997) 177-178
114 E. Perplies, H. Ringsdorf and J.H. Wendorff, Polym. Lett. 13
115 H Finklemann, D. Naegele, H. Ringsdorf, Makromol. Chem., 180 (1979) 803
116 H.J. Coles and R. Simon, Polymer 26 (1985) 1801
117 R. Simon and H.J.Coles, Polymer 27 (1986) 811
118 M.S.A. Abdou, and S. Holdcroft, Can. J Chem., 73, 11 (1995) 1893-1901
119 P. Nagtegaele, and T. V. Galstian, Synth. Met., 127 (2002) 85-87
120 F.Tooley *et al*, Optical Mat., 17 (2001) 235-241
121 T.K.S. Wong *et al*, Mat. Sc. And Eng., B55 (1998) 71-78
122 T.Sano *et al*, Appl. Surf. Sc., 186 (2002) 221-226
123 J. Oguma, R. Kawamoto, H. Goto, K. Itoh and K. Akagi, Synth. Metals, 119 (2001) 537-538
124 H. Goto, K. Itoh, K. Akagi, Synth. Met., 119 (2001) 351-352
125 E. Cloutet *et al*, Polymer, 43,12 (2002) 3489-3495